



# LUND UNIVERSITY

## System analysis of a PV/T hybrid solar window

Davidsson, Henrik

2010

[Link to publication](#)

*Citation for published version (APA):*

Davidsson, H. (2010). *System analysis of a PV/T hybrid solar window*. [Licentiate Thesis, Department of Architecture and Built Environment]. Energy and Building Design, Lund University.

*Total number of authors:*

1

### General rights

Unless other specific re-use rights are stated the following general rights apply:

Copyright and moral rights for the publications made accessible in the public portal are retained by the authors and/or other copyright owners and it is a condition of accessing publications that users recognise and abide by the legal requirements associated with these rights.

- Users may download and print one copy of any publication from the public portal for the purpose of private study or research.
- You may not further distribute the material or use it for any profit-making activity or commercial gain
- You may freely distribute the URL identifying the publication in the public portal

Read more about Creative commons licenses: <https://creativecommons.org/licenses/>

### Take down policy

If you believe that this document breaches copyright please contact us providing details, and we will remove access to the work immediately and investigate your claim.

LUND UNIVERSITY

PO Box 117  
221 00 Lund  
+46 46-222 00 00

# System analysis of a PV/T hybrid solar window

*Henrik Davidsson*

Division of Energy and Building Design  
Department of Architecture and Built Environment  
Lund University  
Faculty of Engineering LTH, 2010  
Report EBD-T-10/11



# Lund University

Lund University, with eight faculties and a number of research centres and specialized institutes, is the largest establishment for research and higher education in Scandinavia. The main part of the University is situated in the small city of Lund which has about 110 000 inhabitants. A number of departments for research and education are, however, located in Malmö. Lund University was founded in 1666 and has today a total staff of 6 200 employees and 46 000 students attending 274 educational programmes and 2 000 single subject courses and 75 international master's programmes offered by 72 departments.

## Division of Energy and Building Design

Reducing environmental effects of construction and facility management is a central aim of society. Minimising the energy use is an important aspect of this aim. The recently established division of Energy and Building Design belongs to the department of Architecture and Built Environment at the Lund University, Faculty of Engineering LTH in Sweden. The division has a focus on research in the fields of energy use, passive and active solar design, daylight utilisation and shading of buildings. Effects and requirements of occupants on thermal and visual comfort are an essential part of this work. Energy and Building Design also develops guidelines and methods for the planning process.

# System analysis of a PV/T hybrid solar window

Henrik Davidsson

Licentiate Thesis

## Keywords

Solar window, PV/T hybrid, building integration, TRNSYS

© copyright Henrik Davidsson and Division of Energy and Building Design.

Lund University, Lund Institute of Technology, Lund 2010.

The English language corrected by L. J. Gruber BSc(Eng) MICE MStructE.

Layout: Hans Follin, LTH, Lund.

Cover photo: Stefan Larsson

Printed by Tryckeriet i E-huset, Lund 2010

Report No EBD-T--10/11

System analysis of a PV/T hybrid solar window.

Department of Architecture and Built Environment, Division of Energy and Building Design,  
Lund University, Lund

ISSN 1651-8136

ISBN 978-91-85147-45-8

Lund University, Lund Institute of Technology  
Department of Architecture and Built Environment  
Division of Energy and Building Design  
P.O. Box 118  
SE-221 00 LUND  
Sweden

Telephone: +46 46 - 222 73 52  
Telefax: +46 46 - 222 47 19  
E-mail: [ebd@ebd.lth.se](mailto:ebd@ebd.lth.se)  
Home page: [www.ebd.lth.se](http://www.ebd.lth.se)

# Abstract

A building-integrated multifunctional PV/T solar window was suggested and developed by Andreas Fieber. The solar window is constructed of PV cells laminated on solar absorbers placed in a window behind the glazing. To reduce the costs of solar electricity, tiltable reflectors have been introduced in the construction to focus radiation onto the solar cells. The reflectors make it possible to control the amount of radiation transmitted into the building. The insulated reflectors also reduce the thermal losses through the window. Fieber discusses the architectural implications of the solar window. The effects on the light distribution are discussed together with effects on the building if different strategies of controlling the reflectors are used. Following this, long term measurements on the energy output from the solar window were performed. A model for simulation of the electric and hot water production was developed and calibrated against the measured values. The model can perform yearly energy simulations where different features such as shading of the cells or effects of the glazing can be included or excluded. The simulation can be run with the reflectors in an active, upright, position or in a passive, horizontal, position. The simulation program was calibrated against measurements on a prototype solar window placed in Lund in the south of Sweden and against a solar window built into a single family house, Solgården, in Älvkarleö in the central part of Sweden. The results from the simulation show that the solar window produces about 35% more electric energy per unit cell area than a vertical flat PV module.

When the solar collector is placed in the window a complex interaction takes place. On the positive side is the reduction of the thermal losses due to the insulated reflectors. On the negative side is the blocking of solar radiation that would otherwise heat the building passively. This might result in an increase of auxiliary energy need compared to a standard solar energy system. However, this might be accepted if the price of the PV/T hybrid is less than the total price of the individual components. To investigate the sum of such complex interaction a system analysis has to be performed. Results from simulations using TRNSYS show that the system with individual solar energy components annually uses 1100 kWh

less auxiliary energy than the system with a solar window. However, the solar window system annually uses 600 kWh less auxiliary energy than a system with no active solar energy system.

# Contents

|   |    |
|---|----|
| <b>Keywords</b>   | 2  |
| <b>Abstract</b>   | 3  |
| <b>Contents</b>   | 5  |
| <b>List of articles</b>                                   | 7  |
| <b>Nomenclature</b>                                       | 9  |
| <b>Acknowledgements</b>                                   | 11 |
| <b>1 Background</b>                                       | 13 |
| 1.1 Energy and environmental problems                     | 13 |
| 1.2 The alternatives                                      | 14 |
| 1.3 Solar energy  | 12 |
| 1.3.1 Solar electricity and Solar thermal                 | 17 |
| 1.3.2 PV cells  | 17 |
| 1.3.3 Thermal collectors                                  | 18 |
| 1.3.4 Hybrid technology                                   | 19 |
| 1.4 Building integrated solar energy                      | 21 |
| 1.5 Energy as a system, feedback mechanisms, energy flows | 21 |
| 1.6 Solgård   | 23 |
| <b>2 The solar window</b>                                 | 25 |
| 2.1 Construction  | 25 |
| 2.2 The existing installations                            | 30 |
| 2.3 The measurements                                      | 31 |
| 2.4 The model   | 33 |
| 2.5 The parameters  | 35 |
| 2.5.1 Radiation, angles                                   | 35 |
| 2.5.2 Transmission through the glazing                    | 36 |
| 2.5.3 Angular dependence of PV cell                       | 37 |
| 2.5.4 Shading   | 38 |
| 2.5.5 Reflector contribution                              | 40 |
| 2.5.6 Diffuse radiation                                   | 43 |
| 2.5.7 Thermal losses                                      | 44 |
| 2.5.8 Passive gains                                       | 49 |
| 2.5.9 Control strategies                                  | 52 |
| <b>3 TRNSYS</b>   | 55 |



|                    |   |     |
|--------------------|---|-----|
| <b>4</b>           | <b>Evaluation</b>   | 61  |
| <b>5</b>           | <b>Results</b>  | 65  |
| 5.1                | Prototype solar window  | 65  |
| 5.2                | Results Solgården solar window                                | 68  |
| 5.2.1              | Electrical Results Solgården                                  | 68  |
| 5.2.2              | Thermal Results.  | 69  |
| 5.2.3              | Development   | 72  |
| 5.3                | Augustenborg  | 76  |
| <b>6</b>           | <b>Conclusions</b>  | 79  |
| <b>7</b>           | <b>Development and future</b>                                 | 83  |
| <b>References</b>  |   | 85  |
| <b>Article I</b>   | Performance of a multifunctional PV/T hybrid solar window     | 89  |
| <b>Article II</b>  | System analysis of a multifunctional PV/T hybrid solar window | 99  |
| <b>Article III</b> | Performance of a multifunctional PV/T hybrid solar window     | 119 |

# List of articles

Davidsson, H., Perers, B., & Karlsson, B. (2010). Performance of a multifunctional PV/T hybrid solar window. *Solar Energy* 84, p 365-372.

Davidsson, H., Perers, B., & Karlsson, B. (2010). System analysis of a multifunctional PV/T hybrid solar window. Submitted to *Solar Energy*.

Davidsson, H., Perers, B., & Karlsson, B. (2008). Performance of a multifunctional PV/T hybrid solar window. *Procidings EuroSun 2008 Lisbon*, article number 364.



# Nomenclature

|                         |   |                      |
|-------------------------|---|----------------------|
| $\alpha$                | solar azimuth   | [°]                  |
| $\gamma$                | solar azimuth   | [°]                  |
| $\theta_z$              | zenith angle  | [°]                  |
| $v$                     | optical axis  | [-]                  |
| $u$                     | absorber tilt   | [°]                  |
| $F$                     | Focal point   | [-]                  |
| $p$                     | Focal length  | [m]                  |
| $h$                     | height of glazing                                     | [m]                  |
| $a$                     | absorber width  | [m]                  |
| $w$                     | angle glazing-absorber plane                          | [°]                  |
| $q_{NS}$                | angle glazing-projected radiation                     | [°]                  |
| $r$                     | vector  | [-]                  |
| $\varphi$               | angle   | [°]                  |
| $T_{in}$                | temperature in to collector                           | [K]                  |
| $T_{out}$               | temperature out of collector                          | [K]                  |
| $Flow$                  | Flow to the collector                                 | [l/s]                |
| $P_{tot}$               | Total delivered power                                 | [W]                  |
| $P_{dir}$               | Delivered power from direct radiation                 | [W]                  |
| $P_{ref}$               | Delivered power from radiation via the reflector      | [W]                  |
| $P_{diff}$              | Delivered power from diffuse radiation                | [W]                  |
| $G_{b,n}$               | beam radiation  | [W/m <sup>2</sup> ]  |
| $G_d$                   | diffuse radiation                                     | [W/m <sup>2</sup> ]  |
| $T_{glass}$             | transmittance through the glazing                     | [-]                  |
| $\alpha_{pv}$           | angular dependence of the absorptance of the PV       | [-]                  |
| $f_{shading}$           | shading of the PV cells                               | [-]                  |
| $f_{ref}$               | correction factor for the shadow effects on reflector | [-]                  |
| $A_{cell}$              | PV cell area  | [m <sup>2</sup> ]    |
| $\eta_{pv}$             | efficiency of PV cell                                 | [-]                  |
| $A_{ref}$               | reflector area  | [m <sup>2</sup> ]    |
| $R_{ref}$               | reflectance   | [-]                  |
| $\theta_1$ - $\theta_5$ | incidence angles                                      | [°]                  |
| $C_1$ - $C_2$           | response function for the diffuse radiation           | [-]                  |
| $P_{loss_p}$            | thermal losses for the prototype solar window         | [W/m <sup>2</sup> K] |

|                  |  |                                    |
|------------------|--|------------------------------------|
| $P_{loss\_s}$    | thermal losses for the Solgården solar window                      | [W/m <sup>2</sup> K]               |
| $U_{s\_out}$     | U-value to the outside for the Solgården solar window              | [W/m <sup>2</sup> K]               |
| $U_{s\_in}$      | U-value to the inside for the Solgården solar window               | [W/m <sup>2</sup> K]               |
| $U_p$            | U-value for the prototype solar window                             | [W/m <sup>2</sup> K]               |
| $A_{window}$     | window area  | [m <sup>2</sup> ]                  |
| $\Delta T_{out}$ | temperature difference, absorber temperature - ambient temperature | [K]                                |
| $\Delta T_{in}$  | temperature difference, absorber temperature - indoor temperature  | [K]                                |
| $\Delta T$       | temperature difference, absorber temperature - ambient temperature | [K]                                |
| $T$              | temperature  | [K]                                |
| $T_h$            | temperature, hot   | [K]                                |
| $T_c$            | temperature, cold  | [K]                                |
| $T_m$            | temperature, medium  | [K]                                |
| $h_c$            | heat losses due to convection                                      | [W/m <sup>2</sup> K]               |
| $h_r$            | heat losses due to radiation                                       | [W/m <sup>2</sup> K]               |
| $q$              | thermal losses   | [W/m <sup>2</sup> ]                |
| $\varepsilon$    | emissivity   | [-]                                |
| $\sigma$         | Stefan-Boltzmann constant  | [W/m <sup>2</sup> K <sup>4</sup> ] |
| $m_{tot}$        | heat resistance, total   | [m <sup>2</sup> K/W]               |
| $m_g$            | heat resistance, glazing   | [m <sup>2</sup> K/W]               |
| $m_{c1, c2}$     | heat resistance, convection  | [m <sup>2</sup> K/W]               |
| $m_r$            | heat resistance, radiation   | [m <sup>2</sup> K/W]               |
| $P_g$            | passive gains, total   | [W]                                |
| $P_D$            | passive gain due to direct radiation                               | [W]                                |
| $P_d$            | passive gain due to diffuse radiation                              | [W]                                |
| $P_t$            | passive gain due to thermal losses in the absorber                 | [W]                                |

# Acknowledgements

This work was financed by the Swedish Energy Agency through the programme Solel 03-07.

I wish to thank my supervisors Prof. Björn Karlsson, Dr. Bengt Perers and Dr. Bengt Hellström for their support. Björn for always making valuable comments and having a never ending supply of knowledge. Bengt Perers for teaching me TRNSYS, the program I have learned to both love and hate. Bengt Hellström for assistance with the heat transfer calculation performed in this thesis. Thank you Dr Håkan Håkansson for assistance with measurements and experimental work. I would also like to thank Johan Nilsson for helping me in the beginning of my Ph.D. His help is priceless for a new Ph.D. student. Johan is acknowledged for the Zemax calculations presented in this thesis. My room mate Luís R. Bernardo deserves special thanks for help regarding many things such as computer issues and lab assistance. I want to thank all the people working at Energy and Building Design for discussions about work and life in general. Of course I would like to thank Andreas Fieber, the inventor of the window. Without Andreas I might have been unemployed today. Stefan Larsson and his family living in Solgården are acknowledged for assistance with measurements and for their acceptance of disturbance due to noise and research related work of different kinds. Thanks also to Håkan Mild for guidance in life. That working hard with a clear focus will result in future success is something I learned from him.

I would like to thank my wife Eva for discussions about the work, language corrections and planning my life. Marrying a physicist is something I can recommend to everybody. Finally I would like to thank my kids Matilda and Albert for giving everything a meaning. Without the next generation this work, and others, has no meaning.



# 1 Background

## 1.1 Energy and environmental problems

”Warming of the climate system is unequivocal, as is now evident from observations of increases in global average air and ocean temperatures, widespread melting of snow and ice and rising global average sea level” (IPCC, 2007).

Few scientific reports have caught the general public’s interest as the IPCC Fourth Assessment Report. In this report IPCC, a scientific intergovernmental body set up by the World Meteorological Organization (WMO) and the United Nations Environment Programme (UNEP), concludes that the increase of the global temperature is about  $0.74^{\circ}\text{C}$  per 100 years for the 100-year linear trend. IPCC also concludes that the rising of the sea level is about 3 mm per year and the annual average Arctic sea ice extent has shrunk by about 2.7% per decade since 1978. IPCC also claims that most of the observed increase in global average temperatures since the mid 20th century is very likely due to the observed increase in concentration of anthropogenic greenhouse gases. The concentration of  $\text{CO}_2$  and  $\text{CH}_4$  in 2005 exceeds by far the natural range over the last 650,000 years. The increase of  $\text{CO}_2$  concentration in the atmosphere is due primarily to fossil fuel use. The consequences are immense. By the end of the 21st century the global average temperature is expected to rise between  $2^{\circ}\text{C}$  and  $4^{\circ}\text{C}$  depending on simulation and emission rate of greenhouse gases. This is expected to lead to drought in some areas and increased water availability in other areas. The ecosystems will suffer significant extinction and about 30% of the global coastal wetlands will be lost.

However, not everybody agrees with the conclusions in the IPCC report. Perhaps the most interesting criticism comes from the Peak Oil theory. Different models show a peak, or a plateau, in the world oil production somewhere between 2007 and 2018 (Aleklett, 2007). The exact year depends on model and increase in oil demand. This shortage of oil will affect the amount of emitted greenhouse gases in more than one way. Of course, the most obvious emission reduction is that if there is no oil to burn there will be no emissions from it. However, shortage of oil will also



affect world markets and if energy prices rise the GNP will most likely grow more slowly. This will slow down the emission rate of greenhouse gases.

What attitude to have to these two theories is of course an individual decision. If you don't believe in either of the theories it is business as usual. If you believe in both of them or if you only believe in one of them the conclusion must be that we need to start working to find alternatives to burning fossil fuel.

“We have climbed high on the “Oil Ladder” and yet we must descend one way or another. It may be too late for a gentle descent, but there may still be time to build a thick crash mat to cushion the fall.” (Alekklett, 2007).

## 1.2 The alternatives

There are many different renewable alternatives to fossil fuel. Some of the more important renewable sources with large potential are wind power, hydro power, geothermal power, bio power and solar power. All the different sources have benefits and drawbacks. The major advantage of renewable energy sources is the low CO<sub>2</sub> emission rate. On the negative side are appearance and sometimes the high initial costs. Solar power is today an expensive way of producing electricity. Wind power stations are by some people considered to ruin the unobstructed view over the landscape. If hydro power stations are built there will be consequences to wildlife. These costs have to be compared to the costs of burning fossil fuel and in the end we have to decide who is going to pay for the energy we use today. If the answer is ourselves the fossil fuel alternative is excluded since the people living on the planet in the future have to pay with high temperature due to the global warming. We are left with the choice of paying with loss of unobstructed view over the landscape, loss of nature values due to construction of dams and hydro power stations or to make large investments to produce and install more solar energy panels.

## 1.3 Solar energy

Solar energy can be defined as energy used on a higher quality level compared to the zero state. The zero state level is the average temperature of the surroundings.

Throughout this thesis the phrase “thermal energy produced in the absorber” or similar phrases will be used. This does not mean that energy

is created out of nothing. As we all know from our physics courses, “energy can not be created or destroyed, only converted into different forms”. The phrase “thermal energy produced in the absorber” thus means “thermal energy converted from solar radiation to thermal energy in the absorber”. However, this last phrase is too long and the language gets complicated, and this is why the shorter phrase, less accurate from a physical point of view, will be used.

Knowledge about the sun and the radiation from it is important for the understanding of solar energy. The sun, practically the only energy supplier to the earth, radiates photons in a broad energy spectrum, see Figure 1.1. The spectrum stretches from UV radiation via visible light to infrared radiation, UV radiation being the most energetic. The many dips in the solar spectrum seen in Figure 1.1 are due to absorption from molecules in the atmosphere. The best known absorption is probably the ozone layer shielding the planet from the dangerous UV radiation. The ozone molecules absorb radiation shorter than 320 nm. When the ozone molecule absorbs the high energetic photon it splits in into one oxygen molecule and one free oxygen atom. Figure 1.1 also shows the sensitivity of two solar cells, a monocrystalline cell and a CIGS (Copper-Indium-Gallium-Diselenide) cell. As can be seen the radiation from the sun with wavelengths longer than approximately 1200 to 1400 nm, depending on PV cell, can not be used for production of electricity in the solar cell. The solar cell is thus transparent to near infrared radiation.

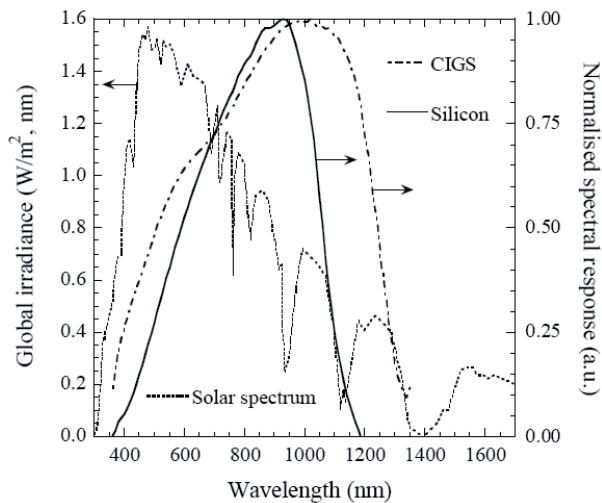


*Figure 1.1 The global solar spectrum (ISO AM1.5) in dashed line. The full line and the broken line are the spectral responses for a monocrystalline PV cell and a CIGS cell respectively. Courtesy of Maria Brogren (Brogren, 2004).*

## Solar angles

Solar radiation can be divided into four parts, shown in Figure 1.2 - the direct radiation from the sun, the diffuse radiation from the sky, the circumsolar radiation and the ground reflected radiation. The circumsolar radiation comes from angles close to the sun but still outside the solid angle of the sun.

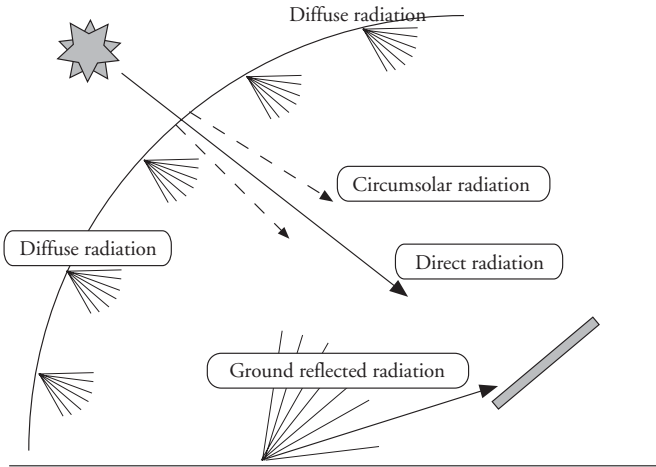


Figure 1.2 Solar radiation divided into direct radiation, diffuse radiation, circumsolar radiation and ground reflected radiation.

The path of the sun in the sky can easily be calculated with simple equations. Knowing date and time and the geographic location the sun's position can be calculated. The position is normally expressed by using the two angles, solar altitude,  $\alpha$  and solar azimuth,  $\gamma$ . The solar altitude is the angle between the ground and the sun. The solar azimuth is the angle between the sun and the south direction, i.e. the azimuth is zero at noon solar time. The angles are illustrated in Figure 1.3 where the zenith angle, defined as  $\theta_z = 90 - \alpha$ , is also shown.

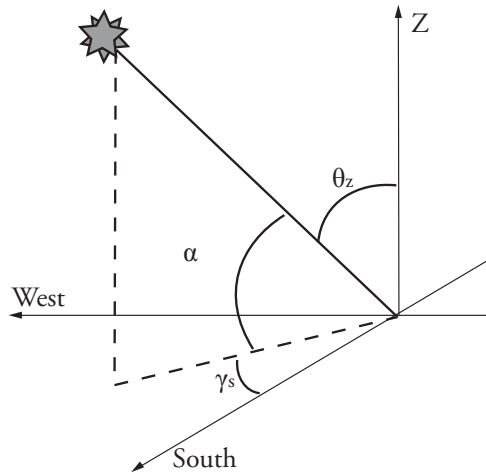


Figure 1.3 The solar angles.  $\gamma_s$  is the solar azimuth.  $\alpha$  is the solar altitude and  $\theta$  is the zenith angle.

### 1.3.1 Solar electricity and Solar thermal

Solar energy is divided into two categories, solar electricity and solar thermal. Solar electricity can be produced in many different ways. The best known technique is to use Photo Voltaic cells, commonly known as PV cells. This technique turns the photon energy into electric energy. Alternatively steam can be produced and used to run turbines to produce electricity.

The alternative form of solar energy is to produce heat. The heat is most commonly delivered and stored in a liquid or a gas. Heat has a lower energy quality and is easier to produce than electricity.

### 1.3.2 PV cells

Single PV cells are normally put together in series or series/parallel in PV modules. Each cell can produce a potential difference of about 0.5 V when irradiated. When put in series these potential differences add up to a total potential. If a module has 36 cells the total maximum potential difference is about 18 V. The PV-modules can also be put in parallel or in series. The array of PV-modules can then be connected to the grid or alternatively to a battery. When connected to the grid there is an inverter that transforms the DC voltage to high AC voltage.

There are many different types of PV cells. They vary in price, appearance and efficiency. The monocrystalline Si cells are the most efficient. These cells are made from one large single crystal. The efficiency of the cells is typically about 17%. The polycrystalline cells are less efficient with an efficiency of about 12%. The polycrystalline cells consist of many small crystals and hence have a speckled appearance. The third type of cell is the thin film cell. This type of PV cell is much thinner than the mono or polycrystalline cells. The thickness of the actual cell is as small as 1  $\mu\text{m}$ . Thanks to the small dimension there is a potential that the thin films will be cheap to produce. Today the efficiency of the thin films is about 8%.

### 1.3.3 Thermal collectors

The thermal collectors are easy to understand on a component level but difficult to understand on a system level. The complication arises due to the losses in the collectors. The PV cells have no such losses. The thermal collectors can be divided into three sections, shown in Figure 1.4. The simplest type of collector is a black painted surface that heats a liquid or a gas. This can be a black painted box that preheats the air before it is let into a building or it can be a black painted sheet of metal that is cooled with water. A pane of glass covers the construction to reduce the heat losses. As the water runs through the collector the water gets heated and is pumped away for storage or use. An uncovered solar collector with black painted sheet of metal will be a poor collector since the losses due to thermal radiation and convection will be large. This limits the use of the collector to a pool heater or similar. To construct a more efficient collector the thermal losses must be minimized. This is done in a standard flat plate collector which has a selective absorber and cover glass, upper left illustration in Figure 1.4. Anti reflection treated glazing (Chinyama, Roos and Karlsson, 1993), (Nostell, Roos and Karlsson, 1999) maximizes the transmission and the glazing itself limits the convectional losses. In order to minimize the losses due to radiation the collector is painted with low emittance paint.

The second type is the vacuum tube, shown in the upper right corner in Figure 1.4. The vacuum tubes are made from low emittance absorbers placed inside a glass cover. The glass cover is evacuated and hence the name vacuum collector. The low emittance coating suppresses the radiation losses and the vacuum limits the convectional losses. The heat is transferred to the water pipes in the manifold via a heat pipe.

The third type is the concentrating collector. This type uses reflecting material to focus radiation onto an absorber. The concentrating collec-

tor is illustrated in the lower left corner in Figure 1.4. The small hot area limits the thermal losses.

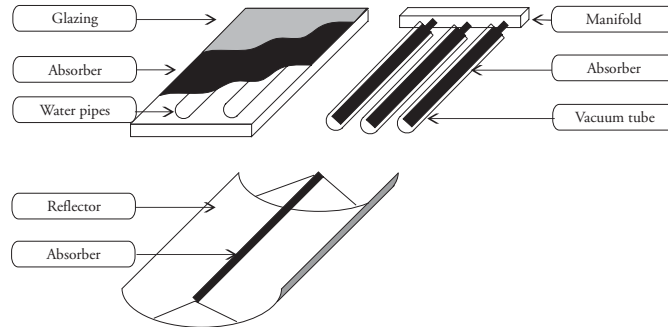


*Figure 1.4 Three types of solar collectors. The upper left is a standard flat plate collector. The upper right is a vacuum tube collector and the lower left is a concentrating collector.*

### 1.3.4 Hybrid technology

Concentrating systems can also be used for decreasing the cell area in PV installations. Concentrating radiation onto the PV cells will lead to high output per cell area and high cell temperatures. Since the PV cells are temperature sensitive the electrical output will decrease with increasing cell temperatures. Even worse, the cells might be permanently damaged if the temperature becomes too high. To solve this problem, the cells are cooled on the back. This results in cool and thereby high efficiency cells and the hot water can be used for space heating or domestic use. This multiple production makes it possible to produce cheap solar energy, (Kalogirou and Tripanagnostopoulos, 2006), (Krauter and Ochs, 2003), (Anderson, Duke, Morrison and Carson, 2009) and (Tonui and Tripanagnostopoulos, 2007). The official homepage of IEA SHC Task 35 PV/Thermal Solar Systems (IEA SHC Task 35) gives a good overview of different hybrid technologies. However, there are problems related to this technique. If PV cells are laminated on top of the absorber the low e-coating will be lost. At the same time the absorber will produce less heat since some of the photons are used to produce electricity. This is shown in Figure 1.5. At 11pm the electric circuit is closed and electrical energy is produced in the hybrid collector. Since the electrical energy is then consumed elsewhere less thermal energy is available for the thermal absorber, hence the dip in thermal energy production. We are only allowed to use the photons once.

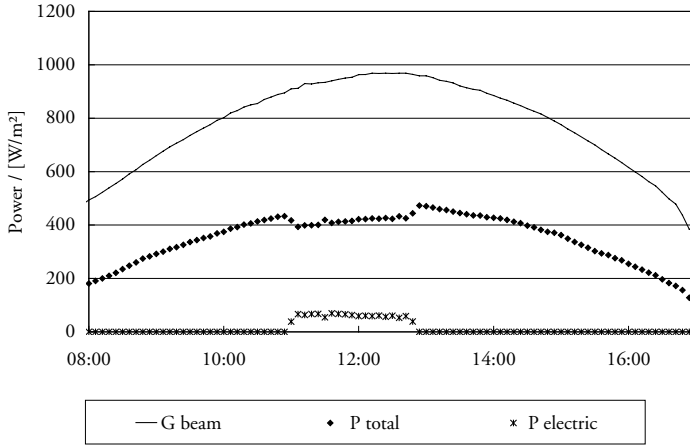


Figure 1.5 The output from a PV/T hybrid collector. At 11:00 the electric load is connected. Measurement performed by Luis R. Bernardo at EBD, LTH Sweden.

## 1.4 Building integrated solar energy

Another way of reducing the price of solar energy is to integrate the collectors and the PV systems in buildings. This saves not only building materials that are replaced by the solar energy systems but also saves work. If the solar collectors or PV modules are introduced into the construction after the building is completed, a significant amount of work has to be performed twice. The integration can be made in many different ways. Figure 1.6 shows building integrated PV modules (left figure) and PV modules installed on a wall to work as sunshade (right figure). Using the PV modules as sunshade results in a lower total cost since no extra investments are required for solar shading.



*Figure 1.6 Left, building integrated PV modules. Right, PV modules working as a sunshade. Thanks to GAIA Solar for photographs.*

There are many reasons, apart from the economical aspects stated above, why solar collectors and PV modules should be building integrated. When, for instance, roofing material is replaced with solar collectors, less energy is needed to produce the materials for the building i.e. less energy is spent in producing and transporting the building materials. Integrated into the roof the thermal losses from the collector are suppressed since the collector is well protected from wind, and at the same time the generally thick roof insulation also works as insulation for the collector.

## 1.5 Energy as a system, feedback mechanisms, energy flows

The energy flows and the energy balance of a whole building are very complex. Some energy aspects are easy to understand e.g. a solar collector that transports heated water to a tank is positive to the energy balance as long as the inlet water is hotter than the outgoing water. The energy flow is in one direction only. Introducing an extra pane of glass in the window is more complicated for the energy flow. On the one hand, the U-value, i.e. the thermal losses, is reduced which is beneficial for the energy balance, at least if cooling is not an issue. On the other hand, the extra glazing will reduce the solar transmission through the window. This means that less energy is let into the building for passive heating. This is negative for the energy balance. Having one positive and one negative effect makes it more complicated to decide the total effect. Introducing large eaves will increase comfort and limit the need for active cooling. However, it will also block some useful radiation. A building is full of such interactions. Some are



more complicated than others. Performing simulations or measurements might answer the questions raised.

The environment which the building is placed in is of great importance for the energy balance. Cold climates will obviously lead to a larger energy need. However, there are other important factors in this equation. The amount of sunshine, especially during the winter months, is also a major factor. The micro climate surrounding the building also affects the energy performance. If, for instance, the building is placed on the north slope of a hill it will receive and benefit less from the solar radiation. If the building is placed in a valley there is a risk of locally colder surroundings, which does not arise if the building is placed on the top of the hill.

The building envelope is the most important part of a building in cold climates. If the envelope is poorly insulated the thermal losses will be very large. This is the reason for the fast growing market in passive houses (Passivhuscentrum a). With thick outer insulation and an effective heat recovery unit the heating system of the building will become redundant. Apart from the free energy from people and electric appliances the passive house is supplied with extra energy for the ventilation only. The extra costs due to thicker insulation and heat recovery unit are partly compensated for by the lack of ordinary heating system such as radiators or underfloor heating (Passivhuscentrum b). The passive house technique has in some ways a less complicated energy balance with its surroundings than a standard house. Since the buildings are well insulated they are less affected by e.g. cold weather. The buildings are also less dependent on the radiation transmitted through the windows since they can utilize less solar energy compared to ordinary buildings. This is not a drawback for passive houses. This is simply a consequence of the fact that the passive houses need less auxiliary energy and have a shorter heating period compared to ordinary buildings.

The domestic hot water and the electric consumption supply the building with a large amount of internal gains. A typical Swedish building with electrical heating uses about 20,000 kWh, including household energy (Energimyndigheten, 2007). If low consuming appliances replace older and high consuming appliances less energy will heat the building. Hence, more auxiliary energy has to be supplied to the heating system. However, only parts of the internal gains will contribute to the heating e.g. the heat gains during the summer will not reduce the auxiliary energy need, they will only add to overheating of the building.

Adding all these more or less complicated energy flows together raises a non trivial question. Are passive houses or “active” houses to prefer? Active houses meaning houses that take advantage of the solar energy in an active way. Is it better to have large windows and a heavy building construction to store the solar gain or is it better to reduce the window

size to minimize the thermal losses? Is it better to have a heat recovery unit that uses relatively large quantities of electrical energy to save thermal energy than to have natural ventilation with preheating of the air in pipes in the ground? Natural ventilation needs less electrical energy but results in considerably higher thermal energy need. To investigate some of these questions the building Solgården located in Älvkarleö in the central parts of Sweden was erected.

## 1.6 Solgården

Solgården, erected in 2005, is a one family house. The architecture is focused on allowing an active utilization of solar energy. The thick solid brick wall in the centre of the building acts as a storage for the solar radiation transmitted during daytime. The south façade of the building is heavily glazed as can be seen in Figure 1.7. The kitchen, bathroom and the master bedroom are placed on the north side. The kitchen is illuminated through the glazed south façade. The outer walls are constructed of expanded polystyrene, EPS. On the inside the EPS blocks are covered with gypsum boards and plywood. The outside is covered with stucco or wooden panelling. The building technique is based on a system engineered by David Hellgren (Hellgren). Apart from the low thermal conduction in the EPS the building technique also makes it possible to build an airtight envelope which is a necessity for the heat recovery to function in an optimal way. The ventilation in Solgården is driven by thermal forces, known as natural ventilation. The idea is to minimize the electrical energy need for fans.



*Figure 1.7      Parts of the south side showing the heavily glazed façade.*

All the appliances in Solgårdén are low energy consuming. This means that Solgårdén benefits less from passive heat gains from electric use. This is also one of the reasons why Solgårdén is not built as a passive house. The passive house definition states that there can be no other heating system in the building apart from the extra energy supplied to the ventilation. Since Solgårdén has an underfloor heating system it does not qualify as a passive house. The underfloor heating system also allows the building to utilize the produced solar thermal energy. The sun does not only heat the solid brick wall, it is also used in an active way since the solar heat is stored in a water storage tank, hence an active solar house. The solar collector in Solgårdén is placed on the inside of a standard window given the name “solar window”.

## 2 The solar window

### 2.1 Construction

The main reason to have a window is to allow daylight to enter the room. The solar radiation transmitted through the window also heats the building passively. However a window suffers large thermal losses during dark and cold hours. This means that an ideal window should have the following properties.

- During dark hours it should have low U-value and correspondingly low heat losses like a well-insulated wall.
- During cold sunny hours it should effectively convert the radiation to heat like a window, i.e. have a low U-value and high total solar transmittance.
- During warm sunny hours solar shades should decrease the solar radiation transmitted through the window.

These properties were all addressed when the solar window was proposed and developed.

The main goal behind the solar window was to lower the cost of solar energy. There are many different techniques to do this. One technique for reducing the cost of solar electricity is to use a reflector for focusing radiation onto the PV cells, thus allowing expensive PV cells to be replaced by considerably cheaper reflector material. This often leads to high cell temperatures and thus cells of low efficiency. Active water cooling on the back of the cell gives both relatively cool, and thereby highly efficient cells, and hot water for domestic use. Further cost reduction is possible if the solar modules can be integrated into the building construction. Integration makes it possible to use existing frames and glazing for the solar modules or, alternatively, to replace roofing material and windows by solar modules. Wall integrated solar collectors using reflectors have been shown to increase the electrical output substantially (Gajbert, Hall and Karlsson, 2007), (Mallick, Eames, Hyde and Norton, 2004) compared to flat vertical PV modules. All these techniques are combined in the solar window proposed and developed by Andreas Fieber, (Fieber, 2003), (Fieber, 2004), (Fieber,

2005). The solar window, see Figure 2.1, is constructed of solar thermal absorbers on which PV cells have been laminated. The absorbers, marked with (a) in the figure, are building integrated into the inside of a standard window, marked with (c) in the figure. This saves frames and glazing and lowers the total cost of the construction. In order to minimize the PV cell area, reflectors, marked with (b) in the figure, have been placed behind the absorbers. When the foldable reflectors are tilted to a vertical position the solar radiation is focused onto the absorbers. When the reflectors are tilted to a horizontal position the solar radiation is let into the building to allow passive heating. This means that in a closed position the reflectors increase the radiation on the cells, reduce the thermal losses through the window and also work as a sunshade. The double glazing of the window in front of the absorbers is anti-reflection treated to maximize the transmittance (Chinyama et al., 1993), (Nostell et al., 1999).

The solar window is not only a solar collector. It is also a sunshade that prevents overheating of the building during the summer. Other innovative solutions for sunshades in buildings have been proposed for instance using thermotropic glass with active dimming (Inoue, Ichinose and Ichikawa, 2008) and electrochromic smart windows (Granqvist et al., 1998). The official homepage of IEA SHC Task 21 Daylight in Buildings (IEA SHC Task 21) gives a good overview of different solar shading systems. Apart from the energy aspects the solar window also gives the room an interesting daylight distribution. After the light is reflected in the reflector it will hit e.g. the ceiling and diffuse. In this way the daylight is transported away from the direct vicinity of the window to the parts further back in the room. However, this thesis is limited to the energy aspects of the solar window. The interested reader is referred to Andreas Fieber's licentiate thesis (Fieber, 2005)

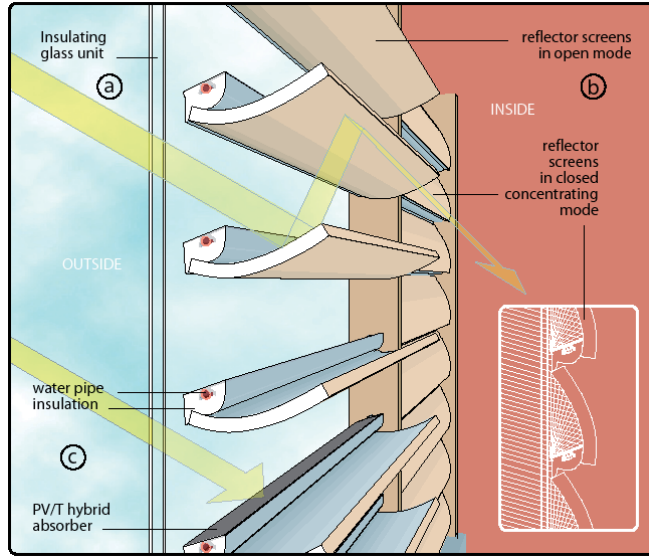


Figure 2.1 *The solar window. The PV cells are laminated on top of the absorbers. Tiltable reflectors are placed behind the absorbers. The large figure shows the solar window with the reflectors in an open mode and the inset in the lower right corner shows the solar window in closed mode. Drawings by Andreas Fieber.*

The geometry of the solar window is shown in Figure 2.2. The optical axis of the parabolic reflector is directed  $15^\circ$  above the horizon with the focus on the front edge of the absorber, i.e.  $v = 15^\circ$ . The absorber tilt,  $u$ , is  $20^\circ$ . This means that all radiation from  $15^\circ$  and higher projected solar altitudes will impinge on the absorber between the focal point,  $F$ , and the reflector. The focal length is denoted  $p$ , the height of the glazing  $h$  and  $a$  is the absorber width. The angle  $w$  is the angle between the glazing and the absorber plane and  $q_{NS}$  is the incident angle of the solar radiation projected in the north-south vertical plane. The reflector parabola is described in Eq. (2.1).  $r$  is a vector from  $F$  to a point on the parabola at angle  $\varphi$ .

$$r(\varphi) = p/\cos^2(\varphi) \quad \text{Eq. (2.1)}$$

Both  $h$  and  $a$  are determined by  $r$  and the two angles  $w=105^\circ$  and  $u+v=35^\circ$ , respectively for the solar window. The ratio between  $h$  and  $a$ , which is defined as the geometrical concentration factor, is 2.45 for the construction.

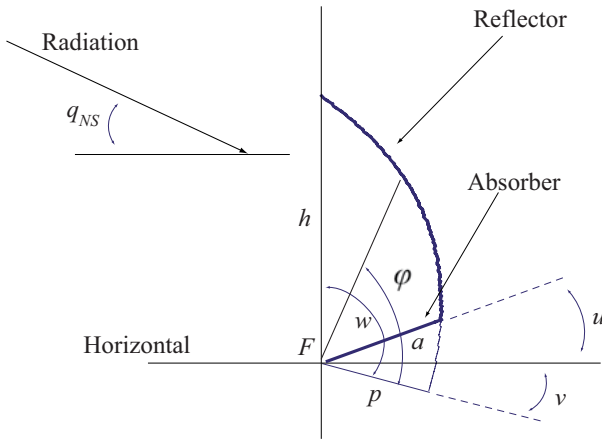


Figure 2.2 Illustration of the parabolic reflector and the absorber.

Figure 2.3 illustrates how the solar radiation is concentrated on the absorber. If the projected solar height is above  $60^\circ$  there is no contribution from the reflector. As the projected solar height is lowered, more and more radiation is focused via the reflector to the absorber. At  $15^\circ$  solar height the contribution from the reflector is at a maximum. If the projected solar height is below  $15^\circ$  the reflection will end up outside the absorber and thus there will be no contribution from the reflector.

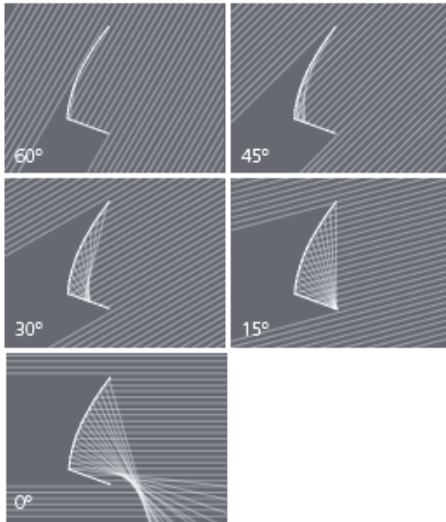


Figure 2.3 The reflection of solar radiation for different projected solar heights. All radiation between  $15^\circ$  and  $60^\circ$  is focused on the absorber. Drawings by Andreas Fieber.

The reflectors in the solar window are constructed of EPS. The front, facing the outside, is covered with reflecting aluminium. The back of the reflectors is laminated with birch veneer. This is illustrated in Figure 2.4. The absorbers are placed in front of the reflectors.

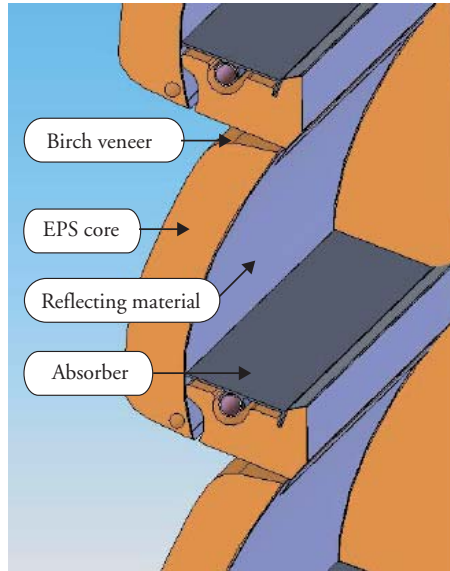


Figure 2.4 The construction of the reflector. Drawings by Stefan Larsson.

The absorbers, seen in Figure 2.5, are laminated with polycrystalline PV cells on the upper side. The water pipe in direct contact with the absorber is insulated with polyurethane.

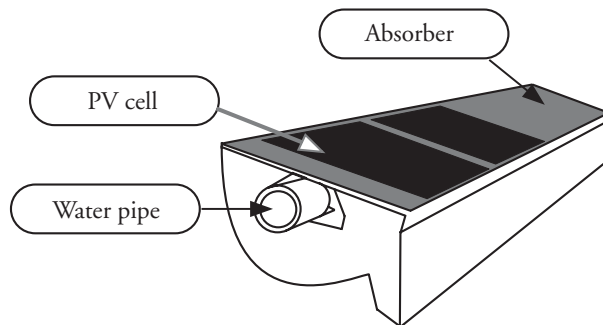


Figure 2.5 The absorber on which the PV cells are laminated.



## 2.2 The existing installations

Three different solar windows have been produced. The first was a prototype shown in Figure 2.6. It was constructed at the Älvkarleby laboratories of Vattenfall Utveckling and later moved to the Solar Laboratory at the Department of Energy and Building Design at Lund University in the south of Sweden (55.44N, 13.12E). The prototype consisting of five absorbers and five reflectors has the upper absorber laminated with PV cells. The prototype solar window is about 1.4 m<sup>2</sup>. The glazing is anti reflection treated in order to minimize the transmission losses. The complete construction was placed in an EPS box to minimize the thermal losses during measurements outdoors. The window was turned to the south during the measurements.



*Figure 2.6 The prototype solar window with five absorbers and five reflectors. The uppermost absorber is laminated with PV cells.*

The solar window in Solgårdén (60.57N, 17.45E), seen in Figure 2.7, is planned for a full area of 16 m<sup>2</sup>. Today only 8 m<sup>2</sup> is in operation. The 8 m<sup>2</sup> collector is divided into four windows. Each window consists of eight absorbers on which eight PV cells per absorber have been laminated. The

insulated reflectors are placed behind the absorbers. The glazing is antireflection treated in order to minimize the transmission losses.



*Figure 2.7 The Solgård solar window with the reflectors in a closed, vertical, position.*

The solar window in Augustenborg in Malmö (55.62N, 13.02E) in the south of Sweden is constructed of altogether 36 absorbers laminated with PV cells. This solar window differs from the other two since these reflectors are not insulated, and since this solar window was retrofitted it has no anti reflection treated glazing. The existing glazing was kept to minimize the cost of the construction. The absorbers are installed in a staircase in a showroom for green roofs (Greenroof). Since the area around the district of Augustenborg has a clear environmental profile in Malmö it was extra interesting to install the collector here. In this way the solar window is used not only to produce hot water and electricity but also to attract people to solar energy.

## 2.3 The measurements

The thermal and electrical output from the prototype solar window was measured during the second half of 2006. An illustration of the measurement can be seen in Figure 2.8.

The temperatures of the system were measured using PT100 sensors. Both  $T_{in}$  and  $T_{out}$  were measured as close to the solar window as possible in order to avoid cooling the water and thus lowering the efficiency of the collector. The water flow was measured using standard Hall technique appliance and the IV-characteristics were monitored simultaneously with the thermal measurements. Unfortunately the IV-receiver was damaged during measurements. At the end of the measurements only the short circuit current was obtained. This problem was however limited since the measurements from the prototype solar window were only used for relative comparisons. The diffuse and direct radiation were measured using pyranometers. Measurements were carried out at 10 second intervals. To avoid filling the memory of the logger, a Campbell CR10, the values were averaged and stored every 6 minutes. The ambient temperature was monitored with a PT100 sensor.

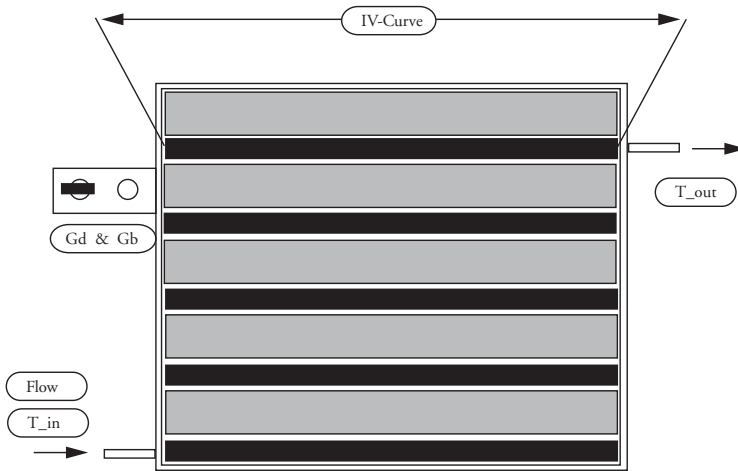


Figure 2.8 The measurement setup for the prototype solar window.  $T_{in}$ ,  $T_{out}$  are the temperatures in respectively out of the collector. Flow is the mass flow of the circulating water. Gd and Gb are the global diffuse radiation and the beam radiation respectively. IV-Curve marks where the current and the voltage were monitored.

The measurements from Solgården were carried out in a similar way using similar equipment. However no IV curves were monitored. Instead the current and the voltage given by the maximum power point tracker (MPP tracker) were monitored.

The Augustenborg solar window used thermocouples to measure the temperature. Also this installation is equipped with a MMP tracker which

means that no IV curves were monitored. The electric output was calculated from current and voltage measurements.

## 2.4 The model

A simulation model was developed to describe the solar window. The goal was to compare the solar window with a more standardized solar energy system made from flat PV modules and flat solar thermal collectors. Another goal was to study whether the solar window can be improved. The model uses the direct and diffuse radiation together with the inlet water temperature, the ambient temperature and the time, and thus the solar angles, as inputs. The outputs are thermal and electrical delivered power. In order to simplify the calculations the total electrical power,  $P_{tot}$ , delivered by the solar window was divided into three components,  $P_{dir}$ ,  $P_{ref}$  and  $P_{diff}$ . The first is  $P_{dir}$ , power caused by the beam radiation that strikes the absorber directly, the second component is  $P_{ref}$  power caused by the beam radiation that goes via the reflector. The third component,  $P_{diff}$  is the power contribution given by the diffuse radiation. Figure 2.9 graphically explains the three different components of radiation.

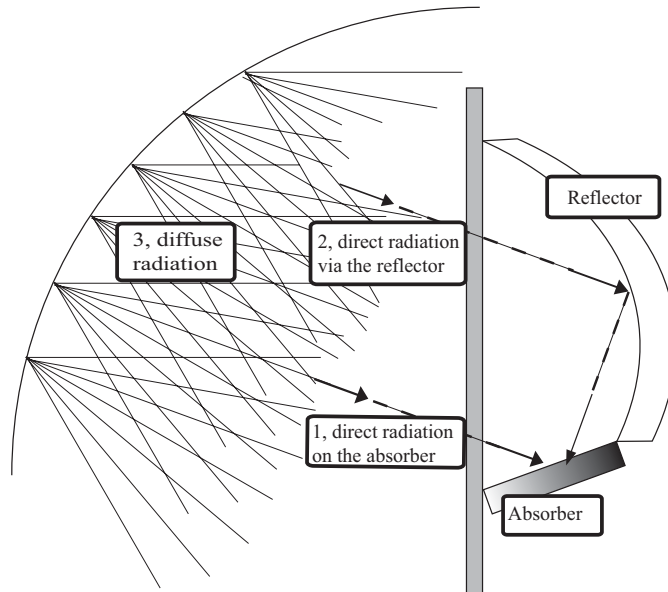


Figure 2.9 Graphical explanation of the calculation method with the three different radiation components.

The expression for the electrical output is shown below.

$$P_{dir} = G_{b,n} \cdot T_{glass}(\theta_1) \cdot \alpha_{pv}(\theta_2) \cdot f_{shading}(\theta_3) \cdot A_{cell} \cdot \eta_{pv} \cdot \cos(\theta_2) \quad \text{Eq. (2.2)}$$

$$P_{refl} = G_{b,n} \cdot T_{glass}(\theta_1) \cdot \alpha_{pv}(\theta_4) \cdot f_{ref}(\theta_5) \cdot A_{ref} \cdot \eta_{pv} \cdot R_{ref} \cdot \cos(\theta_5) \quad \text{Eq. (2.3)}$$

$$P_{diff} = G_d \cdot C_{1,2} \quad \text{Eq. (2.4)}$$

$$P_{tot} = P_{dir} + P_{ref} + P_{diff} \quad \text{Eq. (2.5)}$$

$G_{b,n}$  and  $G_d$  are the beam radiation and the diffuse radiation against the window.  $T_{glass}$  is the angular dependent transmittance through the glazing;  $\alpha_{pv}$  describes the angular dependence of the absorptance of the PV cells, and  $f_{shading}$  describes the shading of the PV cells caused by the window frame.  $f_{ref}$  is a correction factor for the shadow effects of the radiation which is reflected. This function includes the shading of the reflector. The angles  $\theta_1$  to  $\theta_5$  are the incidence angles for the beam towards the components of the solar window.  $A_{cell}$  and  $A_{ref}$  are the areas of the PV cell and the reflector, respectively.  $\eta_{pv}$  and  $R_{ref}$  are the efficiency of the solar cells and the reflectance of the reflector.  $C_{1,2}$  is an empirical response function for the diffuse radiation obtained from measurements during cloudy days, when the beam radiation has negligible influence on the performance. Measurements during cloudy days were performed with the reflector in both the horizontal and vertical positions allowing both response functions  $C_1$ , horizontal reflector, and  $C_2$ , vertical reflector, to be determined.

The transmittance,  $T_{glass}$ , through the window was calculated using the Fresnel equations and Snell's law. The shading factors  $f_{shading}$  and  $f_{reflector}$  were calculated theoretically from the PV/T window geometry. A measurement was performed to determine  $\alpha_{pv}$ , the angular dependence of the PV cells.

In order to calculate the thermal output a fourth term has to be added to describe the thermal losses in the absorber. The thermal losses  $P_{loss\_p}$  for the prototype solar window and  $P_{loss\_s}$  for the Solgården solar window are shown below. Eq. 2.2- Eq. 2.5 are reused but with parameters and functions for the thermal absorbers instead of the PV-cells.

$$P_{loss\_s} = U_{s\_out} \cdot A_{window} \cdot \Delta T_{out} + U_{s\_in} \cdot A_{window} \cdot \Delta T_{in} \quad \text{Eq. (2.6)}$$

$$P_{loss\_p} = U_p \cdot A_{window} \cdot \Delta T \quad \text{Eq. (2.7)}$$

Since the solar window in Solgården experiences thermal losses to two different temperatures, the ambient temperature and the indoor temperature, two different U-values were used. The  $U_{s\_out}$  is the thermal loss to the outside and the  $U_{s\_in}$  is the thermal loss to the inside.  $A_{window}$  is the total window area.  $\Delta T_{out}$  is the difference between the average water

temperature and the ambient temperature.  $\Delta T_{in}$  is the difference between the indoor temperature and the average water temperature. The U-values were estimated from heat transfer analyses. This is discussed later in section 2.5.7.  $U_p$  is the U-value for the prototype solar window and  $\Delta T$  is the difference between the ambient temperature and the average water temperature.

The simulations were carried out with six minute time steps using weather data monitored at the locations for the solar windows.

## 2.5 The parameters

To be able to perform the calculation all the parameters and functions described above have to be known.

### 2.5.1 Radiation, angles

The driving force behind the output is the radiation. It was monitored in the plane of the glazing. However, the simulation model needs the radiation against a number of different surfaces, e.g. the transmission loss through the glazing is dependent on the angle of incidence of the radiation on the glazing,  $\theta_1$ . At the same time the amount of radiation striking the absorber is a function of the angle between the radiation and the normal to the absorber,  $\theta_2$ . If the radiation on the reflector is to be calculated a third angle of incidence has to be calculated,  $\theta_5$ . An illustration of the different angles of incidence can be seen in Figure 2.10. The normal to the reflector was approximated with the normal to the plane connecting the endpoints of the curved reflector. See Figure 2.10 for explanation. Figure 2.11 illustrates how the incidence angles between the solar radiation and the different surfaces change during a day.

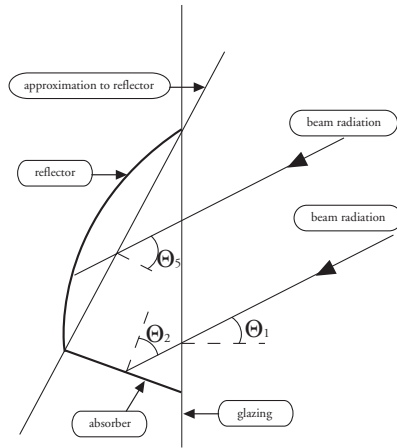


Figure 2.10 The angles of incidence for the solar radiation towards the glazing,  $\theta_1$ , the absorber,  $\theta_2$ , and the approximation to the reflector,  $\theta_5$ .

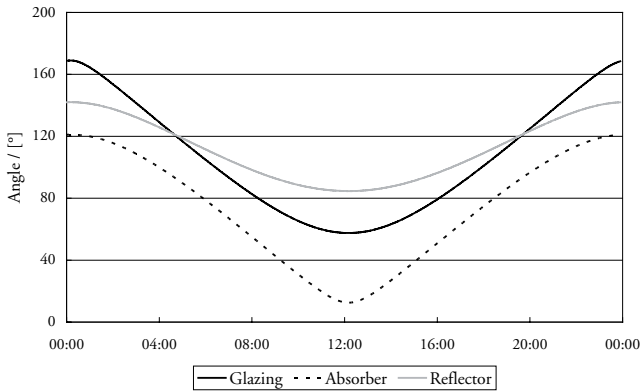


Figure 2.11 The incidence angles for the solar radiation against the glazing, in black, the absorber, in dashed line, and the reflector, in grey.

## 2.5.2 Transmission through the glazing

The transmission through the glazing was calculated theoretically using the Fresnel equations and Snell's law. Figure 2.12 shows the transmission through a standard double glazed window and a double anti reflection treated window. The glazing of the prototype solar window and the Solgård solar window is anti reflection treated while the Augustenborg solar window has a standard glass without antireflection treatment. The Augustenborg solar window thus suffers much greater losses due to the low transmission of the glazing.

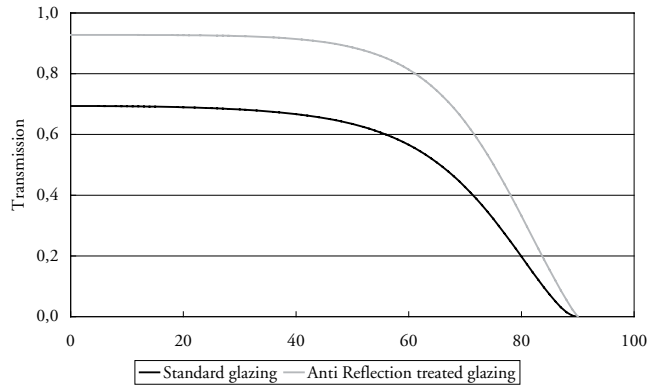


Figure 2.12 Transmission through different types of glazing. Standard double glazing in black and anti reflection treated double glazing in grey.

### 2.5.3 Angular dependence of PV cell

Measurements were performed to determine the angular dependence of a PV cell. Since the experiment is dependent on parallel radiation the inside of the box was painted black to reduce the amount of disturbing reflections. For the same reason the opening on the front of the box is just slightly larger than the PV cell. The PV cell was fastened to a turnable bar and the bar was connected to a potentiometer as can be seen in Figure 2.13. As the bar is turned the potentiometer keeps track of the rotation angle. The PV cell and the potentiometer were connected to a logger for easy measurement.

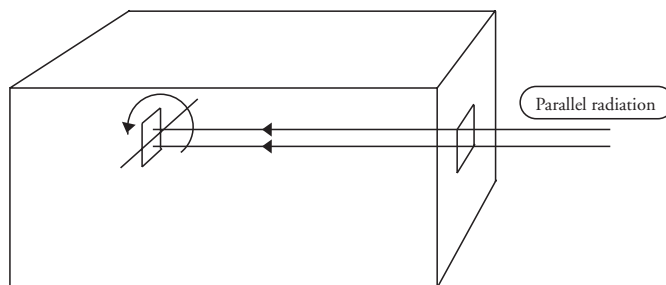


Figure 2.13 Measurement setup to determine the angular dependence of a PV cell. The black painted box reduces the disturbing reflections in the box. The PV cell is located in the centre of the box. The PV cell and a potentiometer are connected to a logger.



The result from the measurements is presented in Figure 2.14. In order to avoid incorporating the cosine dependence, due to the reduction of the projected area, the results were divided by the cosine of the rotated angle. As can be seen in the figure the PV cell has a low angular dependence for angles below 60°. Above 60° the output falls quickly. This result was used for all three solar windows.

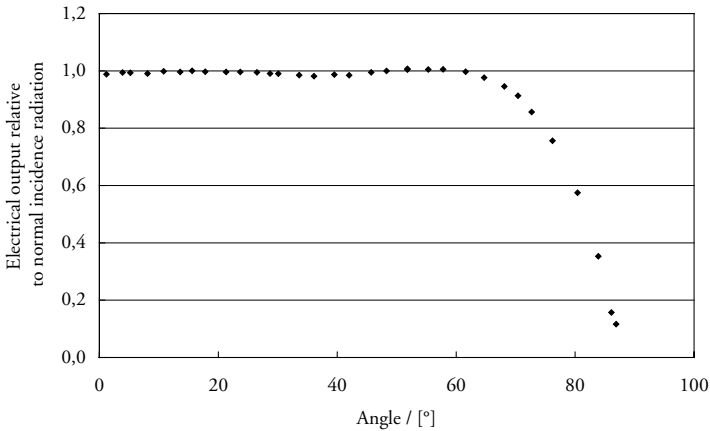
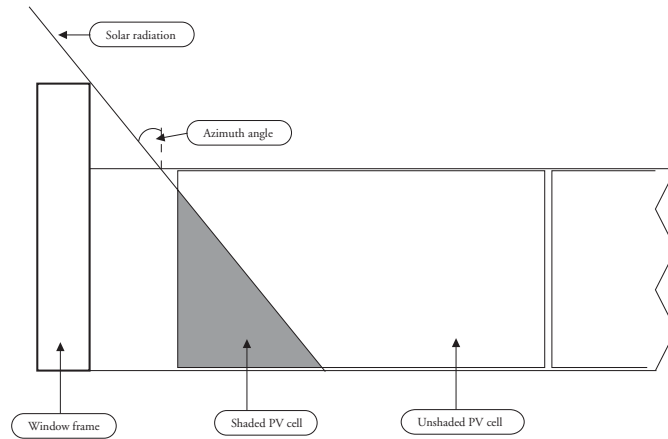


Figure 2.14 Measured angular dependence of a PV cell.

## 2.5.4 Shading

Shading due to large frames is normally not a problem for standard PV modules. The solar window is different since it is located on the inside of a standard window and is thus shaded by the window frames and mouldings. A theoretical calculation was performed to determine the amount of shading as a function of the solar azimuth angle. Since the most shaded cell limits the electrical output only the outer cells were investigated. The problem is also assumed to be symmetric on both sides. Figure 2.15 illustrates the geometry.



*Figure 2.15 The absorber with the PV cells seen from above. Shading of the PV cells due to the window frame. In the illustration about 20% of the cell is shaded.*

As can be seen in Figure 2.16 the PV cells suffer from losses due to shading caused by the window frame from azimuth angles up to about  $-30^\circ$  if the window faces south. During noon the shading is zero. One way of reducing the shading is to increase the space between the frame and the outermost cell. Shading of the full, thermal, absorber is also shown in the figure. It is clear that the shading will have a much smaller influence on the thermal output than on the electrical output. The results from the three different solar windows differ slightly due to different construction of frames and buildings.

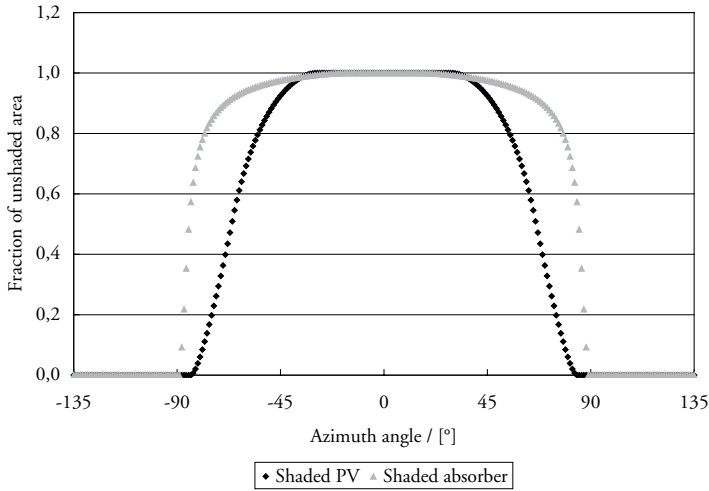


Figure 2.16 Result from a calculation of the unshaded part of the PV cell as a function of the solar azimuth in black and the unshaded part of the full absorber in grey. The results are from the prototype solar window facing south.

### 2.5.5 Reflector contribution

The contribution of energy from the absorbers due to the reflectors is limited by the shading of the frames in the window. Calculating the contribution of the reflectors to the output is one of the most complicated parts of the model. When the projected solar height is  $15^\circ$  all the radiation striking the reflector will be reflected to the focal point, i.e. the front edge of the PV cells. If the projected solar height is larger than  $15^\circ$ , still less than  $60^\circ$ , the reflected radiation will be distributed throughout the absorber as illustrated in Figure 2.17. The figure is from a simulation using Zemax (Zemax). The projected solar height is  $25^\circ$ . As can be seen most of the reflected radiation strikes the absorber between 20 to 30 mm from the front edge. This is normally referred to as the light band. In order to simplify the calculations the centre of reflection was determined. The centre of reflection is defined as the line on the absorber where 50% of the reflected radiation is on either side of the line. In Figure 2.17 the centre of reflection was determined to be 25.9 mm from the front edge. In Figure 2.18 the centre of reflection for different solar heights has been plotted in the same diagram. In the calculations for the contribution from the radiation that goes via the reflector all radiation is assumed to end up on this line.

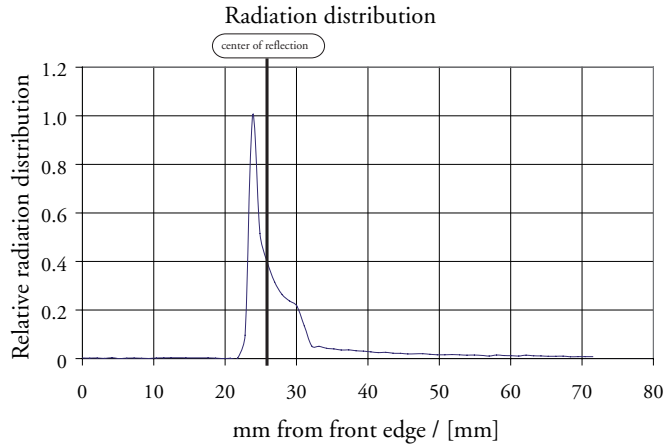


Figure 2.17 The distribution of radiation on the absorber from radiation that was reflected on the reflector from a projected solar height of  $25^\circ$ . The centre of reflection, marked with a black line, is 25.9 mm from the front edge.

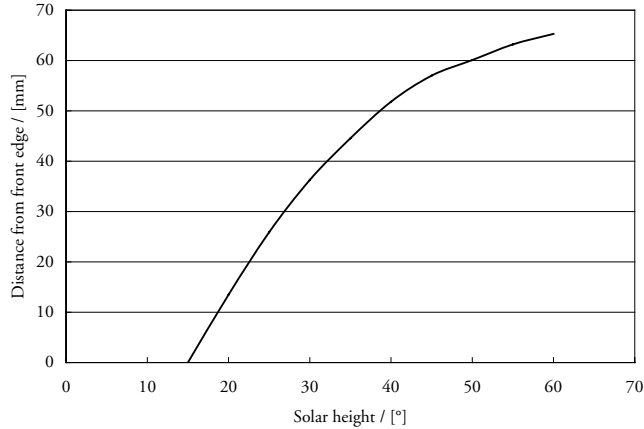


Figure 2.18 The centre of reflection as a function of projected solar height.

When the centre of reflection is known together with the solar angles and the geometry of the window, the points A and B in Figure 2.19 can be determined. A is the point to which the radiation that goes via the lower part of the reflector is reflected. B is the point to which the radiation that

goes via the upper part of the reflector is reflected. It is assumed that the radiation that hits the reflector anywhere between the top and the bottom ends up between A and B and that the increase of radiation from A to B is linear. This means that point B will be fully lit and A will be the starting point of radiation. Figure 2.19 illustrates the solar radiation. Since the increase of radiation from A to B is assumed to be linear the degree of illumination can be calculated for all points on the absorber. The degree of illumination for the total PV cell can be calculated using Eq. 2.8;

$$f_{ref}(\Theta) = \frac{X_2 \cdot \frac{1}{2} + X_3 \cdot 1}{X_1 + X_2 + X_3} \quad \text{Eq. (2.8)}$$

where  $X_1$  is the part of the PV cell where no reflected radiation impinges,  $X_2$  is the distance between A and B and  $X_3$  is the distance of the cell that is fully illuminated.  $f_{ref}(\Theta)$  is the degree of illumination for the total cell. See Figure 2.20 for an explanatory illustration.

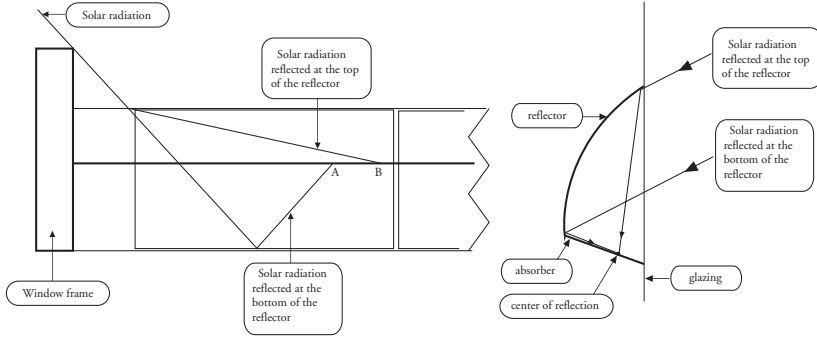


*Figure 2.19 The reflection of solar radiation. Left figure; A is where the radiation reflected from the lower part of the reflector impinges and B is where the radiation reflected from the upper part of the reflector impinges. Right figure; All the radiation reflected along the reflector is assumed to end up on the same line, the centre of reflection.*

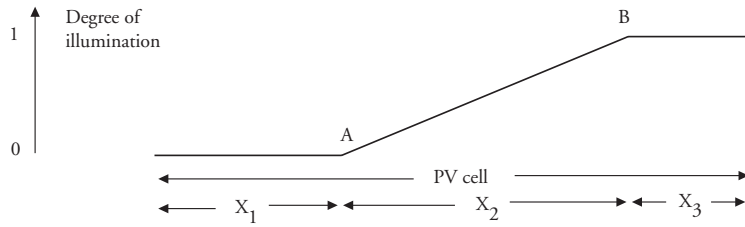


Figure 2.20 The radiation distribution on the PV cell as a function of distance from the edge. A is the point where the radiation reflected from the lower part of the reflector impinges and B is the point where the radiation reflected from the upper part of the reflector impinges.

### 2.5.6 Diffuse radiation

In order to investigate the influence of diffuse radiation on the total electric and thermal output, measured data was analysed. Choosing the cloudiest days and plotting the generated current versus the diffuse radiation generates the results shown in Figure 2.21. The response function in Eq. 2.4 for horizontal reflectors,  $C_1 = 0.002$ , and for vertical reflectors,  $C_2 = 0.0026$ .  $C_1$  and  $C_2$  are the proportionality constants for the relationship between incident radiation and electrical output. The same technique was used to determine the influence of diffuse radiation on the thermal output.

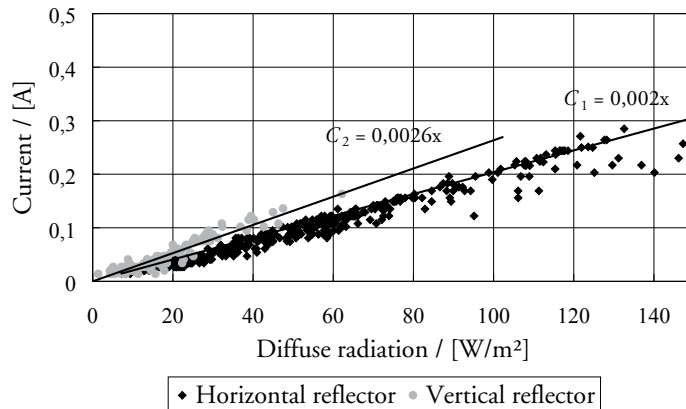
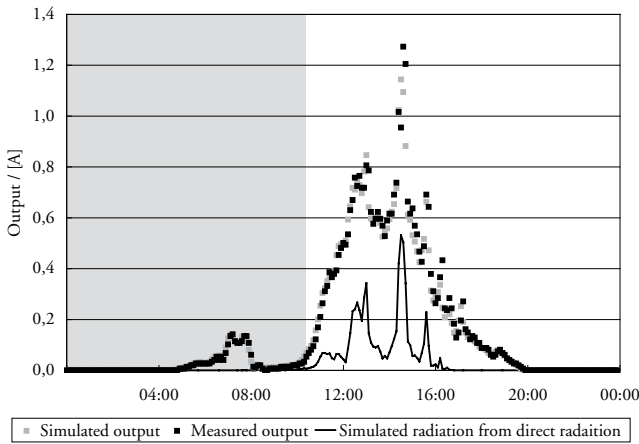


Figure 2.21 The influence of the diffuse radiation on the electrical output. Results using horizontal reflectors are in black and vertical reflectors in grey.

Another way to validate  $C_1$  and  $C_2$ , the response functions for the diffuse radiation, is to plot the simulated and the measured electrical output in the same graph. The influence of the direct radiation is almost zero during the cloudiest days. This is shown in Figure 2.22, also seen in Fig 4.1 section 4. This graph indicates that the electrical output due to the diffuse radiation is modelled in an accurate way. The periods marked with grey in the graph are periods where the direct radiation has little or no influence on the electrical output. The period marked with grey is from a period where the direct radiation plays a small role in the total output. The model is accurate also during period with both direct and diffuse radiation.



*Figure 2.22 Contribution of diffuse radiation to the electrical output. The black dots are the full simulation and the grey dots are from the measurement. The black line is the influence due to the direct radiation. The areas marked with grey are periods with little or no influence due to the direct radiation, and the white area is from a period with a significant contribution from the direct radiation to the electrical output.*

## 2.5.7 Thermal losses

### Prototype solar window

The thermal measurement was performed using three different inlet temperatures, 30°C, 45°C and 60°C, to the collector. Since the pump was running continuously the values from the night could be used to determine the thermal output without impact from the solar radiation. The result can be seen in figure 2.23.

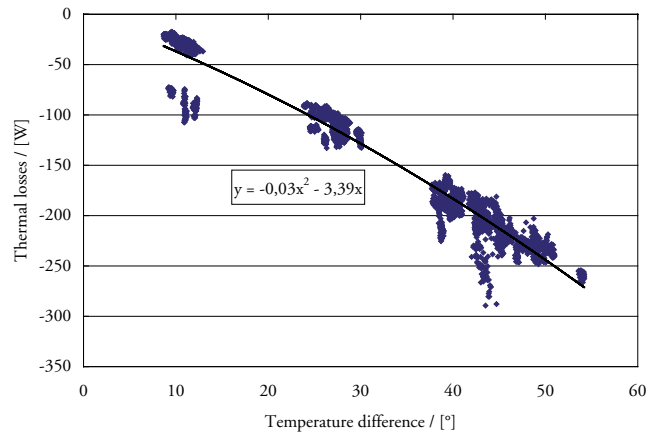


Figure 2.23 Thermal losses from the prototype solar window.

### Solgården solar window

Whether the heat is lost backwards or forwards is insignificant for the performance of the prototype solar window. This will not be the case for the Solgård solar window. If the losses are to the front, i.e. to the surroundings, the energy is lost. If the heat is dissipated backwards, i.e. to the building, the energy is utilized as passive heating in the house. There was no possibility to measure the loss in different directions for the solar window. Instead the U-values of the solar window in the two directions were derived theoretically. Since the total thermal losses from the solar window were measured the calculations of the total losses could be calibrated. The calculations are presented below;

The calculations are divided into four modes: Into the room with open or closed reflectors or out from the window with open or closed reflectors. Figure 2.24 shows the different modes.

### General

When the measurements and the calculations were performed the solar window was not completed. The insulation on the back of the reflector was still to be attached. All the calculations are therefore based on the status of the window at the time of measurement. This is discussed in more detail in section 5.2.3.



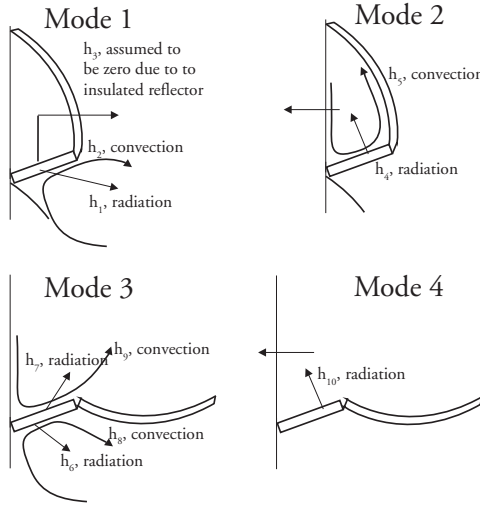


Figure 2.24 Thermal losses from the solar window. Mode 1: Closed reflectors, losses to the room. Mode 2: Closed reflectors, losses to the surroundings. Mode 3: Open reflectors, losses to the room. Mode 4: Open reflectors, losses to the surroundings.

### Assumptions

- General; All the modes use the same convection and radiation heat transfer coefficients
- Mode 1; no losses through the insulated reflector.
- Mode 2; same heat transfer coefficient as in Mode 1.
- Mode 3; all convection ends up in the room. Convection coefficients  $h_8$  and  $h_9$  in Figure 2.24 are of equal size. Half the radiation is radiated towards the glazing and half towards the room.
- Mode 4; no contribution from convection to the surroundings.

The heat radiation losses ( $q$ ) for a body can be calculated using the formula  $q = \epsilon_{eff} \sigma T^4$ , where  $\epsilon_{eff}$  is the effective emissivity and  $q = 5.67 \cdot 10^{-8}$  is the Stefan-Boltzmann constant. The heat loss coefficient due to radiation can be calculated using Eq. 2.9 below, derived from  $q = \epsilon_{eff} \sigma T^4$ .

$$\begin{aligned}
 q &= \varepsilon_{eff} \sigma (T_h^4 - T_c^4) \\
 q &= \varepsilon_{eff} \sigma (T_h^2 + T_c^2)(T_h + T_c)(T_h - T_c) \\
 \Delta T &= (T_h - T_c) \Rightarrow \\
 \Rightarrow h_r &= \frac{q}{\Delta T} = \varepsilon_{eff} \sigma (T_h^2 + T_c^2)(T_h + T_c) \\
 T_m &= \frac{(T_h + T_c)}{2} \Rightarrow \\
 \Rightarrow h_r &= 4\varepsilon\sigma \cdot 4T_m^3
 \end{aligned}
 \tag{Eq. (2.9)}$$

Where  $T_m$  is the mean temperature of the radiator, with temperature  $T_h$ , and the radiated object with temperature  $T_c$ . The losses due to convection,  $h_c$ , can be calculated for the specific mode but a standard value from the Swedish Standards Institute (SIS, 1997) of 3.6 W/m<sup>2</sup>K was used instead. The value is for convections from glass panes. Since the fresh air intake for the ventilation of the building is located directly in front of the solar window this number will increase. In the calculations a value of 4 W/m<sup>2</sup>K was used.

The contribution to the total thermal loss,  $h_{tot}$  from convection and radiation is summed up in Eq. 2.10. In Eq. 2.11 this number is divided by the concentration factor,  $c$ , of the geometry to get the heat transfer coefficient,  $h$ , per glazed area instead of per absorber area.

$$h_{tot} = h_c + h_r \tag{Eq. (2.10)}$$

$$h = \frac{h_{tot}}{c} \tag{Eq. (2.11)}$$

Two of the modes described above are calculated in more detail below.

Mode 1: closed reflectors, heat losses to the room.

Assuming a mean temperature of 300 K (27°C) and  $\varepsilon=0.9$  results in;

$$h = \frac{h_{tot}}{c} = \frac{h_c + h_r}{c} = \frac{4\varepsilon\sigma \cdot 4T_m^3 + h_r}{c} = \frac{5.5 + 4}{2.45} \approx 3.9 \text{ W/m}^2\text{K}$$

Mode 2: closed reflectors, heat losses to the surroundings.

Mode 2 will be used for explaining the calculation technique with a thermal network. The same heat transfer coefficients as in mode 1 are used. The

heated air between the absorber and the glazing will experience a heat transfer coefficient of 4 W/m<sup>2</sup>K going to the glazing i.e. the heat will encounter a resistance of 0.25 m<sup>2</sup>K/W. The resistance is defined as the inverse of the heat transfer coefficient. The full calculation is easier to understand using the analogy of electrical circuits. In Figure 2.25 the total resistance ( $m_{tot}$ ) is calculated using the resistance in the glazing ( $m_g$ ), the resistance from the radiation ( $m_r$ ), the resistance for the convection from the absorber to the air pocket ( $m_{c1}$ ) and the resistance for the heat from the air pocket to the inner glazing ( $m_{c2}$ ). As can be seen in the figure the two convective resistances will be added together, meaning that the energy has to overcome two “difficulties”. The analogy to electrical circuits is that the total resistance R from two resistors R1 and R2 in series is simply  $R = R1 + R2$ . The heat transfer from convection can now be added to the heat transfer from the radiation. The analogy to electrical circuits is that the total resistance for two resistors in parallel is  $R = 1/(1/R1 + 1/R2)$ . This total resistance is added to the heat resistance from the inner glazing to the ambient air, i.e.  $m_g$ . In Figure 2.25 this formula is displayed. The total resistance adds up to 0.5 m<sup>2</sup>K/W; hence the heat transfer coefficient is 2 W/m<sup>2</sup>K.

## Mode 2

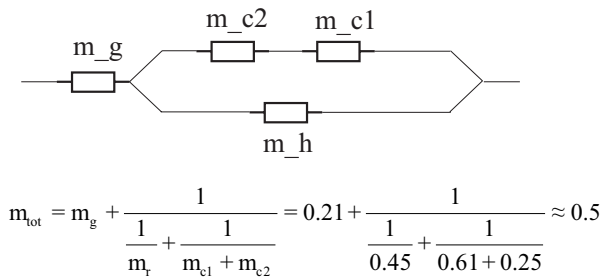


Figure 2.25 The analogy between heat transfer resistance and electrical resistance.  $m_g$  is the resistance in the glazing,  $m_r$  is the resistance for the radiation,  $m_{c1}$  is the resistance for the convection from the absorber to the air and  $m_{c2}$  is the resistance for the convection from the air to the glazing.

Performing the same kind of calculations for mode 3 and mode 4, taking reflection in the glazing into account, results in U-values of 5.9 W/m<sup>2</sup>K and 1.3 W/m<sup>2</sup>K respectively.

Table 2.1 The thermal losses for the solar window.

| U-value / [W/m <sup>2</sup> K], Solar window PV/T Collector |               |     |             |     |
|---|---------------|-----|-------------|-----|
| Closed/open mode  | Closed window |     | Open window |     |
| Direction of thermal loss                                   | In            | Out | In          | Out |
| Standard Window   | 3.9           | 2.0 | 5.9         | 1.3 |

## Discussion

The calculations described above are surrounded with large uncertainties. The complex design of the collector creates air pockets between absorber and reflector, resulting in air movements in the space between reflectors and glazing which give rise to a heat transfer that is difficult to estimate and it offers a wide range of possibilities for the heat to disappear. Apart from this the solar window is located in front of the ventilation exhaust. This also adds uncertainty to the calculation. However, the total thermal losses are included in the validation of the model, see section 4. As can be seen in Figure 4.1, shown later, there is a high correlation between measurements and simulation. This indicates that the U-values, shown in Table 2.1, found in the calculations are reasonable to use. In the calculations the convective heat losses from the solar window, using open reflectors, will end up in the building. This means that the use of the solar window in a building is slightly overestimated.

## 2.5.8 Passive gains

When the reflectors in the solar window are closed no radiation is transmitted into the building. This is both positive and negative for the energy balance. During the summer, this is good since the overheating of the building is limited. During the winter, this might be bad since the free solar energy through the windows contributes to heat the building. Even if the reflectors are open there will still be large losses of passive heating compared to a standard window since the absorbers are blocking parts of the incoming radiation. This is illustrated in Figure 2.26.

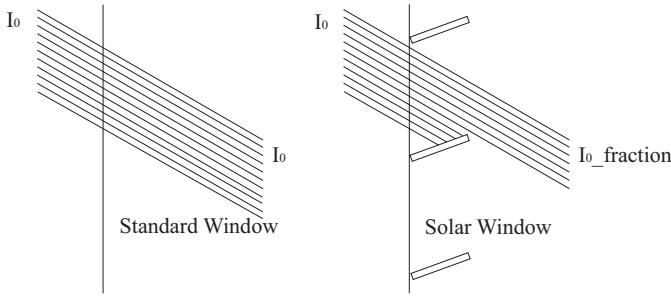


Figure 2.20 Left, transmission through a standard window. Right, transmission through the solar window.

The amount of radiation let into the building varies with solar height. This is shown in Figure 2.27. The figure shows that no radiation from  $60^\circ$  projected solar altitude or above enters the building. This is mostly positive since radiation from these angles only occurs during the summer when no extra heat is wanted in the building. This is also illustrated in Figure 2.28. Figure 2.28 shows Figure 2.27 in numbers. The figure shows the fraction of transmitted radiation compared to the amount of radiation transmitted through the window. For high solar angles almost no radiation is transmitted.

The results of integration of the diffuse radiation over the entire sphere show that about 35% of the diffuse radiation is transmitted into the building. Since there is more radiation from low projected solar heights this will be weighted more than the radiation from the less common high projected solar heights.

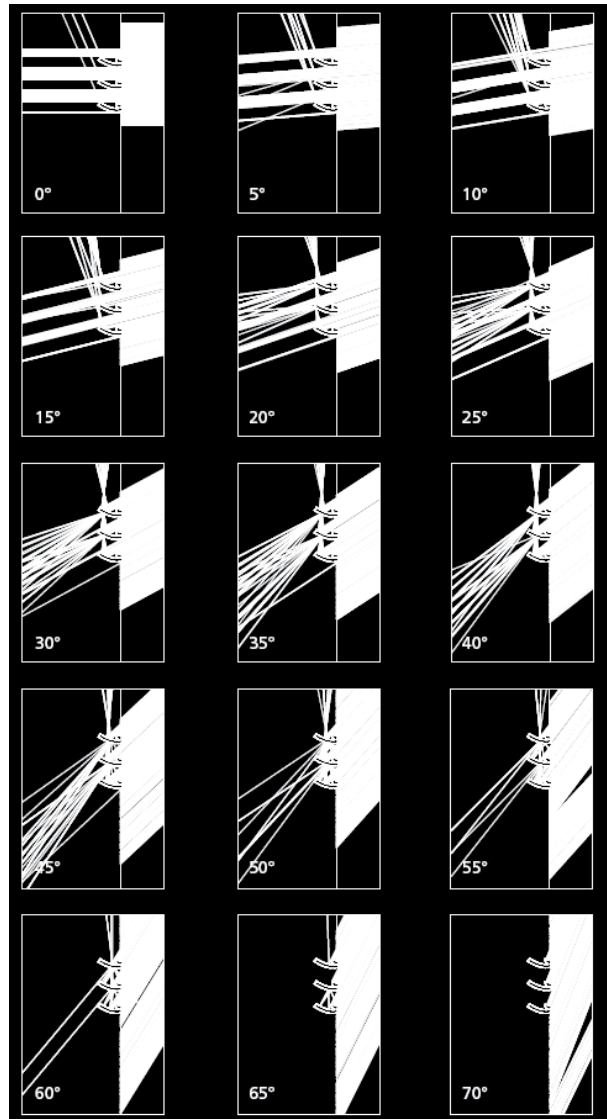


Figure 2.27 *The amount of radiation transmitted into the building as a function of the projected solar height. Drawings by Andreas Fieber.*

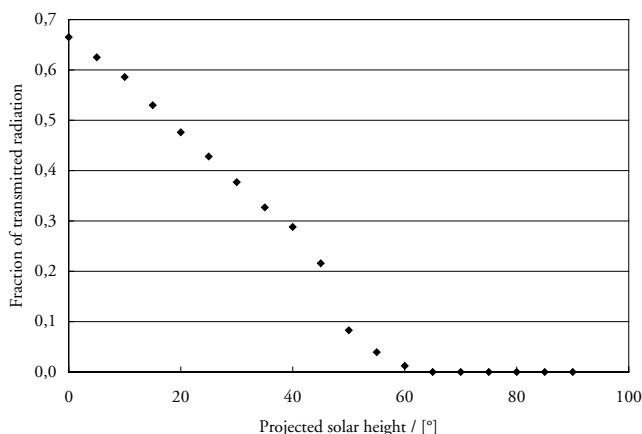


Figure 2.28 The fraction of transmitted solar radiation compared to the total radiation hitting the window. The projected solar height is on the x-axis and the fraction of transmitted radiation on the y-axis.

## 2.5.9 Control strategies

If all energy flows, such as thermal losses, passive heating and energy production, caused by the solar window are known, a decision can be made whether the reflectors are to be closed or open. Different control strategies for opening and closing the reflectors have been evaluated.

The tiltable reflectors in the solar window were controlled using four different monitoring mechanisms. The control strategies are listed below;

1. Always open, horizontal, reflectors.
2. Always closed, vertical, reflectors.
3. The reflectors are open if the solar radiation lies between two user defined values. If the radiation falls below the interval the reflectors close in order to decrease the U-value of the window to prevent the building from cooling down. If the radiation exceeds the interval the reflectors close to avoid overheating of the building.
4. If the temperature in the building falls below a user defined value the window endeavours to heat the building. This means that the model calculates the energy balance for open reflectors and for closed reflectors and then selects the most energetically favourable alternative. If the indoor temperature exceeds the upper user defined value the window tries to minimize the energy admitted into the building. This means

that during periods with overheating the reflectors will typically be closed during daytime to hinder the passive heating and they will typically be open during night time in order to have a large U-value and in this way ventilate the heat out of the building. If the temperature is between the two stated temperatures the window will be closed to fill the batteries and the collector tank to a preset level. When this condition is fulfilled the reflectors will be opened for aesthetic reasons.





### 3 TRNSYS

The thermal performance of a solar thermal collector is dependent on the irradiance to a much higher extent than a PV module. Apart from external factors such as temperature, wind and irradiance, the thermal solar collectors are also highly dependent on the load and the storage capacity of the system. The annual output from a collector will differ strongly between high and low domestic water demands. If the load is high for the system the bottom of the storage tank will be cold due to the fresh water that is let into the tank. If the system has a low water usage the tank will be full of hot water and the inlet temperature to the collector will be high. This will lead to high thermal losses in the collector. The annual output is also dependent on when the water is used. Whether the water is consumed in the morning or in the evening will affect the system since the collector will be working at different temperature levels.

The solar window in Solgården is part of a system. This means that the level of complexity is much higher for the Solgården solar window compared to the prototype solar window. Therefore it is interesting to study the electrical output and the thermal output. During the evaluation of the solar window four people lived in the house, two of them teenagers, which gives a high water demand throughout the year.

To be able to analyse such a complex system as the solar window a flexible simulation tool is required. In this case TRNSYS (2000) was used. TRNSYS (Transient Systems Simulation Program) is a dynamic simulation program frequently used in the field of solar energy. It has been commercially available since 1975. It was first developed by the Solar Energy Laboratory at the University of Wisconsin, USA. Since then the development has continued around the world. One of main advantages of TRNSYS is the open structure allowing new components to be constructed. The new types are relatively easy to implement with the standard components. TRNSYS is used to investigate new energy products such as solar collectors, heat exchangers, PV panels etc. Apart from products, control strategies and system solutions can also be tested. The flexibility is large.

The modern version of the interface known as Simulation Studio is shown in Figure 3.1. The figure shows how types have been linked to a so

called deck. In the figure the deck has been simplified for clarity. Printers and connections have been removed.

Each type has parameters, inputs and outputs. The parameters are fixed throughout the simulation while the inputs are varying. The inputs are either fixed numbers or calculated from other types. The outputs are calculated in the specific types and then sent as inputs to other types, alternatively as outputs to a file.

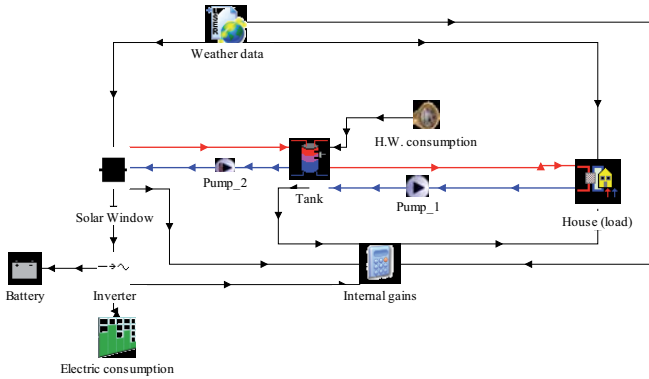


Figure 3.1 The developed TRNSYS deck. The different flows are marked with arrows.

Most of the different types can be found in the standard library in TRNSYS. This is the case for all the types used in this work except for the solar window. Since this is a new product a new type had to be developed. The type, given the name type 760, is written in FORTRAN. It is a direct translation from the Excel program discussed in sections 2.4 to 2.5.8.

The list below shows some of the parameters for the most important types in the TRNSYS deck. All types used in the simulations except the solar window type are standard types from the standard library.

- **Battery/Inverter and load.** A battery bank of 10.6 kWh and a constant electrical load of 375 W throughout the year, i.e. 3285 kWh annually.
- **Tank.** The tank, type 60, is set to have a volume of 620 litres. The hot water consumption was set to 9 litres per hour throughout the year. The type is easy to use since there is a possibility to use two inlets and two outlets, at the same time as there is an internal heat exchanger.

- **Building.** The one zone building, type 12, model is a lumped capacitance degree hour model with internal gain. This simplification equates to a building with an open plan layout, which is the case for Solgård. The building has a UA-value of 110 W/K and a thermal capacitance of 40 000 kJ/K. The UA-value of the building is lowered to 95 W/K for the developed solar window, discussed in section 5.2.3, simulation since the U-value is reduced from 2.43 W/m<sup>2</sup>K to 1.5 W/m<sup>2</sup>K. The UA-value is reduced to 80 W/K for the simulations for system 2 and system 3 since the 16 m<sup>2</sup> large solar window is replaced with a 8 m<sup>2</sup> large standard window.
- **Weather data.** The weather data used for the simulation is derived with meteonorm (Meteonorm 5.0) for Gävle, about 20 km from Älvkarleö. The simulation uses type 109 to process the weather information. Type 109 both reads weather data from a file and calculates the solar radiation for different directions. The solar radiation can be calculated for any surface geometry.
- **Solar window.** A new TRNSYS component, the solar window, was constructed (Davidsson, Perers and Karlsson, 2010).
- **PV and solar collector.** Separate PV and solar collectors were used to model the solar energy system in system 3, discussed in section 5.2.3. They are simplified first order models taking into account solar beam and diffuse radiation, incidence angle, inlet and ambient temperature with  $\eta_{direct} = 0.75$ ,  $\eta_{diffuse} = 0.68$  and with a U-value of 4 W/m<sup>2</sup>K.
- **Internal gain.** The thermal losses from the storage tank, the used electricity, the heat produced by the people in the house and the radiation let into the building through the windows are added as internal gains for the building.

The types in TRNSYS are calculated in subroutines of the main program. All types are calculated separately and in sequential order. Quite often the components are dependent on each other. For instance the output of a solar collector is dependent on the temperature of the storage tank and the temperature of the storage tank is dependent on the output from the collector. This is solved by iteration in TRNSYS. The iteration continues until a predefined tolerance limit value is reached. If the loop for some reason does not converge the last calculated value is used and a warning is printed to a file. After a user defined number of warnings the simulation is terminated and action has to be taken to solve the problem. Typically this can be to decrease the time step. The time step is the length of each calculation step. A short time step means that the outputs are calculated

often. Normally this results in longer computational time but a more stable simulation.

If they are used correctly, simulation programs can be powerful tools. However, they are also risky. If the program is not used correctly the output might be completely wrong. Often the biggest mistakes are corrected since the output is unreasonable. Smaller mistakes are more difficult to find. They can be anything from mistakes with units to misplaced connections. Therefore it is important to critically analyse the results.

This is of course a problem that has to be minimized. There are a couple of things that can be done to prevent this problem. The most common way to find mistakes is to connect all the outputs to online printers. The online printers print the calculated values on the screen as the calculation is in progress. This enables the user to quickly check if there is something wrong with the simulation. Other actions that can be taken are to set up ideal situations. Running simulations with no thermal losses in the collector, no thermal losses in the building or no hot water use can produce simple checks for the user. Also annual checks can be made. Adding all the energy flows to and from the storage tank including the thermal losses must add up to the energy stored in the tank.

## The program, type760

In TRNSYS there is a program that generates the structure of the code for a new type. The program generates for instance the parameters, inputs and outputs. Since more or less the entire structure is generated the programmer is left to fill in the mathematical equations describing the type.

Since the solar window is a new product there was no type available to use. The solar window type, given the name 760, is constructed as a translation from the developed excel sheet used to evaluate the prototype solar window. Type 760 has the option to choose control strategy for the reflectors as discussed in section 2.5.9.

Before the actual calculation starts in the program four matrices are read from files that describe the reflectors. These matrices describe the impact that the reflectors have on both the thermal and the electrical output from the solar window. Two of the matrices are for the thermal calculations and the other two for the electrical calculations. The matrices describe the radiation on the absorber due to the reflector during 11 different days of the year. Each day is divided into 240 points, i.e. every six minutes. Other days are extrapolated from the existing data. Following this the program calculates all the different limiting factors described in Eq. (2.2-2.5) in the section 2.4. The different limiting factors are described with a polynomial of the 6:th degree. Using a polynomial has no physical meaning but makes

the calculations easy and fast. After this,  $P_{dir}$ ,  $P_{refl}$ ,  $P_{diff}$  and hence  $P_{tot}$  are calculated, see section 2.4. The thermal calculations are carried out in the same way. The only difference is the iteration performed to calculate the temperature of the absorber. Also the passive gains from the window are calculated. This calculation is performed for two cases, open or closed reflectors. If the reflectors are open the passive gains are calculated to be,

$$P_g = P_D + P_d + P_t$$

Where  $P_g$  is the total passive gains,  $P_D$  is the passive gains due to direct radiation that goes between the absorbers,  $P_d$  is the passive gains due to diffuse radiation that goes between the absorbers and  $P_t$  is the thermal losses from the absorbers that is lost to the room. In the case of closed reflectors  $P_D$  and  $P_d$  will be zero and  $P_t$  will decrease compared to open reflectors. See Figure 3.2 for an explanatory sketch. The effects of lowering the U-value of the building when the window is closed are added separately outside the type 760. This is possible since one of the outputs from type 760 is whether the reflectors are open or closed.

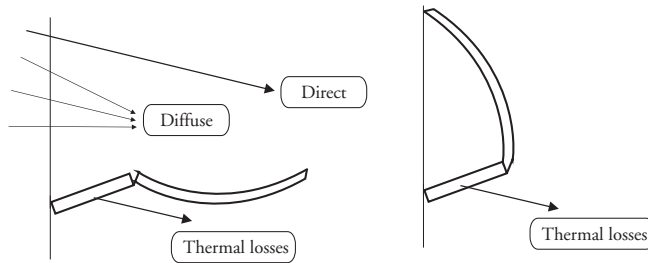


Figure 3.2 *Passive gains to the building. Left; open reflectors allow radiation to enter the room. Right; closed reflectors block radiation from entering the room.*

The last step in the program is to decide if the reflectors are to be open or closed. The annual auxiliary energy need for a building including a solar window using control strategies 1 and 2, see section 2.5.9, is simple to calculate since the reflectors are always open or always closed by definition. The annual auxiliary energy need using control strategy 3 is also simple to calculate since the reflectors are to be open if the radiation is in the interval stated in the parameter list for the type. Control strategy 4 is however more complicated. This control strategy requires that the total energy balance is calculated for open and for closed reflectors. The best option is then chosen. If the temperature in the building is below the lower control

parameter the reflectors will be used to maximize the energy flow into the building. If the temperature is above the higher parameter the opposite will happen, i.e. the reflectors will maximize the energy flow out of the building. If the temperature is between the parameters the reflectors will be closed to maximize the energy production in the solar window. The energy balance is shown in Figure 3.3. If the reflectors are closed instead of open the U-value of the building is lowered, less radiation is admitted into the building and the thermal energy production is high in the absorbers. Summing up all contributions and comparing them to each other lets strategy 4 decide whether or not to open the reflectors.

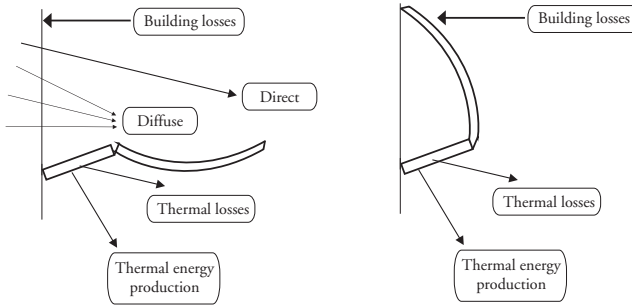
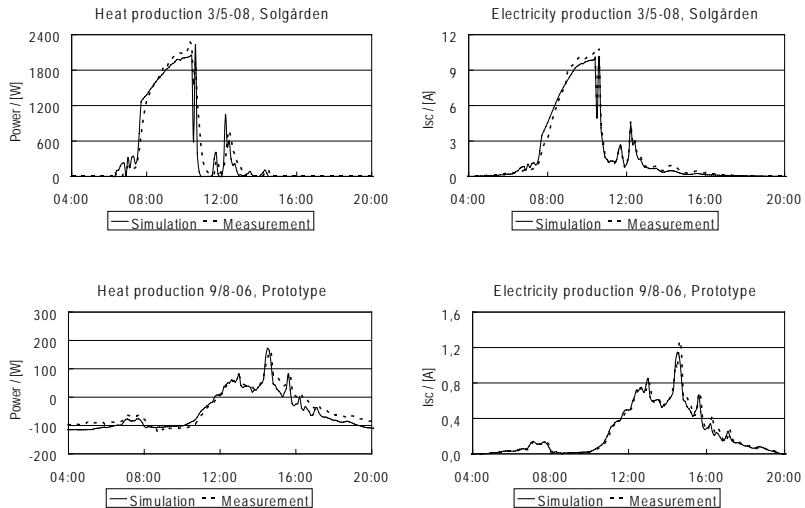


Figure 3.3 The two different situations for the thermal balance calculations. The most energetically favourable is chosen by control strategy 4.

## 4 Evaluation

The results from the simulation model were validated against measured data. This was performed in two different ways. The first way was plotting the measured daily output in the same graph as the simulated output. This was performed for both electrical and thermal output. Figure 4.1 shows the electrical and the thermal output validation for both the prototype solar window and the Solgård solar window. The days were chosen to illustrate different weather conditions and different parts of the year. The correlation is high for all four graphs.



*Figure 4.1 Validation of the simulation model. The upper graphs are from the Solgård solar window and the lower graphs are from the prototype solar window. The graphs on the left side are for thermal output validation and the graphs on the right are for electrical validation.*

In Figure 4.2 the simulated electrical output from the prototype solar window is shown in the same graph as the measured values for two differ-



ent days. The simulated output with the reflectors in a passive, horizontal, position and the radiation has also been plotted in the same graph. The area under the output graph is the daily electrical output. It is apparent that the reflector has greater impact during days with low projected solar height, e.g. winter days for the northern hemisphere. For the 12/9, left graph, the reflector accounts for 30% of the total output while it accounts for about 50% of the total output for the 3/11, right graph. However if the projected solar height drops below the critical angle of  $15^\circ$  the reflector will not contribute to the output. The radiation will be reflected out of the construction.

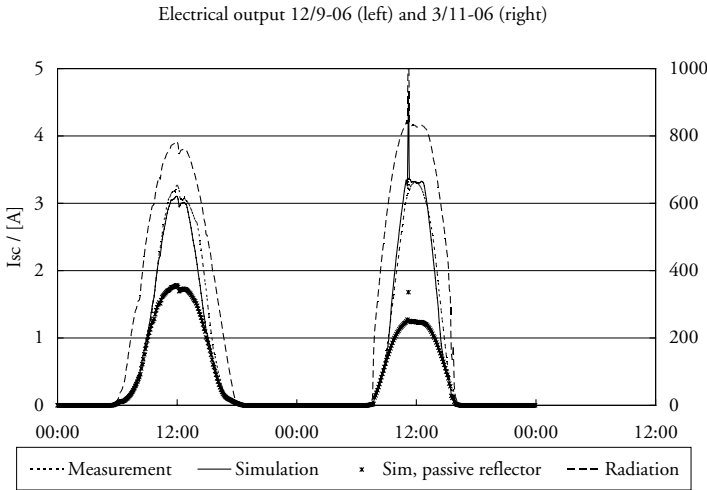


*Figure 4.2 Measured and simulated electrical output from the solar window. The dashed line for the radiation uses the right y-axis. The peak during 3/11 is due to a reflection.*

Two different loggers were used for the measurement of the prototype solar window. One logger was used to register the electrical measurements and one logger to register the thermal measurements and the radiation on the wall. During cloudy weather with sunny intervals the problem of synchronisation could arise since the two loggers were not perfectly synchronised. This means that if the electricity was measured during a cloudless moment and the radiation was measured during cloudy conditions there will be a very poor correlation between measurement and simulation. To overcome this problem the output from the window was integrated day by day. Then this irregularity will even out. The result from this validation is shown in Figure 4.3. The simulated values are plotted on the x-axis

and the measured values on the  $y$ -axis. A perfect fit between simulation and experiment would place all the dots on the line  $x=y$ . The left figure is the validation for the thermal model and the right figure is the validation for the electrical model. The black dots are from the Solgården window and the white dots are from the prototype solar window. The correlation between measurement and simulation is high for all cases.

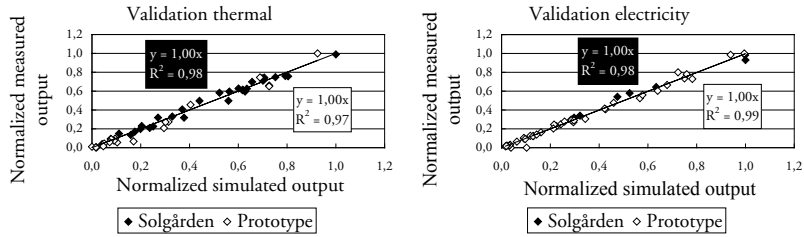


Figure 4.3 Validation of the thermal, left figure, and the electrical, right figure, simulation. The black dots are from the Solgården solar window and the white dots are from the prototype solar window. The simulated output is on the  $x$ -axis and the measured output on the  $y$ -axis.



## 5 Results

All the simulations from the prototype solar window are on a component level. The results are obtained from the developed Excel sheet. The results from the Solgården solar window are on a system level. All the results are from the developed TRNSYS-deck. The results from the Augustenborg solar window are also on system level.

### 5.1 Prototype solar window

At the Division of Energy and Building Design at Lund University, long term weather measurements are recorded. Using data from this station allows annual simulations for electrical output from the solar window to be performed. Data from one full year without interruptions could however not be found. Days ruined by logger problems e.g. frost on the pyranometer or misplaced diffuse ring were all removed. In the end 46 full weeks were left. The removed weeks were fairly evenly distributed over the year.

A simulation for the prototype solar window can be seen in Figure 5.1. In this figure the total annual output from the solar window has been plotted together with simulations for two different flat PV-modules. The PV-modules, placed at  $20^\circ$  on a roof and at  $90^\circ$  on a wall, have the same efficiencies and areas as the string module in the solar window, but the PV-modules have no reflectors, are unshaded and they use single glazing instead of the double glazing as in the solar window. The black part of the diagrams is electricity generated caused by the radiation that impinges directly on the PV cell. The white part is electricity generated by direct radiation that goes via the reflector. The light grey part is electricity from diffuse radiation and the dark grey part is electricity from the diffuse radiation that goes via the reflector. As can be seen in the figure the electricity from the diffuse radiation is heavily suppressed in the solar window. This is mostly due to the vertical position and also to the double glazing of the solar window. The increase of electricity from the direct radiation for the roof module compared to the solar window, not including the reflector, is due to more preferable solar angles and the single glazing. Also part of

the radiation that comes from behind the building can be utilized by the roof mounted module. This is not possible for the solar window. The total output is 35% larger for the solar window than for a flat solar module placed vertically on a wall. However the roof mounted collector produces 17% more than the solar window. All figures have been normalized to the total output from the solar window. The model assumes isotropic diffuse radiation.

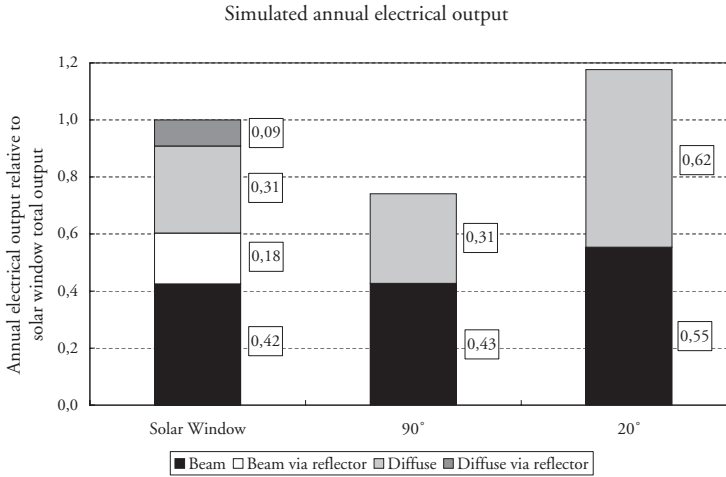


*Figure 5.1 The annual electrical output from the prototype solar window and from two flat PV-modules on a wall at 90° tilt and on a roof at 20° tilt. The black part is electricity generated by the beam radiation that strikes the absorber directly. The white part is the electricity generated by beam radiation via the reflector. The light grey part is electricity from the diffuse radiation which directly impinges on the absorber and the dark grey part is the electricity generated by the diffuse radiation via the reflector. All results have been normalized to the total annual output from the solar window.*

## Limiting effects

Different simulations, omitting angular dependence and shading effects in  $\alpha_{pv}(\theta_2)$ ,  $f_{shading}(\theta_3)$ ,  $T_{glass}(\theta_1)$  of the equations Eq 2.2 - Eq 2.3, were performed to investigate the potential of developing the solar window. This is obtained by setting these parameters to unity. The results are shown in Figure 5.2. Even if the angular dependence of the PV cell could be removed the annual output would only increase by about 1%. Angular dependence of PV cells is apparent only for large solar angles and large angles are already heavily shaded and affected by the low transmission in

the glazing. Thus, removing the angular dependence of the PV cell will have only small effects. If the shading could be removed the annual output would increase by almost 20%. Shading of the PV cells is most apparent at the edges. If the shading is large it might be better to remove one of the cells and in this way have a larger space between the outer cell and the frame of the window. If the anti reflection treated double glazing could be removed completely the annual output would increase by 23%.

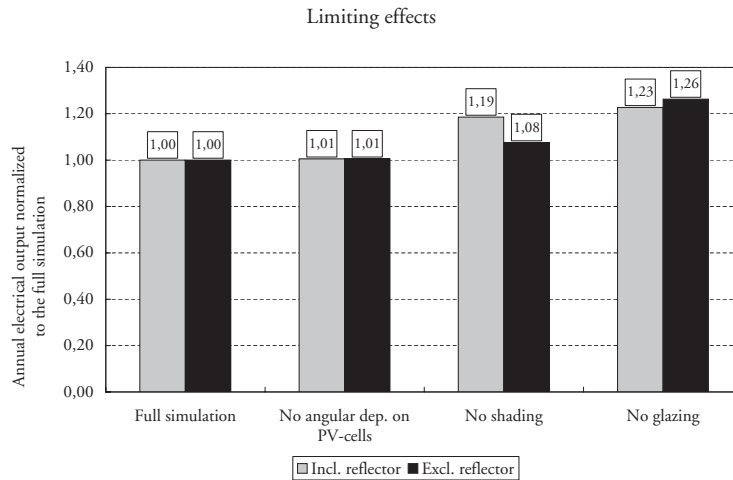


*Figure 5.2 Different limiting factors affecting the solar window. The two bars to the left correspond to the original simulation. For the second pair the angular dependence of the PV cells has been removed. For the third pair all shading effects have been removed and for the last pair the transmission losses due to the glazing have been removed. The black bars correspond to simulations performed without the influence of the reflector and the grey ones include the reflector contribution.*

No thermal simulations were performed for the prototype solar window. The reason is that the thermal output is strongly dependent on the overall system design. The size of the storage tank, the load profile of hot water use and the surrounding temperature are very important parameters for the solar window. To be able to perform such simulations a more advanced simulation program has to be used. TRNSYS, described in section 3, was chosen as a simulation program suitable for solving simulation tasks for the solar window.

## 5.2 Results Solgården solar window

### 5.2.1 Electrical Results Solgården

Depending on how the reflectors are controlled the electrical energy output will vary. In Figure 5.3 four different curves are shown. The black curve is the electrical energy output per month for control strategy 1, the white curve is for strategy 2. The broken line is for control strategy 3 with the control lower parameter set to 100 and the upper parameter set to 400. This will be denoted lower/upper parameters in the following. The dashed line is for control strategy 4 with control parameters 22/26. Obviously the second strategy produces the most electrical energy since this strategy has constantly closed reflectors that maximize the output. The maximum production, strategy 2, produces 435 kWh of electrical energy per year. The total cell area is 4 m<sup>2</sup> and the efficiency is about 10% for the cells. During the most productive month, i.e. May, the average electrical production is 2 kWh per day. Since the daily energy use is about 9 kWh there is no risk of saturating the battery bank. This would otherwise result in a loss of electrical output since the electric system does not register grid delivery.

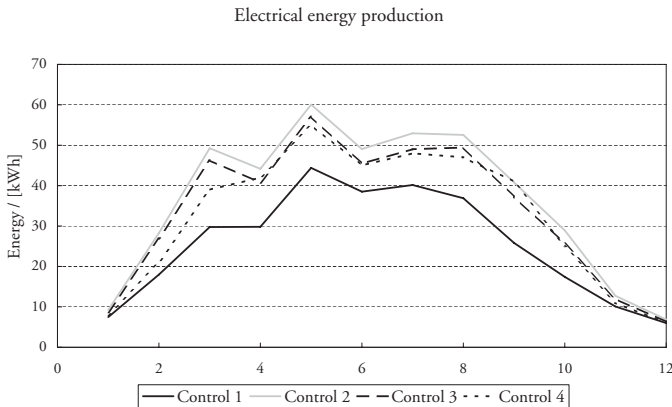


*Figure 5.3 The electrical output during one year. The black curve is for control strategy 1, the white curve is for control strategy 2, the broken curve is for control strategy 3 and the dashed curve is for control strategy 4. The y-axis is the produced energy in kWh.*

### 5.2.2 Thermal Results.

The results from the thermal simulations in Solgården are much more complex than the electrical simulation. The thermal output from the solar window is a function of the indoor temperature which is a function of the thermal losses from the window etc. The main goal can not only be to maximize the energy performance of the building, the comfort demand for the people living in the building has to be taken into account. One such example is control strategy 4 that opens the reflectors to cool the building at night time. This is not optimized from an energy point of view since it would be better to overheat the building to maximum temperatures in order to save future heating costs. This is of course not a strategy that the inhabitants would allow. The consequences of using strategy 3 or strategy 4 were therefore analysed in more detail. In Figure 5.4 the control strategy 3 is analysed. As can be seen, the best control strategy is to use  $100 \text{ W/m}^2$  as the low parameter. The high parameter is from an energy point of view chosen wisely in the range  $600\text{-}800 \text{ W/m}^2$ . The results show that the solar window is optimized for low energy consumption if the reflectors are tilted backwards to allow for passive heating. This is understood since it is more energetically favourable to heat the building passively compared to heating it actively through the absorber and the underfloor heating system. The same analysis for the control strategy 4 is shown in Figure 5.5. In this graph it can be seen that the optimized control parameters are  $26^\circ\text{C}$  for the lower parameter and  $30^\circ\text{C}$  for the upper parameter. Since the upper parameter is used only to lower the temperature in the building, i.e. to lower the energy content, it is always better to have an infinitely large upper parameter. The situation is more complicated for the lower parameter. If the lower parameter is low this means that less energy is stored in the building from day to day since the reflectors will close to maximize the energy production in the absorbers. If the lower parameter is set to a high value the situation will be the opposite. Large amounts of energy will be stored in the building from day to day but the energy production in the absorbers will be down prioritized. Which scenario to choose is difficult, or even impossible, to answer without simulations. In Figure 5.5 it can be seen that if the upper parameter is fixed to  $30^\circ\text{C}$  the optimum low parameter from an energy point of view is  $26^\circ\text{C}$ . Both  $24^\circ\text{C}$  and  $28^\circ\text{C}$  will result in higher energy need.



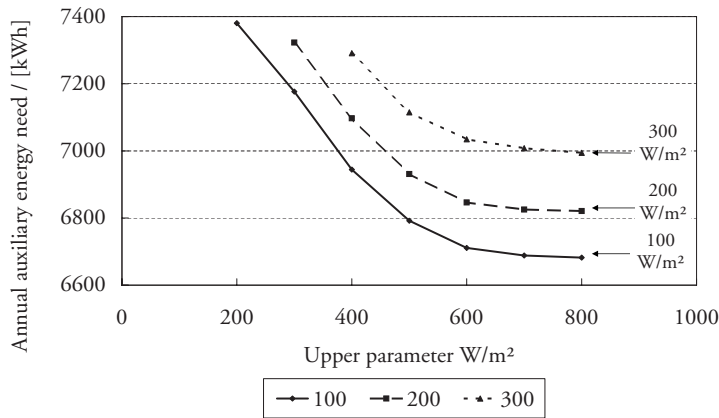


Figure 5.4 The auxiliary energy need for Solgården with a solar window using control strategy 3. The black graph is with the lower parameter at 100  $W/m^2$ . The dashed line is 200  $W/m^2$  and the broken line is 300  $W/m^2$ . The upper control parameter is on the x-axis and the annual auxiliary energy need on the y-axis.

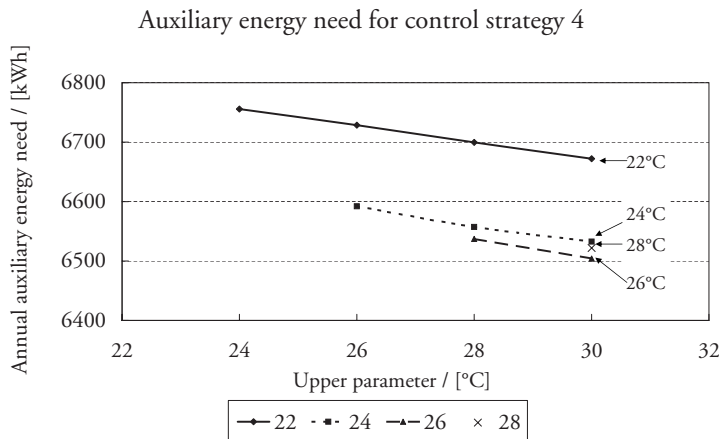
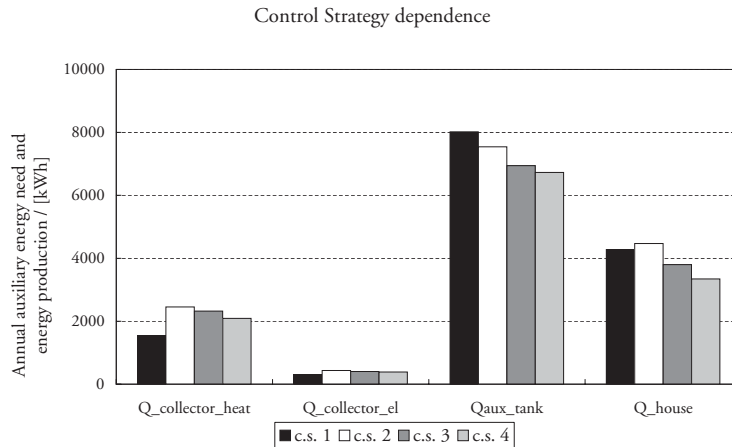


Figure 5.5 The auxiliary energy need for Solgården with a solar window using control strategy 4. The black graph is with the lower parameter at 22  $^{\circ}C$ . The dashed line is 24  $^{\circ}C$ , the broken line is 26  $^{\circ}C$  and the star is for 28  $^{\circ}C$ . The x-axis is the upper control parameter and the y-axis is the annual auxiliary energy need.

In Figure 5.6 it can be seen that control strategy 2 produces the most thermal and electrical energy. This is however not the control strategy that minimizes the auxiliary energy need. As can be seen in Figure 5.6; using control strategy 3 with parameters 100/400 or control strategy 4 with parameters 22/26 results in a lower auxiliary energy need. The reason for this is that no passive heating is utilized if the reflectors are constantly closed.



*Figure 5.6 The annual energy production and need. The thermal and the electrical energy production, the auxiliary energy need and the space heating need for one full year are on the x-axis. Control strategy 1 is in black, the 2: nd in white, the 3: rd in dark grey and 4: th control strategy in light grey. The energy production and need are on the y-axis.*

Which control strategy to choose is however a more complicated question. In Table 5.1 the control strategies and control parameters are listed. The most interesting parts of the table have been marked with a grey background. As stated before, control strategy 2 produces the most thermal and electrical energy. However, it will result in a large auxiliary energy need since it fails to utilize passive heating of the building. Instead control strategy 4 turns out to be the best solution from an energy point of view. Control strategy 4 is also the best way to control the reflectors to avoid overheating of the building. Using control strategy 3 with the parameters 100/800 will result in about the same auxiliary energy need as using control strategy 4 with parameters 22/26. However, the building is overheated almost twice as often with control strategy 3.

Table 5.1 Parameter study of different control strategies for the reflectors. The parameter row shows what values were used for lower and upper parameters for the control strategy. Control strategy 1 & 2 have no parameters. Overheated building is the percentage of the year with temperature above 30° C. The most optimized control strategies and parameters are marked with grey background.

|                             | Control 1 | Control 2 | Control 3 |         | Control 4 |       |
|-----------------------------|-----------|-----------|-----------|---------|-----------|-------|
| Parameters                  | X         | X         | 100/400   | 100/800 | 22/26     | 26/30 |
| Auxiliary energy need / kWh | 8000      | 7500      | 6900      | 6700    | 6700      | 6500  |
| Produced ther. energy / kWh | 1500      | 2500      | 2300      | 1700    | 2100      | 2000  |
| Produced el. energy / kWh   | 300       | 430       | 400       | 330     | 390       | 370   |
| Over heated building / %    | 27        | 23        | 27        | 33      | 18        | 20    |

### 5.2.3 Development

To maximize the output from the solar window the glazing was anti reflection treated. For the same reason no low-e coating was put on the glazing since this coating decreases the solar transmittance. This results in a window with high solar transmittance and a high U-value. In order to investigate the potential of improving the solar window a new simulation was performed with a developed solar window with a low-e coated glazing and insulation on the back of the absorbers. Apart from the low-e coating the developed solar window was also insulated better on the back of the absorbers. The consequences of these improvements are shown in Table 5.2. The drastic decrease in the thermal losses to the inside is due to increased insulation on the back. The table shows thermal losses from the absorbers in both directions, in and out of the building, for the standard and the developed solar window with both open and closed reflectors. The transmission through the low-e coated glazing is assumed to decrease by 20% compared to the solar window glazing. The U-values for the construction are lowered to 0.6 W/m<sup>2</sup>K for closed reflectors and 1.5 W/m<sup>2</sup>K for the open reflectors. The values for the developed solar window are estimates and it is questionable if a window with these parameters can be constructed.

Table 5.2 Thermal losses from the absorbers for the open and closed solar window towards the inside and the outside for both the standard and the developed solar window. The solar transmission relative to the standard solar window and the U-values for the thermal losses through the solar window.

| Thermal losses / [ $\text{W}/\text{m}^2\text{K}$ ], Solar window<br>PV/T Collector |               |     |             |     |                                      |                   |                 |
|--|---------------|-----|-------------|-----|--------------------------------------|-------------------|-----------------|
| Closed/open mode   | Closed window |     | Open window |     | Transmission rel.<br>to Solar Window | U-value<br>Closed | U-value<br>Open |
| Direction of thermal<br>loss dissipated from<br>the absorber                       | In            | Out | In          | Out |                                      |                   |                 |
| Standard Window  | 3.9           | 2.0 | 5.8         | 1.3 | 1.0                                  | 1.3               | 2.43            |
| Developed Window   | 0.7           | 1.3 | 3.5         | 0.7 | 0.8                                  | 0.6               | 1.5             |

The solar window was also compared to a reference case where the  $16 \text{ m}^2$  solar window was replaced by an  $8 \text{ m}^2$  large standard window with U-value  $1.1 \text{ W}/\text{m}^2\text{K}$ . This reference case was also equipped with a solar collector and a PV-module of the same size as the solar window constituents. The different systems are shown in Figure 5.7. System 1 is the solar window. The standard and the developed case look the same. System 2 is the reference case without a solar collector installed on the roof. System 3 is the reference system with a solar energy system on the roof. The solar energy system in system 3 is tilted  $20^\circ$  from the horizontal, as is the roof at Solgård. The reference cases will be labelled system 2 and system 3.

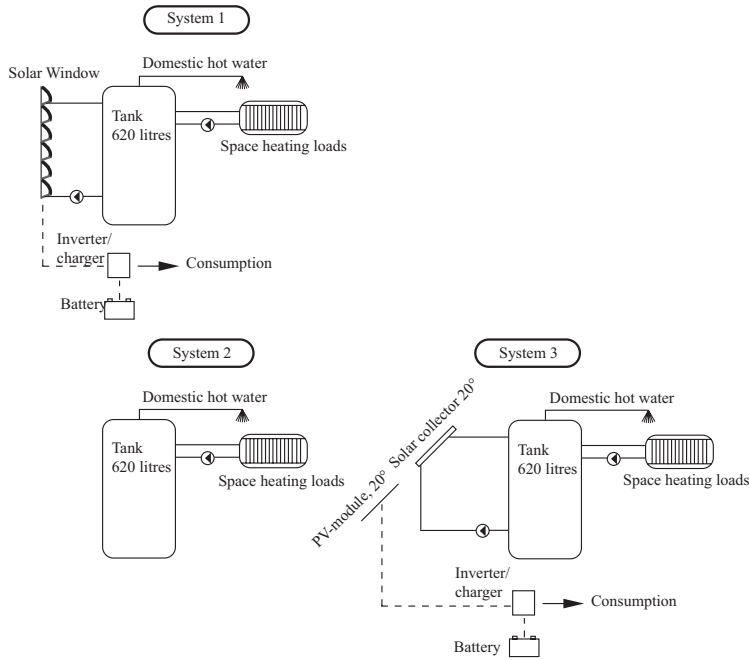
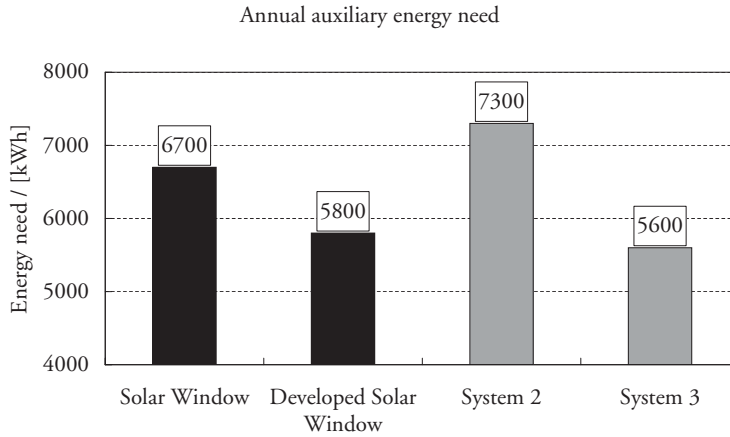


Figure 5.7 System 1 is the solar window. System 2 is the reference case and system 3 is the reference case including a solar energy system.

Figure 5.8 shows that it is more important to minimize the thermal losses through the solar window than to maximize the thermal output from the collector part. The developed solar window performs better than the standard solar window. This difference is significant. The standard solar window alternative needs about 600 kWh less energy per year than system 2. However the standard solar window performs worse than system 3. The reason for this is the increased UA-value of the building with the solar window. A building equipped with a developed solar window requires about the same amount of auxiliary energy as a building equipped with system 3. This analysis is performed with no regard to electric energy production.



*Figure 5.8 The first bar is the solar window using control strategy 4 with parameters 22/26. The second bar is the developed solar window using the same strategy. The third bar is system 2 and the fourth bar is system 3.*

Due to the vertical placement of the solar window the annual distribution of produced thermal and electrical energy is fairly uniform, i.e. there is no sharp peak during the summer. This means that it is possible to install a larger solar window to utilize the solar energy more. The simulation performed to investigate this uses a solar window 50% larger than the standard window. For comparison system 3 was also increased by 50%. The results from these simulations are shown in Figure 5.9. The solar window uses control strategy 4 with parameters 22/26. As can be seen the auxiliary thermal energy need increases instead of decreases. This is due to the larger window and thus larger thermal losses from the building. The increase in thermal losses from the building is greater than the increase in thermal energy production in the solar window. Hence, the energy consumption is larger with a large solar window. For system 3 the situation is different. Increasing the collector area has no negative feedbacks. A large part of the increased thermal energy production is utilized by the building. Hence, the energy use is lower if the collector area is larger.

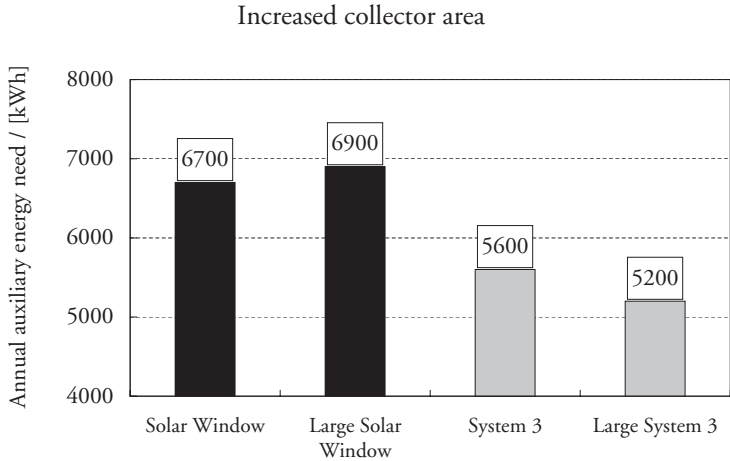


Figure 5.9 *Annual auxiliary energy need for the solar window of standard size and increased by 50% and system 3 including a solar energy system of standard size and system 3 with the solar energy system increased by 50%.*

### 5.3 Augustenborg

The solar window at Augustenborg in Malmö differs from the other solar windows in several respects. The window is facing approximately 40° to west. The reflectors behind the absorbers are not insulated, nor is the glazing in front of the absorbers anti reflection treated. The solar window connected to a storage tank is used to preheat the incoming water before it is heated. In this way the water temperature in the system can be kept low. This is also one of the reasons why the reflectors are not insulated. The simulations for the solar window in Augustenborg were performed using the Solgård solar window TRNSYS deck. However there are some differences. The water consumption and the temperature of the water flowing into the tank were set to values that resulted in a temperature profile of the water entering the collector that was in agreement with the measurements performed at Augustenborg.

## Results

The results presented for the Augustenborg solar window with closed reflectors are for the full year. The results from the simulations show that a flat PV module placed at 20 degrees with an azimuth of  $37^\circ$  to west will produce about 50% more electrical energy than the solar window. The main reason is the effects from the glazing. Since the existing window has standard glazing without anti reflection treatment, the transmission losses will be large. The orientation of the solar window also affects the annual output. At 11.30 at the end of July, half of the outermost cell is still shaded from the sun by the window frame. The cell is partly shaded until after 12.00. This shading is most apparent for the electrical output since the output is limited by the most shaded cell; which is not the case for the thermal output.

The electrical output for the Augustenborg solar window was simulated to be about 110 kWh. The thermal output was calculated to be about 700 kWh annually.

Figure 5.10 shows the electrical output from the solar window during 40 consecutive days. The left side of the graph, in white, is with the reflectors in a closed position and the right side, in grey, is with the reflectors in an open position.

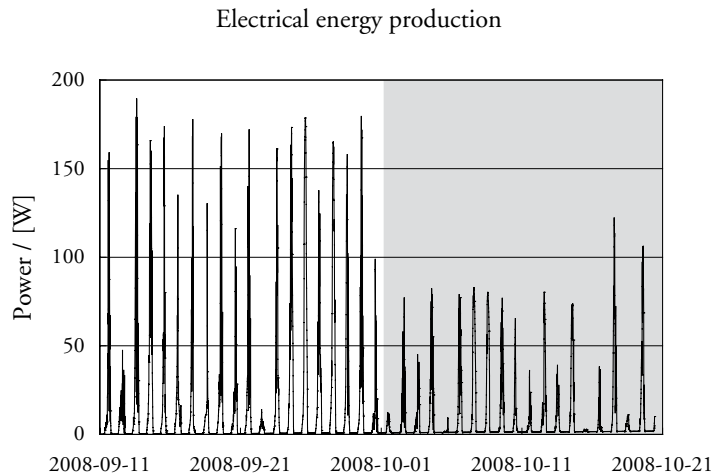


*Figure 5.10 Electrical output from the solar window in Augustenborg. The white part is with active reflectors and the grey part is with passive reflectors.*





## 6 Conclusions

The solar window was developed to lower the total investment cost of a solar energy system. Apart from the energy perspective the solar window also works as a sunshade and directs the daylight to the back of the room. Daylighting and aesthetics are however not investigated in this work. This was covered by Andreas Fieber in his licentiate thesis (Fieber, 2005). This work aims to investigate the energetic consequences of the solar window both on a component level and on a system level.

In the end it would have been nice to answer the question; is the solar window an energy efficient product? This question will however not be answered. It is too complicated to answer since it involves more than just numbers. It is difficult to put a value on the sunshade provided by the reflectors. Also the benefit of transporting the light further back into the building is difficult to value. This work only answers the question about the energetic consequences of installing a solar window.

The evaluation shows that the model is in good agreement with the measured data. This is true for the prototype solar window as well as for the Solgård solar window, the electrical and the thermal output and for open and closed reflectors.

The results in Figure 5.1 show that the solar window produces about 35% more energy per PV cell area than a flat PV module placed vertically on the wall even though it is located on the inside of a window. If space is the limiting factor when PV modules are installed on the roof, the solar window is an interesting product in high-rise houses and staircases. However, if space is not a problem, Figure 5.1 shows that it is better to install the PV modules on the roof. This will result in an additional 17% electrical energy per module area. It was shown in Figure 5.2 that the shading of the cells in the solar window lowers the annual output substantially. If the shading were removed the output would increase by about 20% annually. Also the transmittance losses are significant despite the fact that the glazing is anti reflection treated. If the glazing were removed the annual electrical output would increase by about 25%. One of the problems is that the performance of PV cells is always limited in some way. During the winter the incidence angle between the sun and the absorber is high. This

means that the sun can not see the absorber very well. During the summer the angle between the sun and the absorber is more preferable. However during the summer the incidence angle between the glazing and the solar radiation is high. This means that the transmission losses will be at their highest level during the time when the irradiance is at its maximum. The angular dependence of the PV cells is however not an important factor. However, during the winter the reflector increases the output. The angle between the sun and the normal to the reflector is small. This means that the sun can see the whole reflector.

In Table 5.1 it was shown how the performance of the solar window depends on the choice of control strategy for the reflectors. Maximizing the annual electrical output using control strategy 2, always closed reflectors, will result in high auxiliary energy need for a building. This is of course very dependent on the geographical location of the building. If the building is located in the south of Europe the result will be completely different from the results from Sweden. If the auxiliary energy need is to be minimized control strategy 4 is preferable. This is also the best strategy from a comfort point of view, resulting in relatively low overheating. Control strategy 3 was chosen for the solar window in Augustenborg since sensors for solar radiation are a standard solution on the market. Control strategy 4 is much more complex and sensors and controllers have to be specially assembled. The main reason why control strategy 4 is better than control strategy 3 is the possibility to utilize high solar irradiance during the winter. If the solar radiation is high during a cold winter day it is better to open the reflectors to heat the building passively. If control strategy 3 is used there is a risk that the window will close during hours of high irradiation.

During the tests on the Solgården solar window the absorbers were not insulated correctly. The consequences of improving this and adding a low emission coating on the glazing were studied theoretically. The U-value and the transmission through the glazing were lowered. The results show that the annual energy use is lowered and hence it is more important to lower the heat losses than it is to maximize the PV and the thermal output.

The solar window was also compared to reference systems. In the reference case the 16 m<sup>2</sup> solar window was replaced by an 8 m<sup>2</sup> standard window. The reference case was simulated with and without system 3 and system 2 respectively, a solar energy system of the same size as the solar window. The reason for choosing to replace the solar window with a 8 m<sup>2</sup> window and not an 16 m<sup>2</sup> window is the access to daylight. If the reflectors are open about half the radiation transmitted through the glazing ends up on the absorber. This means that the solar window must be twice the size of a standard window in order to have the same amount of daylight reaching the room. As was shown in Figure 5.8 the solar window performs better than system 2. The heat produced in the solar window during the summer

is more important than the increased thermal losses during the winter due to the heavily glazed façade. However, if the solar window is compared to the reference case including the solar energy system the result is the opposite. System 3 performs better than the solar window. This is one of the most important conclusions. It is energetically more favourable to install the thermal absorbers and the PV-cells on the roof than in the window. System 3 was simulated with the solar system at  $20^\circ$  tilt, i.e. the same tilt as the roof in Solgårdén. This is not an optimal tilt. If the simulation had been performed with the modules at a higher inclination, the difference between the solar window and system 3 would be even larger.

One of the problems with the solar window is that the absorbers and reflectors block the solar radiation from entering the building. This means less passive heating of the building. The problem becomes clear when the solar window is compared to system 3. A thermal collector can be installed in a window to build something that looks like the solar window or it can be installed on for instance the roof. This is illustrated in figure 6.1. If the collector is installed on the roof as was proposed by (Corbin and Zhai, 2010) the active area collecting the solar radiation is the sum of the individual areas. In the figure this means  $A + B$ . If the thermal collector is installed in the window the active area is still just  $A$ . The thermal collector is now shading the window. In other words, a photon can not be used for simultaneously heating the collector and the building.

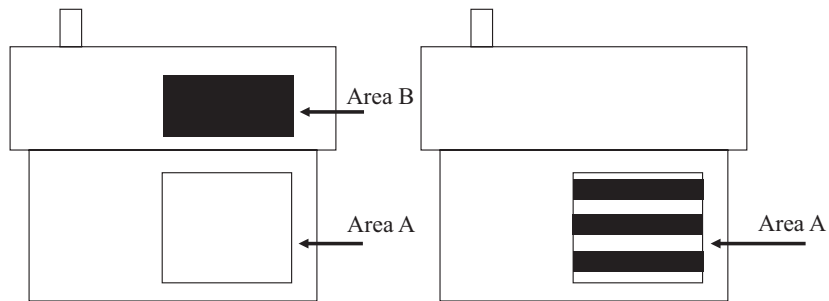


*Figure 6.1 Left, Building with a window of size A and a solar collector of size B on the roof. Right, Building with a window of size A in which a solar collector of size B has been placed.*

Since the solar window is located vertically the annual energy distribution is rather flat, i.e. there is no peak during the summer. The simulations suggest that it would be possible to increase the window area in order to gain more energy from the sun. This is why the investigation was performed with increased solar window area and increased collector area for system

3. It was shown in figure 5.9 that increasing the solar window area will lead to higher auxiliary energy need. This is due to the increased thermal losses caused by the window. The increase in thermal losses is larger than the extra solar thermal energy produced by the window. This is not the case for system 3. If the solar collector is located on the roof all the extra energy will be used to lower the energy need. There is no negative effect that ruins the positive effect. This is of course a problem for the solar window.

## 7 Development and future

The solar radiation and the ambient temperature vary substantially at different sites. The weather conditions for a building vary both seasonally and from day to night. This variation leads to different problems and possibilities. When the conditions change it is often a good idea to try to adjust to these changes.

A standard wall gives good insulation but does not utilize the irradiance falling on it. A window uses the solar radiation in an effective way for saving energy for heating. However it has high heat losses during the dark hours and may contribute to overheating during periods of high ambient temperatures and requires a sunshade. A solar collector uses the high solar intensities for delivering hot water, but its contribution to the heating of the building is limited. A PV-module converts around 10% of the solar radiation to electric energy, while the rest is lost to the surroundings as heat. This means that there is a demand for a dynamic façade element that combines the properties of a wall, a window and a solar collector or a PV-module. The ideal façade element should combine the following properties:

- During dark hours it should have low U-value and correspondingly low heat losses like a well-insulated wall.
- During cold sunny hours it should effectively convert the radiation to heat like a window, i.e. have a low U-value and high total solar transmittance.
- During warm sunny hours it should deliver hot water or electricity like a solar collector or a PV cell and simultaneously give sunshade to the building.

The solar window fulfils to some extent the requirements for an ideal element. A weak point of the solar window is the high U-value, even in a closed position.

The solar window has to be improved in a number of ways to become an attractive solar energy product. Most important is the U-value. This has to be lowered considerably. If a low emittance coating is added on the window glazing the transmission through the glazing will be reduced.

This is a problem for the window during both the summer and the winter. During the winter valuable radiation for passive heating is lost. The low emittance coating will also lower the energy output from the window when the transmission is reduced. One way of solving this problem might be to put the collector between the two panes of glass. This would result in higher transmission and thus higher output since the radiation only has to pass through one pane of glass. The inner glazing could be single or double and, most importantly, it can be low emittance treated without affecting the collector. The construction of the window might become more complicated but that is most likely a price that has to be paid. Another advantage is that the cells will not become dusty, which is a problem with the construction today. If the collector is placed between the panes the sunshading properties will be improved since less energy will be lost from the absorber to the room. The solar window can also be improved if the shading of the cells is reduced by having a larger distance between the outer cell and the window frame.

# References

- Aleklett, K. (2007) Peak oil and the evolving strategies of oil importing and exporting countries. Discussion paper No 2007-17. Web page visited 2010-01-18 from internationaltransportforum: <http://www.internationaltransportforum.org/jtrc/DiscussionPapers/Discussion-Paper17.pdf>
- Anderson, T.N., Duke, M., Morrison, G.L., & Carson, J.K. (2009). Performance of a building integrated photovoltaic/thermal (BIPVT) solar collector. *Solar Energy* 83 (2009), p 445-455.
- Brogren, M. (2004). *Optical Efficiency of Low-Concentrating Solar Energy Systems with Parabolic Reflectors*. ISSN 1104-232X, ISBN 91-554-5867-X. Uppsala: Uppsala University. Department of Engineering Science. Available at; <http://urn.kb.se/resolve?urn=urn:nbn:se:uu:diva-3988> visited 2010-03-18
- Chinyama, G.K., Roos, A. & Karlsson, B. (1993). Stability of antireflection coatings for large area glazing. *Solar Energy* 50 1993, p 105-111.
- Corbin, C.D., & Zhai, Z.J. (2010). Experimental and numerical investigation on thermal and electrical performance of a building integrated photovoltaic-thermal collector system. *Energy and Buildings* 42 (2010), p 76-82.
- Davidsson, H., Perers, B., & Karlsson, B. (2010). Performance of a multifunctional PV/T hybrid solar window. *Solar Energy* 84 (2010), p 365-372.
- Energimyndigheten (2007). Energistatistik för småhus 2007. Web page visited 2010-01-18, from energimyndigheten: ([http://www.energimyndigheten.se/Global/Press/ES2009\\_1.pdf](http://www.energimyndigheten.se/Global/Press/ES2009_1.pdf))
- Fieber, A., Gajbert, H., Håkansson, H., Nilsson, J., Rosencrantz, T., & Karlsson, B. (2003). *Design, Building integration and performance of a hybrid solar wall element*. Proceedings of ISES Solar World Congress 2003 Gothenburg, Sweden



- Fieber, A., Nilsson, J., & Karlsson, B. (2004). *PV performance of a multi-functional PV/T hybrid solar window*. Proceedings of 19th European photovoltaic solar energy conference and exhibition 2004, Paris, France
- Fieber, A. (2005). *Building Integration of Solar Energy*. Lic. Thesis Report, EBD-T--05/3, p 107-192. Lund: Lund University, Lund Institute of Technology, Department of Construction and Architecture, Division of Energy and Building Design. Available at; [http://www.ebd.lth.se/fileadmin/energi\\_byggnadsdesign/images/Publikationer/AvhandlingWEB\\_alt\\_Andreas.pdf](http://www.ebd.lth.se/fileadmin/energi_byggnadsdesign/images/Publikationer/AvhandlingWEB_alt_Andreas.pdf) visited 2010-01-18
- Gajbert, H., Hall, M., & Karlsson, B. (2007). Optimisation of reflector and module geometries for stationary, low-concentrating, façade-integrated photovoltaic systems. *Solar Energy Materials and Solar Cells* 91 (2007), p 1788-1799.
- Granqvist, C.G., Azens, A., Hjelm, A., Kullman, L., Niklasson, G.A., Rönnow, D., Strømme Mattsson, M., Veszeli, M. & Vaivars, G. (1998). Recent advances in electrochromics for smart windows applications. *Solar energy* 63 (1998), p 199-216.
- Greenroof. Augustenborgs botanical roof garden. Web page visited 2010-01-18, from Green Roof: <http://www.greenroof.se/>
- Hellgren, D. Hellgrens Ingenjörbyrå, web page visited 2010-01-18 from Hellgrens homepage [www.davidhellgren.se](http://www.davidhellgren.se)
- IEA SHC Task 21. IEA SHC Task 21 Daylight in Buildings, web page visited 2010-01-18 from IEA Task 21 homepage: <http://www.iea-shc.org/task21/index.html>
- IEA SHC. Task 35 PV/Thermal Solar System, web page visited 2010-01-18, from IEA Task 35 homepage: [www.iea-shc.org/task35/index.html](http://www.iea-shc.org/task35/index.html)
- Inoue, T., Ichinose, M., & Ichikawa, N. (2008). Thermotropic glass with active dimming control for solar shading and daylighting. *Energy and Buildings* 40 (2008), p 385-393.
- IPCC. (2007). Climate Change 2007: Synthesis Report, Summary for Policymakers. Web page visited 10-01-18, from IPCC: [http://www.ipcc.ch/pdf/assessment-report/ar4/syr/ar4\\_syr\\_spm.pdf](http://www.ipcc.ch/pdf/assessment-report/ar4/syr/ar4_syr_spm.pdf)
- Kalogirou, S.A., & Tripanagnostopoulos, Y. (2006). Hybrid PV/T solar systems for domestic hot water and electricity production. *Energy conversion and management* 47 (2006), p 3368-3382.

- Krauter, S., & Ochs, F. (2003). Integrated solar home system. *Renewable energy* 29 (2003), p 153-164.
- Mallick, T.K., Eames, P.C., Hyde, T.J., & Norton, B. (2004) . The design and experimental characterisation of an asymmetric compound parabolic photovoltaic concentrator for building façade integration in the UK. *Solar Energy* 77 (2004), p 319-327.
- METEONORM 5.0. Global meteorological database for solar energy and applied meteorology, webpage visited 2010-01-18 from Metotest: [www.meteotest.ch](http://www.meteotest.ch)
- Nostell, P., Roos, A., & Karlsson, B. (1999). Optical and mechanical properties of sol-gel antireflective films for solar energy applications. *Thin solid films* 351, p 170-175.
- Passivhuscentrum. The market for passive houses. Web page visited 2010-01-18, from [passivhuscentrum: \(http://www.passivhuscentrum.se/marknaden.html?&L=1&hafslwvcybiitcm\)](http://www.passivhuscentrum.se/marknaden.html?&L=1&hafslwvcybiitcm)
- Passivhuscentrum. Frågor och svar om passivhus. Web page visited 2010-01-18, from [passivhuscentrum: \(http://www.passivhuscentrum.se/fragorochsvar.html?&aqwunluknkjk\)](http://www.passivhuscentrum.se/fragorochsvar.html?&aqwunluknkjk) visited 2010-01-18
- SIS, Swedish Standards Institute (1997). SS-EN 673 Byggnadsglas - Bestämning av värmegenomgångskoefficient (U-värde) - Beräkningsmetod. Stockholm: SIS Förlag AB.
- Tonui, J.K., & Tripanagnostopoulos, Y. (2007). Improved PV/T solar collectors with heat extraction by forced or natural air circulation. *Renewable Energy* 32 (2007), p 623-637.
- TRNSYS Reference Manual. (2000). Klein, S.A., Beckman, W.A., Mitchell, J.W., Duffie, J.A., Duffie, N.A., & Freeman. T.L., Madison: Solar Energy Laboratory, University of Wisconsin.
- Zemax. Software For Optical System Design. Web page visited 2010-01-18 from Zemax: <http://www.zemax.com/> visited 2010-01-18



# Article I



Available online at [www.sciencedirect.com](http://www.sciencedirect.com)

ScienceDirect

Solar Energy 84 (2010) 365–372

SOLAR  
ENERGY[www.elsevier.com/locate/solener](http://www.elsevier.com/locate/solener)

## Performance of a multifunctional PV/T hybrid solar window

Henrik Davidsson\*, Bengt Perers, Björn Karlsson

*Energy and Building Design, Lund University, P.O. Box 118, SE 221 00 Lund, Sweden*

Received 4 March 2009; received in revised form 18 November 2009; accepted 19 November 2009  
Available online 22 December 2009

Communicated by: Associate Editor Matheos Santamouris

### Abstract

A building-integrated multifunctional PV/T solar window has been developed and evaluated. It is constructed of PV cells laminated on solar absorbers placed in a window behind the glazing. To reduce the cost of the solar electricity, tiltable reflectors have been introduced in the construction to focus radiation onto the solar cells. The reflectors render the possibility of controlling the amount of radiation transmitted into the building. The insulated reflectors also reduce the thermal losses through the window. A model for simulation of the electric and hot water production was developed. The model can perform yearly energy simulations where different features such as shading of the cells or effects of the glazing can be included or excluded. The simulation can be run with the reflectors in an active, up right, position or in a passive, horizontal, position. The simulation program was calibrated against measurements on a prototype solar window placed in Lund in the south of Sweden and against a solar window built into a single family house, Solgården, in Älvkarleö in the central part of Sweden. The results from the simulation shows that the solar window annually produces about 35% more electric energy per unit cell area compared to a vertical flat PV module.

© 2009 Elsevier Ltd. All rights reserved.

**Keywords:** Solar window; PV/T; Building integration

### 1. Introduction

A diversity of technical solutions needs to be applied and developed if solar electricity is to become cheap enough to compete with grid electricity. One technique for reducing the cost of solar electricity is to use a reflector for focusing radiation onto the PV cells, thus allowing expensive PV cells to be replaced by considerably cheaper reflector material. Active water cooling on the back of the cell gives both relatively cool, and thereby high efficient cells, and hot water for domestic use. Photo Voltaic/Thermal (PV/T) hybrid collectors producing electricity and thermal energy simultaneously have been reported earlier as cost effective collectors (Kalogirou and Tripanagnostopoulos, 2006; Krauter and Ochs, 2003; Assoa et al., 2007; Tonui and Tripanagnostopoulos, 2007). The official homepage of IEA SHC Task

35 PV/Thermal Solar Systems (IEA SHC) gives a good overview of different hybrid technologies. Further cost reduction is possible if the solar modules can be integrated into the building construction. Integration makes it possible to use existing frames and glazing for the solar modules or, alternatively, to replace roofing material and windows by using solar modules. Wall integrated solar collectors using reflectors have been shown to increase the electrical output substantially (Gajbert et al., 2007; Mallick et al., 2004) compared to flat vertical PV modules. All technologies mentioned above have been combined in the PV/T hybrid technology that is presented in this work.

A building-integrated multifunctional solar window was proposed and developed by Andreas Fieber (Fieber et al., 2003, 2004). The solar window (Fig. 1) is constructed of solar thermal absorbers on which PV cells have been laminated. The absorbers are building-integrated into the inside of a standard window, thus saving frames and glazing and lowering the total cost of the construction. In order

\* Corresponding author. Tel.: +46 46 2224851; fax: +46 46 2224719.  
E-mail address: [henrik.davidsson@ebd.lth.se](mailto:henrik.davidsson@ebd.lth.se) (H. Davidsson).

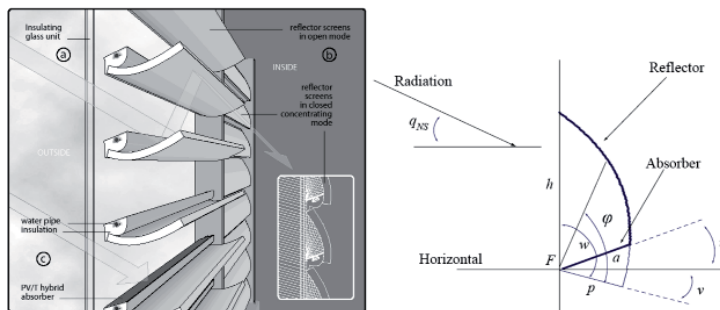


Fig. 1. Left: the solar window. Right: illustration of the parabolic reflector and the absorber.

to minimize the PV cell area, reflectors have been placed behind the absorbers. When tilting the foldable reflectors to a vertical position the solar radiation is focused onto the absorbers. When the reflectors are tilted to a horizontal position the solar radiation is let into the building to allow for passive heating. This means that the reflectors in a closed position increase the radiation on the cells, reduce the thermal losses through the window and also work as a sun shade. The double glazing of the window in front of the absorbers is anti-reflection treated to maximize the transmittance (Chinyama et al., 1993; Nostell et al., 1999; Brogren et al., 2000). Two solar windows have been monitored and characterized, one prototype solar window placed in the solar laboratory at Lund University in the south of Sweden and one solar window integrated into a single family house in Älvkarleö in the central part of Sweden. A detailed construction of the PV/T collector and the architectural implications such as light distribution is presented in Fieber et al. (2003, 2004, 2005). Following this, long term measurements were performed regarding energy production of heat and electricity. This was carried out on both of the solar windows.

In this paper, we describe a model developed to simulate the yearly energy production of the hybrid window system from climatic data. The model uses a combination of both experimentally measured and theoretically derived parameters and functions in the calculations. It takes into account shading caused by the window frames and also includes the transmittance through the glazing and the angular dependence of the efficiency of the PV cells. The model also allows for analyzing different limiting effects such as shading or transmittance through the glazing. This gives an opportunity to study possible improvements for the solar window.

### 1.1. Geometry

The geometry of the solar window is shown in Fig. 1. The optical axis of the parabolic reflector is directed  $15^\circ$

above the horizon with focus on the front edge of the absorber, i.e.  $v = 15^\circ$ . The absorber tilt,  $u$ , is  $20^\circ$ . This means that all radiation from  $15^\circ$  and higher projected solar altitudes (Rönnelid and Karlsson, 1997) will hit on the absorber between the focal point,  $F$ , and the reflector. The focal length is denoted  $p$ , the height of the glazing  $h$  and  $a$  is the absorber width. The angle  $w$  is the angle between the glazing and the absorber plane and  $q_{NS}$  is the incident angle of the solar radiation projected in the north-south vertical plane. The absorbers are 113 cm long and 7 cm wide while the PV cells covering the absorber are 12.5 cm by 6.25 cm each. This means that a fraction of 80% of the absorber is covered with solar cells. The solar window in Solgården is constructed of eight absorbers per window unit while the prototype solar window is constructed of five absorbers (Fig. 2). The Solgården solar window has 64 PV cells in series and the prototype solar window has 8 PV cells in series. The total window area is  $16 \text{ m}^2$  in Solgården and about  $1.2 \text{ m}^2$  in the case of the prototype solar window. The reflectors are made of conventional anodized aluminium from Alanod, Germany, and the anti-reflection treated low iron glazing is from Sunarc, Denmark. The anti-reflection treatment increases the transmittance, weighted by the spectral sensitivity of the PV-cell, by about 5% for each glass pane (Chinyama et al., 1993).

The reflector parabola is described in Eq. (1).  $r$  is a vector from  $F$  to a point on the parabola at angle  $\phi$ .

$$r(\phi) = p / \cos^2(\phi) \quad (1)$$

Both  $h$  and  $a$  is determined by  $r$  and the two angles  $w = 105^\circ$  and  $u + v = 35^\circ$ , respectively, for the solar window. The ratio between  $h$  and  $a$ , which is defined as the geometrical concentration factor, is 2.45 for the construction.

### 2. Methods

Measurements of the performance of the multifunctional PV/T hybrid solar window were carried out during



Fig. 2. Left: the prototype solar window. Right: the solar window in Solgården with closed reflectors.

2006 on a prototype solar window placed in Lund, Sweden (55.44N, 13.12E). A full scale system combining four of these solar windows was installed in a single family home called Solgård in Älvkarleö, Sweden (60.57N, 17.45E) and evaluated during 2006–2008. This window was directed 23° towards east from south. The solar windows can be seen in Fig. 2. The measurements of the generated current and voltage produced by the prototype solar window were carried out using a Campbell CR1000 logger. The radiation, temperatures and water flow through the absorbers were measured using a Campbell CR10 logger. The temperature measurements were carried out using PT100 sensors. All measurements made in Solgården were conducted by using a Campbell CR10.

The water flow was kept at a constant level throughout the measurements for the prototype solar window. The Solgård solar window was equipped with a PV module driven pump. This means that the water flow will vary with the solar radiation. The radiation was monitored using Kipp and Zonen pyranometers for the measurements in Lund and Li-COR pyranometers in Solgård. Measurements were monitored both with the reflectors in a horizontal and in a vertical position. The measurements were carried out with a 10 s sampling interval and the average values were stored every sixth minute. This will determine the resolution. The prototype solar window was supplied with water of constant inlet temperatures and the measurements were carried out during both day and night. Night time data were used for determining the thermal losses of the window. The typical flow in the thermal circuit is 100 liter per hour and the temperature increase is typically 15°. The accuracy in each measurement is around 1% and the accuracy in the thermal measurements adds up to 2–3%. The accuracy of the pyranometer is 3% and the measurements of the current from the solar cells have accuracy below 1%.

A simulation model was developed to describe the solar window. The model uses the direct and diffuse radiation together with the inlet water temperature, the ambient temperature and the time, and thus the solar angles, as inputs. The outputs are thermal and electrical delivered power. In

order to simplify the calculations the total electrical power,  $P_{tot}$ , delivered by the solar window was divided into three components,  $P_{dir}$ ,  $P_{ref}$ , and  $P_{diff}$ . The first component,  $P_{dir}$ , is the power caused by the beam radiation that hits the absorber directly. The second component,  $P_{ref}$ , is the power caused by the beam radiation that goes via the reflector. The third component,  $P_{diff}$ , is the power contribution given by the diffuse radiation. Fig. 3 explains graphically the three different components of radiation.

The expression for the electrical output is shown below.

$$P_{dir} = G_{b,n} \cdot T_{glass}(\theta_1) \cdot \alpha_{pe}(\theta_2) \cdot f_{shading}(\theta_3) \cdot A_{cell} \cdot \eta_{pe} \cdot \cos(\theta_2) \quad (2)$$

$$P_{refl} = G_{b,n} \cdot T_{glass}(\theta_1) \cdot \alpha_{pe}(\theta_4) \cdot f_{ref}(\theta_5) \cdot A_{ref} \cdot \eta_{pe} \cdot R_{ref} \cos(\theta_5) \quad (3)$$

$$P_{diff} = G_d \cdot C_{1,2} \quad (4)$$

$$P_{tot} = P_{dir} + P_{ref} + P_{diff} \quad (5)$$

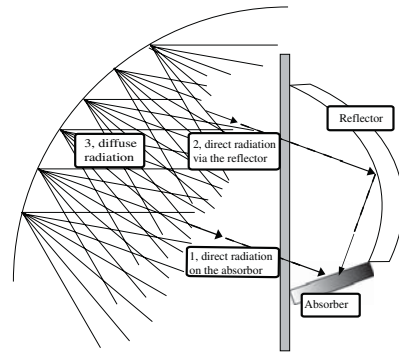


Fig. 3. A graphical explanation of the calculation method with the three different radiation components.



$G_{b,n}$  and  $G_d$  are the beam radiation and the diffuse radiation against the window.  $T_{glass}$  is the angular dependent transmittance through the glazing;  $\alpha_{pv}$  describes the angular dependence of the absorptance of the PV cells, and  $f_{shading}$  describes the shading of the PV cells caused by the window frame.  $f_{ref}$  is a correction factor for the shadow effects of the radiation which is reflected. This function includes the shading of the reflector. The angles  $\theta_1$  to  $\theta_5$  are the different incidence angles for the beam towards the components of the solar window.  $A_{cell}$  and  $A_{ref}$  are the areas of the PV cell and the reflector, respectively.  $\eta_{pv}$  and  $R_{ref}$  are the efficiency of the solar cells and the reflectance of the reflector.  $C_{1,2}$  is a response function for the diffuse radiation obtained from measurements during cloudy days, when the beam radiation has negligible influence on the performance. Measurements during cloudy days were performed with the reflector in both horizontal and in vertical positions allowing both response functions  $C_1$ , horizontal reflector, and  $C_2$ , vertical reflector, to be determined.

The transmittance,  $T_{glass}$ , through the window was calculated using the Fresnel's equations and Snell's law. The shading factors  $f_{shading}$  and  $f_{reflector}$  were calculated theoretically from the PV/T window geometry. A measurement was performed to determine  $\alpha_{pv}$ , the angular dependence of the PV cells. Fig. 4 shows the transmission through the glazing, the angular dependence of the PV cell, the angular impact of shading on the performance of the PV cell and on the optical efficiency of the thermal collector.

In order to calculate the thermal output a fourth term has to be added to describe the thermal losses in the absorber. The thermal losses  $P_{loss,p}$  for the prototype solar window and  $P_{loss,s}$  for the Solgård solar window are shown below. The Eqs. (2)–(5) are reused but with parameters and functions for the thermal absorbers instead of the PV-cells.

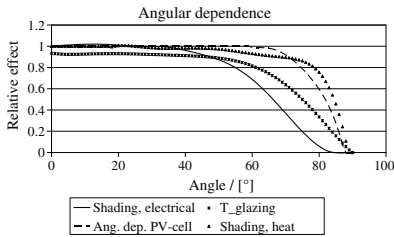


Fig. 4. The angular dependence for the different functions describing the solar window.

Table 1  
U-values for the prototype solar window.

| Thermal losses/[W/m <sup>2</sup> K], solar window PV/T collector |               |     |             |     |
|--|---------------|-----|-------------|-----|
| Closed/open mode   | Closed window |     | Open window |     |
| Direction of thermal loss dissipated from the absorber           | In            | Out | In          | Out |
| U-value/[W/m <sup>2</sup> K]                                     | 3.9           | 2.0 | 5.9         | 1.3 |

$$P_{loss,s} = U_{s,out} \cdot A_{window} \cdot \Delta T_{out} + U_{s,in} \cdot A_{window} \cdot \Delta T_{in} \quad (6)$$

$$P_{loss,p} = U_p \cdot A_{window} \cdot \Delta T \quad (7)$$

Since the solar window in Solgård experiences thermal losses to two different temperatures, the ambient temperature and the indoor temperature, two different U-values were used. The  $U_{s,out}$  represents the thermal loss to the outside and the  $U_{s,in}$  the thermal loss to the inside.  $A_{window}$  is the total window area.  $\Delta T_{out}$  is the temperature difference between the average water temperature and the ambient temperature.  $\Delta T_{in}$  is the temperature difference between the indoor temperature and the average water temperature. The U-values, in Table 1, were estimated from heat transfer analysis.  $U_p$  is the U-value for the prototype solar window and  $\Delta T$  is the temperature difference between the ambient temperature and the average water temperature. The separately measured thermal losses through the solar window are 1.3 W/m<sup>2</sup>K with reflectors closed and 2.4 W/m<sup>2</sup>K with reflectors open.

The simulations were carried out with 6 min time steps using weather data monitored at the locations where the solar windows were placed.

### 3. Results

Two different types of graphs were used to validate the model regarding thermal and electrical output. The first type is shown in Fig. 5, where results from measurements and simulations are compared during a day period. To be able to perform easy and reliable measurements, the short circuit current was monitored and simulated instead of the delivered power. In this way the measurements do not depend on maximum power point tracking. The days were chosen to illustrate different weather conditions, such as different ambient temperatures and cloudy weather with sunny intervals. Results from both the prototype and from Solgård are shown in Fig. 5. Fig. 5 combined with Fig. 7, discussed later, show that different seasons and thus different solar angles are handled correctly by the model. Fig. 5 illustrates the performance during partly cloudy days.

During the measurements on the prototype solar window, two different, not perfectly synchronized, loggers for monitoring the electrical output and the radiation were used. This means that synchronization problems could arise during partly cloudy days with quickly changing solar irradiance. To solve this problem the simulated and the measured output was integrated daily. Then this irregularity will disappear. The result from this analysis is shown in Fig. 6, where the integrated daily measured output on the

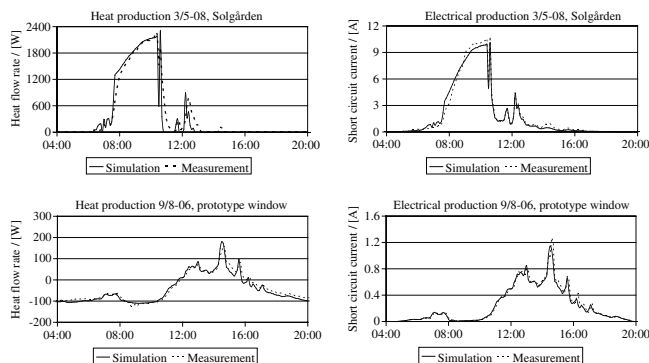


Fig. 5. Measured and simulated thermal and electrical output for 8 m<sup>2</sup> window in Solgården (upper) and for 1 m<sup>2</sup> window in the prototype (lower).

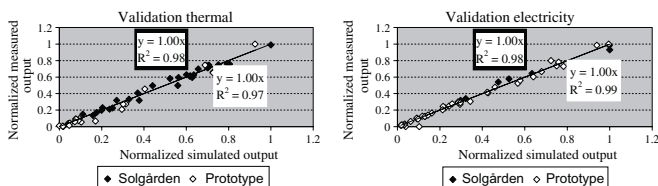


Fig. 6. Comparison of measured and simulated daily thermal and electrical performance of the solar window.

y-axis is plotted versus the integrated daily simulated output on the x-axis. A perfect agreement between simulation and measurement would put all the points on the line,  $x = y$ . This analysis was performed both for the thermal output, left figure, and the electrical output, right figure. Validation from the Solgården solar window is in filled circles and the validation from the prototype solar window is in empty circles. All values have been normalized to the highest output in each series. The correlation is high for all four validations.

The impact of the reflector on the electrical and thermal output is larger during periods of low solar altitude. This can be seen in Fig. 7 where two simulations have been plotted. The solid black line represents a simulation with active, vertical reflectors, and the dashed black line (the lowest) represents a simulation with passive, horizontal reflectors. The area between the solid black line and the dashed black line is thus the contribution to the electrical output from the reflector. In the left graph dated 12/9-06 the reflector contributes to about 30% of the daily output while the contribution is about 50% in the right graph dated 3/11-06. The filled circles in the figure are from measurements during both days. The correlation is high between measurement and simulation. In the empty squares the irradiance

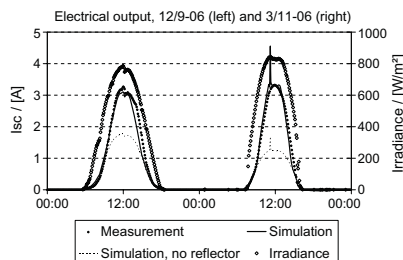


Fig. 7. Measurement and simulation of the electrical output during 12/9-06 (left) and 3/11-06 (right).

during the two days is shown. The right y-axis represents the solar irradiance.

Yearly simulations were made for the prototype solar window and for two flat PV-modules. The PV-modules have the same efficiencies and areas as the string module in the solar window, but they have no reflectors, are unshaded and use single glazing instead of double glazing

as in the solar window. The PV-modules were installed on a wall or on the Solgård roof, tilted  $20^\circ$ . The wall mounted PV module benefits less from the diffuse radiation compared to the solar window due to less favourable view angles between the cells and the sky. The results from the simulation show that the performance of the solar window is suppressed by shadow and transmittance effects. However, annually it delivers about 35% more electric energy per unit cell area compared to a vertical flat PV module.

When the PV module is located on a roof at a low tilt, it receives more diffuse radiation than a wall mounted PV module since the module can see a larger part of the diffuse radiation from the sky. This is clearly visible in Fig. 8. The increase of the electrical output from the direct radiation on the roof mounted PV module compared to the solar window is due to lower losses in the glazing and the possibility for the roof module of utilizing the radiation which comes from directions behind the wall. Note that the increase of the diffuse radiation on the roof mounted module compensates for the reflector contribution on the cells in the solar window. The diffuse irradiation is treated as isotropic.

A similar analysis, in this case using TRNSYS, was performed to investigate the thermal properties of the solar window connected to the thermal system of the house. A TRNSYS-deck including the solar window or flat solar collectors, pumps, a storage tank, etc. and a heating load was constructed. In the simulation all parameters except the areas of the wall collector and the roof collector were kept constant.

The thermal performance of the solar window cannot be compared with a solar collector of the same area, since it will give a substantial over production during the summer period. Therefore a comparison was performed between two solar thermal systems with the same annual energy production. Fig. 9 shows that  $8.3 \text{ m}^2$  of wall collectors or  $6.0 \text{ m}^2$  of roof collectors tilted  $20^\circ$  annually delivers the same amount of heat as the solar window with  $16.0 \text{ m}^2$  glazed area and  $5.06 \text{ m}^2$  of absorber areas. The wall and roof collectors are assumed to have  $\eta_{\text{direct}} = 0.75$  and  $\eta_{\text{diffuse}} = 0.68$ . The  $U$ -value of the collectors is assumed to

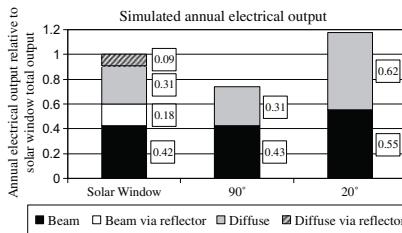


Fig. 8. The annual electrical output from the prototype solar window and from two flat PV-modules on a wall at  $90^\circ$  tilt and on a roof at  $20^\circ$  tilt.

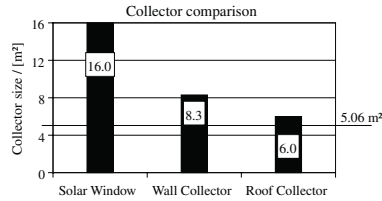


Fig. 9. The required areas of the wall collector and the roof collector to produce an equal annual amount of thermal energy compared to the Solgård solar window. The wall collector is placed vertically and the roof collector is installed at  $20^\circ$  tilt.

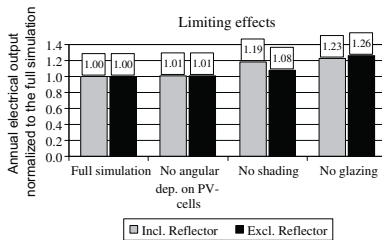


Fig. 10. Limiting factors affecting the performance of the solar window.

be  $4 \text{ W/m}^2\text{K}$ . All systems are supposed to be oriented  $23^\circ$  from south towards east.

This means that the solar window per absorber area delivers a similar amount of electric and thermal energy as PV-modules and thermal collectors each of the same area as the absorber in the solar window.

To study the limiting factors in the solar window a simulation was carried out where the factors  $T_{\text{glass}}(\theta_1)$ ,  $\alpha_{\text{pv}}(\theta_2)$  and  $f_{\text{shading}}(\theta_3)$  in Eqs. (2)–(4) were in turn set to 1, see Fig. 10. The impact of setting  $\alpha_{\text{pv}}(\theta_2)$  to 1 was small, since the angular dependence of the efficiency of the PV cells is negligible except for such high angles that the shading is already strongly affecting the performance. If the anti-reflection treated glazing were removed the yearly electrical output would increase by about 23% and if the shading effects could be removed completely the increase would be as much as 19%.

#### 4. Discussion

A standard wall gives good insulation but does not utilize the irradiance falling on it. A window uses the solar radiation in an effective way for saving energy for heating. However it has high heat losses during the dark hours and may contribute to overheating during periods of high ambient temperatures and requires a sun shade. A solar

collector uses the high solar intensities for delivering hot water, but its contribution to the heating of the building is limited. A PV-module converts around 10% of the solar radiation to electric energy, while the rest is lost to the ambient as heat. This means that it is a demand for a dynamic façade element that combines the properties of a wall, a window and a solar collector or a PV-module. The ideal façade element should combine the following properties:

- During dark hours it should have low  $U$ -value and correspondingly low heat losses like a well-insulated wall.
- During cold sunny hours it should effectively convert the radiation to heat like a window, i.e. have a low  $U$ -value and high total solar transmittance.
- During warm sunny hours it should deliver hot water or electricity like a solar collector or a PV cell and simultaneously giving sun shade to the building.

The solar window fulfils to some extent the requirements on an ideal element. A weak point of the solar window is the high  $U$ -value, even in a closed position. The large area of the solar window also contributes to the high heat losses. This can be improved by designing the reflector with a thicker insulation and to be tighter in the closed state. The  $U$ -value can also be suppressed if the glazing is coated with low emitting films. These films will however also decrease the transmittance with roughly 10%.

Solar cells in concentrating system are principally required to have a lower series resistance due to a high and non-uniform irradiance. The solar window can however be equipped with standard cells since the concentration is relatively low. If the reflectors are flat or have a white diffuse coating, then the irradiance will be uniform. But this also means that the performance will deteriorate significantly.

The reflectors will be closed when there is a demand for production of electricity and heat. During these hours the window will act more like a wall than a window. This is often a disadvantage, even if sometimes a sun shade is demanded. During the summer period, when the projected solar altitude is high, a large fraction of the solar beam goes directly onto the absorber with a low contribution from the reflector. Then the reflector can be partly opened and the window delivers heat, electricity and light. This is probably the ideal use of the solar window. This period will be extended when the window is moved to lower latitudes. However, at lower latitudes the annual irradiation on a vertical wall is decreasing, which means that the solar window will deliver less heat and electricity. Principally also the optical axis of the reflector parabola should be shifted with the latitude. The impact of the optical axis on the annual performance is however not so strong.

The solar window is designed for installation in a south window. However, if the window is designed with a horizontal optical axis it accepts all radiation and it can be installed in all directions. The concentration factor is then

limited to a factor of 2. It is difficult to design external sun shades for standard windows in east and west since the solar altitude is low in the morning and afternoon, respectively. There the solar window has the proper design since it effectively darkens the window in its closed position.

An alternative design of the solar window is to construct it without glazing and thermal circuit on the outside of the wall. Then the electric output will be considerably increased (Gajbert et al., 2007). The long term stability of an unprotected aluminium reflector will however be limited. If the standard solar window does not have a cooling circuit then the cells will be hot and the heat will be delivered to the inside, so the sun shade function will not work.

## 5. Conclusions

The overall goal of the project presented in this article is to reduce the total costs of the PV and solar thermal systems for a building. An alternative for achieving this goal is to use PV/T hybrid collectors using reflectors which concentrate the irradiance onto the absorbers. Different designs have been proposed (Gajbert et al., 2007; Mallick et al., 2004). But very few geometries, which allows for building integration, have been presented. A multifunctional PV/T hybrid which can be integrated in a window was proposed by Andreas Fieber (Fieber et al., 2003, 2004). This solar window replaces installations of PV-modules, solar thermal collectors and sun shades. The performance of this solar window is analyzed in detail in this paper.

The results from the simulation program developed to evaluate the window, closely match the measured data. The simulated annual electrical energy production clearly shows the importance of utilizing the diffuse radiation. About 40% of the electrical energy produced in the window is due to diffuse radiation. The comparison performed in Fig. 8 shows that the solar window produces about 35% more electrical energy per unit area of PV cells compared to a flat PV module placed on a wall at a 90° tilt. The simulation presented in Fig. 9 shows that the solar window produces more thermal energy per absorber area than a flat plate solar collector placed on the roof of Solgården at 20° tilt. If the flat plate collector is installed at an optimum tilt of 45° the annual output increases by around 5%.

These values were found using weather data from Lund at latitude 55.4° in the south of Sweden. They are representative also for Stockholm at latitude 59.3°. It is important to point out that vertical collectors and windows are more energy effective on high than on low latitudes.

The best method for analyzing the performance of the solar window is to compare it with conventional systems that deliver a comparable amount of heat and electricity. The paper shows that the hybrid absorber in the solar window can be replaced by 8.3 m<sup>2</sup> of collectors and 5.4 m<sup>2</sup> of PV-modules installed on the wall. The solar window requires less solar cell-, absorber-, and glazing areas than

the conventional systems. This implies that the materials cost are lower for the solar window. However, the solar window requires a relatively complicated thermal system and tiltable reflectors. The tested solar window is an early prototype, which means that it is difficult to estimate the real cost for a complete installation.

The solar window has a geometrical concentration factor of 2.45, while the real annual concentration is limited to a factor of 1.33 only. The substantial difference is explained by effects of optical axis of the reflector, optical losses in the reflector and glazing, shadow effects and the impact of the diffuse irradiance. The optical axis at 15° means that the beam irradiance vector will be below the optical axis during December and January. If a reflector with a horizontal optical axis is chosen then the geometrical concentration is limited to a factor of 2. Fig. 10 shows that the transmittance of the double glazing decreases the performance by almost 20 percent. The shading is also an important factor that limits the performance of the collector. All of these factors adds up to a total annual concentration factor that is about half of the theoretical value. The low absorbing anti-reflection treated glazing has a very high transmittance and can be improved only marginally. This means that the largest potential for improvement is obtained by minimizing the shadow effects. This can be accomplished by having a sufficient distance between the outer cells and the frame.

As can be seen in Figs. 7 and 8 it is possible to run simulations with the reflectors in either active, vertical, or passive, horizontal, positions. This keeps the simulation realistic by allowing control mechanisms, based on human behaviour, to decide whether or not to have closed reflectors. For instance there is a possibility to cool the building at night by simply opening the reflectors and thus increasing the  $U$ -value of the window. This is not an option for a standard window with a low  $U$ -value.

In conclusion, the developed calculation model for the PV/T hybrid solar window is in good agreement with measurements from both the prototype solar window and from the Solgård solar window. The model describes correctly both the electrical and the thermal output from the window. The solar window, placed vertically in a wall, produces about the same amount of electric energy as a roof integrated PV-module per unit cell area. Simultaneously the solar window produces about the same amount of thermal energy per unit absorber area as a solar collector integrated in the same roof tilted 20°.

## Acknowledgements

This work was supported by the Swedish Energy Agency through the Program Solel 03-07. B. Hellström and H. Håkansson at Lund University and S. Larsson at Vattenfall Development are acknowledged for assistance during measurements and evaluation.

## References

- Assoa, Y.B., Menezes, C., Fraisse, G., Yezou, R., Brau, J., 2007. Study of a new concept of photovoltaic-thermal hybrid collector. *Solar Energy* 81, 1132–1143.
- Brogren, M., Nostell, P., Karlsson, B., 2000. Optical efficiency of a PV-thermal hybrid CPC module for high latitudes. *Solar Energy* 69, 173–185.
- Chinyama, G.K., Roos, A., Karlsson, B., 1993. Stability of antireflection coatings for large area glazing. *Solar Energy* 50, 105–111.
- Fieber, A., Gajbert, H., Håkansson, H., Nilsson, J., Rosencrantz, T., Karlsson, B., 2003. Design, building integration and performance of a hybrid solar wall element. In: *Proceedings of ISES Solar World Congress 2003*, Gothenburg, Sweden.
- Fieber, A., Nilsson, J., Karlsson, B., 2004. PV performance of a multifunctional PV/T hybrid solar window. In: *Proceedings of 19th European Photovoltaic Solar Energy Conference and Exhibition 2004*, Paris, France.
- Fieber, A., 2005. Building Integration of Solar Energy. Lic. Thesis Report, Division of Energy and Building Design, Department of Construction and Architecture, Lund University, Lund Institute of Technology, Report EBD-T – 05/3, pp. 107–192. Available from: <[http://www.ebd.lth.se/fileadmin/energi\\_byggnadsdesign/images/Publikationer/AvhandlingWEB\\_alt\\_Andreas.pdf](http://www.ebd.lth.se/fileadmin/energi_byggnadsdesign/images/Publikationer/AvhandlingWEB_alt_Andreas.pdf)>.
- Gajbert, H., Hall, M., Karlsson, B., 2007. Optimisation of reflector and module geometries for stationary, low-concentrating, façade-integrated photovoltaic systems. *Solar Energy Materials and Solar Cells* 91, 1788–1799.
- IEA SHC Task 35 PV/Thermal Solar System. Available from: <[www.iea-shc.org/task35/index.html](http://www.iea-shc.org/task35/index.html)>.
- Kalogirou, S.A., Tripanagnostopoulos, Y., 2006. Hybrid PV/T solar systems for domestic hot water and electricity production. *Energy Conversion and Management* 47, 3368–3382.
- Krauter, S., Ochs, F., 2003. Integrated solar home system. *Renewable Energy* 29, 153–164.
- Mallick, T.K., Eames, P.C., Hyde, T.J., Norton, B., 2004. The design and experimental characterisation of an asymmetric compound parabolic photovoltaic concentrator for building façade integration in the UK. *Solar Energy* 77, 319–327.
- Nostell, P., Roos, A., Karlsson, B., 1999. Optical and mechanical properties of sol-gel antireflective films for solar energy applications. *Thin Solid Films* 351, 170–175.
- Rönnelid, M., Karlsson, B., 1997. Irradiation distribution diagrams and their use for estimating collectable energy. *Solar Energy* 61, 191–201.
- Tonui, J.K., Tripanagnostopoulos, Y., 2007. Improved PV/T solar collectors with heat extraction by forced or natural air circulation. *Renewable Energy* 32, 623–637.

## Article II



# System analysis of a multifunctional PV/T hybrid solar window

Henrik Davidsson\*, Bengt Perers, Björn Karlsson

*Energy and Building Design, Lund University, B.O Box 118, SE 221 00 Lund, Sweden*

\* Corresponding Author, Tel.: +46-46-2224851, fax: +46-46-2224719  
*E-mail address:* henrik.davidsson@ebd.lth.se

## Abstract

The work presented in this article aims to investigate a PV/T hybrid solar window on a system level. A PV/T hybrid is an absorber on which solar cells have been laminated. The solar window is a PV/T hybrid collector with tiltable insulated reflectors integrated into a window. It simultaneously replaces thermal collectors, PV-modules and sunshade. The building integration lowers the total price of the construction since the collector utilizes the frame and the glazing in the window. When it is placed in the window a complex interaction takes place. On the positive side is the reduction of the thermal losses due to the insulated reflectors. On the negative side is the blocking of solar radiation that would otherwise heat the building passively. To investigate the sum of such complex interaction a system analysis has to be performed. In this paper we present results from such a system analysis showing both benefits and problems with the product. The building system with individual solar energy components uses 1100 kWh less auxiliary energy than the system with a solar window. However, the solar window system uses 600 kWh less auxiliary energy than a system with no active solar energy system.

*Keywords:* PV/T hybrid; solar window; building integration; TRNSYS



## 1 Introduction

If solar electricity is to become cheap enough to compete with electricity from the grid a number of different techniques have to be combined. These techniques can be PV/T technology combining PV cells with solar thermal collectors. It can be to utilize reflectors to focus the solar radiation onto the cells or it could be building integration where building materials can be replaced by the solar collectors and solar modules. All these techniques have the potential for decreasing the cost of solar energy. However, when a product is used for multiple purposes there is always a risk of complex interactions with the surrounding.

A PV/T solar window has been developed, (Fieber, 2003, 2004, 2005). An analysis on a component level (Davidsson et al., 2009) shows that the solar window produces 35% more electric energy per cell area compared to a PV module installed vertically on a south wall. Other PV/T hybrid collectors have been reported earlier as cost effective collectors (Anderson et al., 2009; Kalogirou and Tripanagnostopoulos, 2006; Krauter and Ochs, 2003; Tonui and Tripanagnostopoulos, 2007). The solar window, shown in Fig. 1, is a multifunctional PV/T hybrid constructed of absorbers on which PV cells have been laminated. To reduce the total cost of the construction the solar window is building integrated into a standard window. Tiltable reflectors are introduced in the construction behind the absorbers. When the reflectors are placed in a vertical position they focus radiation onto the absorbers. If the reflectors are tilted to a horizontal position they allow daylighting and passive heating of the building. Located in a window, the solar collector will influence the building in both positive and negative ways. When the insulated reflectors are placed vertically the thermal losses through the window are reduced. However, placed in a window, the collector will block some of the radiation that would otherwise heat the building passively. This problem is not shared by PV/T collectors integrated on the envelope of the building (Corbin and Zhai, 2010).

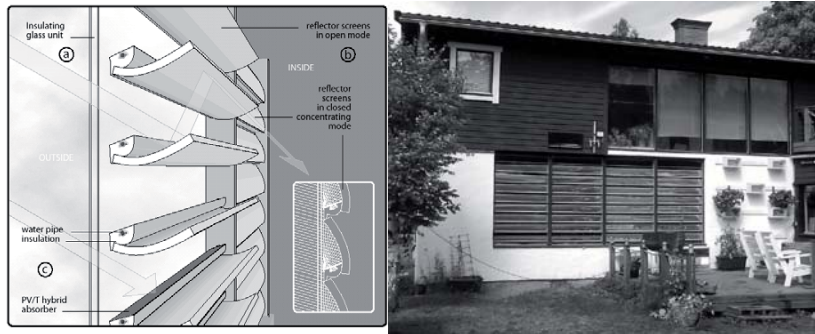


*Fig. 1 Left; the solar window with water cooled PV cells, tiltable reflectors and anti reflection treated glazing. Right; the solar window in Solgården.*

The tiltable reflectors also make it possible to control the intensity of solar radiation transmitted into the building. An efficient control strategy for the reflectors can both minimize the auxiliary energy required and at the same time keep the indoor temperature at a desired level. The control strategy can for instance allow the reflectors to be open at night to have a high U-value and thus cool down the building. This is not an option for a standard window with low U-value.

Other types of mechanisms to control the amount of solar radiation let into the buildings have been reported, for instance using thermotropic glass with active dimming (Inoue et al., 2008) or electrochromic smart windows (Granqvist et al., 1998). The official homepage of IEA SHC Task 21 Daylight in Buildings (IEA SHC) gives a good overview of different solar shading systems.

### 1.1 Solgården, the building

The solar window is installed in a one family building, shown in Fig. 1, called Solgården in Älvkarleö (60.57N, 17.45E) in the central parts of Sweden. The building is constructed from large blocks made of Expanded Poly Styrene, EPS (davidhellgren). This technique gives the building a well insulated skin without plastic films which is still airtight and suitable for efficient heat recovery from the ventilation system. Solgården is a low energy building but does not qualify as a passive house due to the active underfloor heating system.

The solar window is connected to a thermal storage tank of 620 litres where thermal energy is stored. The auxiliary thermal energy need is produced with a 9 kW pellet burner. The heating and electrical system is adapted for a future Stirling engine. The produced electrical power from

the solar window is stored in a battery bank using a combined regulator, charger and inverter. The battery bank ensures that no electric energy is lost due to mismatch between the electric production in the PV cells and consumption of electricity in the building. The capacity of the battery bank is far larger than the daily electrical energy usage. A sketch of the system is illustrated in Fig. 2.

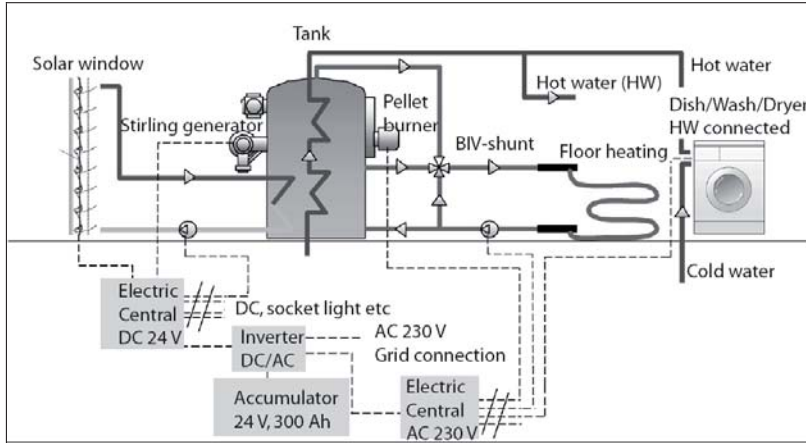
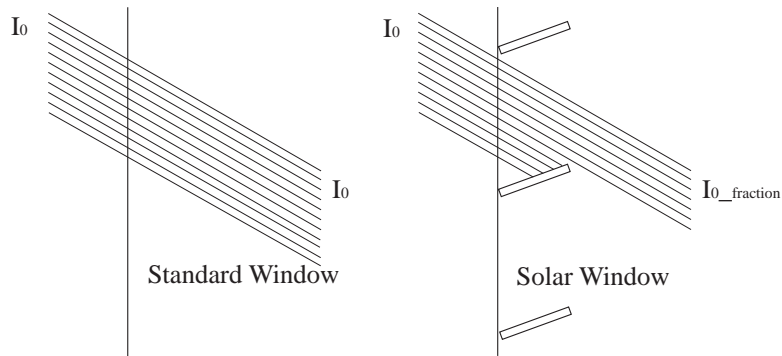


Fig. 2 The energy system in Solgården.

## 1.2 Energy balance of the solar window.

Since the solar system components are located on the inside of a standard window, this will affect the energy balance in the building in both positive and negative ways. On the positive side are the effects of lowering the U-value of the total construction when the reflectors are closed, in an upright position. Closing the reflectors during hot and sunny days will reduce the risk of overheating. However, there are also effects that have a negative impact on the energy balance in the building. Since the collectors are placed in the window the absorbers will block some of the radiation that would otherwise illuminate and heat the building, as illustrated in Fig. 3. This is compensated for by installing a larger window. If the reflectors are closed, put in an upright position, there will be very little light entering the room. This has to be compensated for with extra artificial lighting. This effect was however not included in the simulations presented in this article.



*Fig 3 Left, a standard window; all the transmitted radiation heats the building. Right the solar window; only a fraction of the radiation heats the building directly as one part is collected in the absorbers. The reflectors have been removed for clarity.*

The glazing of the window is anti reflection treated (Nostell et al., 1999) in order to maximize the transmission through the window. The panes have no low emittance coatings since these would decrease the transmittance and the PV-performance. The negative effect of having no low emittance coating is that it results in a high U-value and hence high thermal losses for the large area window.

An analysis was made to investigate the potential for improving the performance of the solar window. In this developed solar window a low-e coating was put on the glazing to lower the thermal losses. The absorbers were also better insulated for minimizing the losses. The low-e coating will not only lower the thermal losses but also lower the transmission through the glazing. We estimate a reduction of the transmission by 20% compared to the glazing in the standard solar window. The warm solar window collector has thermal losses to two different temperatures, the ambient and the indoor temperature. The losses from the solar window to the inside of the building heat the building passively. Table 1 presents the heat transfer coefficients for heat dissipated from the absorbers to the surroundings or indoors. In the table the open mode is the solar window with horizontal reflectors and the closed mode is the case with the reflectors in a vertical position. All the numbers in Table 1 are calculated values. The total loss from the standard solar window using closed reflectors was calibrated against measured data. Since the solar window was not completed when the measurements took place the absorbers could not be tilted to an open position. However, the theoretical basis for the calculations it is the same as in the closed mode. In the open mode all the convectational losses are assumed to be lost to the room. This will slightly overestimate the heat

gain to the room. In the developed solar window all the values for the thermal losses have been derived theoretically.

Table 1 Heat transfer coefficients of the solar window collector.

| Thermal losses / [ $\text{W}/\text{m}^2\text{K}$ ], Solar window PV/T Collector |               |     |             |     |
|---|---------------|-----|-------------|-----|
| Closed/open mode  | Closed window |     | Open window |     |
| Direction of thermal loss dissipated from the absorber                          | In            | Out | In          | Out |
| Standard Window   | 3.9           | 2.0 | 5.8         | 1.3 |
| Developed Window  | 0.7           | 1.3 | 3.5         | 0.7 |

The standard conventional U-value of the window was determined to be  $2.4 \text{ W}/\text{m}^2\text{K}$  for open reflectors and  $1.3 \text{ W}/\text{m}^2\text{K}$  for closed reflectors (Fieber 2005). For the developed solar window the U-value was estimated to be reduced to  $1.5 \text{ W}/\text{m}^2\text{K}$  for open reflectors and  $0.6 \text{ W}/\text{m}^2\text{K}$  for closed reflectors.

### 1.3 Reflector control strategy

The tiltable reflectors in the solar window were controlled using four different strategies. The strategies are listed below;

1. Always open, horizontal, reflectors.
2. Always closed, vertical, reflectors.
3. The reflectors are open if the intensity of the solar radiation onto the window plane lies between two user defined values. If the intensity falls below the interval the reflectors close in order to lower the U-value of the window to prevent the building from cooling down. If the radiation goes above the interval the reflectors close to avoid overheating of the building.
4. If the temperature in the building falls below a user defined value the window aims to heat the building directly, i.e. the hot water production and the electrical production are of less importance. This means that the model calculates the energy balance for open reflectors and closed reflectors and chooses the most energetically favourable alternative. If the indoor temperature exceeds the upper user defined value the window endeavours to minimize the energy transmitted into the building. This means that during periods with overheating the reflectors will typically close during daytime to prevent passive heating and open during night time for increasing the U-value and thus the heat losses to dissipate the heat out from the building. If the temperature lies between the two

stated temperatures the window will be closed to fill the batteries and the collector tank to a preset level. When this condition is fulfilled the reflectors will be opened for daylighting.

All these control strategies were simulated.

## 2 Method

The work presented in this article aims to investigate the solar window on a system level. The parameters used in the simulations were found experimentally (Davidsson et al., 2009).

Simulations were used to investigate the complex interaction between the solar window and the building in which it is installed. The building with the solar window was compared to an identical building without the solar window, with and without a more conventional solar energy system. Fig. 4 shows the three different systems. System 1 is the solar window system. System 2 is a reference system where the 16 m<sup>2</sup> solar window was removed and replaced by an 8 m<sup>2</sup> large standard window with U-value 1.1 W/m<sup>2</sup>K. System 3 is the reference system including a solar energy system of the same size as the solar window system i.e. 4 m<sup>2</sup> PV-cells and 5.06 m<sup>2</sup> solar thermal absorbers. The solar collector used is assumed to be characterized by  $\eta_{\text{direct}} = 0.75$ ,  $\eta_{\text{diffuse}} = 0.68$  and with a U-value of 4 W/m<sup>2</sup>K.

The main reason for installing a window is to get daylight into the building. Since the absorbers and reflectors in the solar window block a substantial part of the glazing the solar window has to be larger in size than a standard window. This is why the reference case was equipped with a window half the size of the solar window. Depending on the fraction of direct and diffuse solar radiation and the solar altitude about half the solar window is blocked by absorbers and reflectors.

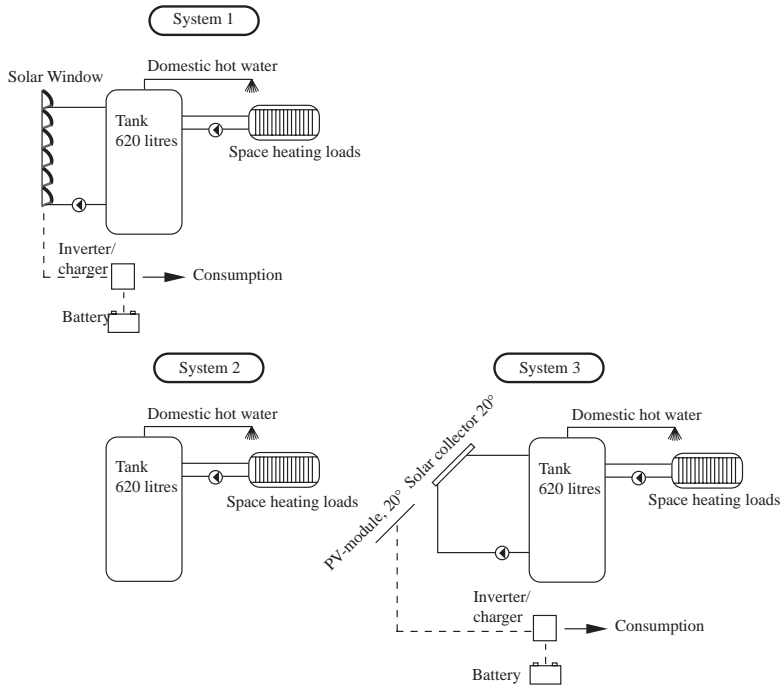


Fig 4 The three different simulated systems. System 1 shows the system for the solar window, system 2 is the reference system without solar energy system and system 3 is the reference system including a solar energy system.

## 2.1 TRNSYS Modelling

The modelling of the system was performed using TRNSYS. The TRNSYS deck was calibrated against measured consumption of wood pellets and electricity for the building Solgård. Some of the most important parameters are listed below,

- **Battery/Inverter and load.** A battery bank of 10.6 kWh and a constant electrical load of 375 W throughout the year, i.e. 3285 kWh annually.
- **Tank.** The tank, TRNSYS type 60 (Klein et al. 2000), has a volume of 620 litres. The hot water consumption was set to 9 litres per hour throughout the year.
- **Building.** The one zone building, TRNSYS type 12 (Klein et al. 2000), model is a lumped capacitance degree hour model with internal gain. This simplification equates to a building with an open plan layout,

which is the case for Solgården. The building has a UA-value of 110 W/K and a thermal capacitance of 40000 kJ/K. The UA-value of the building is lowered to 95 W/K for the developed solar window simulation since its U-value is reduced from 2.43 W/m<sup>2</sup>K to 1.5 W/m<sup>2</sup>K. The UA-value is reduced to 80 W/K for the simulations for system 2 and system 3 since the 16 m<sup>2</sup> large solar window is replaced with an 8 m<sup>2</sup> large standard window.

- **Weather data.** The weather data used for the simulation is derived with meteonorm (Meteonorm) for Gävle, about 20 km from Älvkarleö.
- **Solar window.** A new TRNSYS component for the solar window was constructed.
- The separate PV and collector used to model the solar energy system in system 3 are simplified first order models taking into account solar beam and diffuse radiation, incidence angle, inlet and ambient temperature.
- The thermal losses from the storage tank, the used electricity, the heat produced by the people in the house and the radiation transmitted into the building through the windows are added as internal gains for the building.

The developed TRNSYS deck allows the electrical and thermal energy production to be simulated. When the control strategies 3 and 4 are simulated the upper and lower solar radiation intensity limits have to be specified. The choice of intensity limits will affect both energy production and hence the auxiliary energy need and the thermal comfort in the building. If the upper parameter for control strategy 3 is set too high, i.e. the reflectors are open during high levels of irradiance; the building is likely to become overheated during hot and sunny summer days. Setting the lower parameter too low will result in open reflectors during hours of low irradiance, hence giving large thermal losses.

To investigate the importance and difference in energy production and auxiliary energy need for the building a parametric study was performed for the standard solar window using control strategies 3 and 4 with varying upper and lower parameters. How to control the reflectors is a highly complex question and there are most likely many answers. The choice of optimizing energy production, thermal comfort or daylight is in many cases a personal preference.

The results of the simulations of the required auxiliary energy need should primarily be used for comparative studies. The building in the TRNSYS deck serves as a load for the solar energy system. For a complete evaluation of the building itself a more detailed house model than the TRNSYS type 12 has to be used.



### 3 Results

The parameter study using the 3:rd control strategy was performed for different upper and lower levels according to Fig. 5. The figure shows simulations with the lower parameter set to 100, 200 and 300 W/m<sup>2</sup> respectively indicated with arrows. On the x-axis is the upper parameter. The lowest energy consumption is obtained using 100 W/m<sup>2</sup> as lower parameter and 800 W/m<sup>2</sup> as the upper parameter. This means that the window is open during practically all the bright hours. Problems might arise during summer hours with strong irradiance. Windows with open reflectors can easily overheat the building.

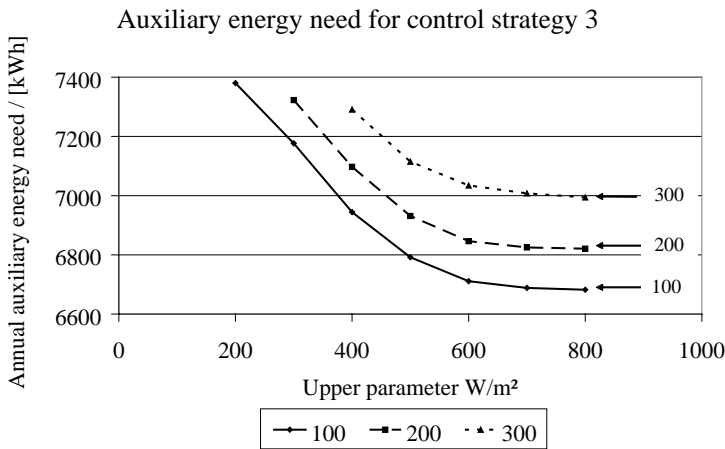


Fig. 5 The annual auxiliary energy need using control strategy 3 for the reflectors as a function of the upper control level for different lower levels.

The same kind of analysis for control strategy 4 is presented in Fig. 6. The lower and the upper parameter were allowed to vary between 22°C and 30°C. As can be seen in the figure the difference in auxiliary energy need is rather small. The lowest energy consumption is obtained using 26°C as lower parameter and 30°C for the upper parameter. However, these are not levels of indoor temperature that are normally preferred by the inhabitants. The solar window is thus not used in an optimal way for the thermal comfort. The preferred levels will be different for different persons and from different location of installation. The strategy might for instance differ between a staircase and an office room.

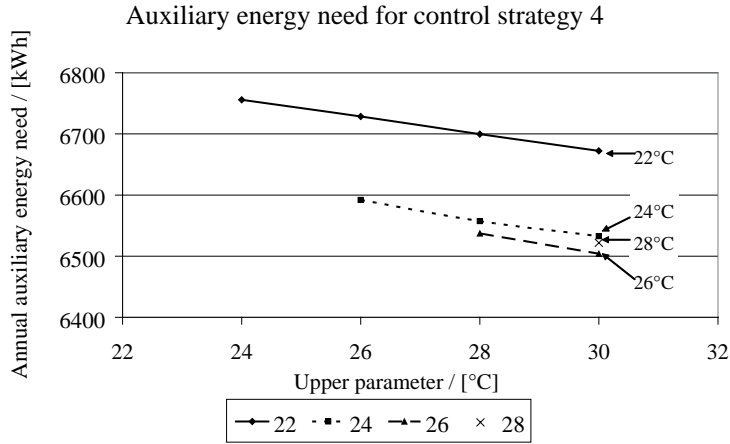


Fig. 6 The annual auxiliary energy need using control strategy 4 for the reflectors.

The choice of control strategy and control parameters will not only affect the annual auxiliary energy demand for heating but also the electrical energy production and the thermal comfort in the building. This is illustrated in Table 2. Depending on what is optimized the control strategy must be changed. If the priority is to maximize the electrical energy production control strategy 2 should be used. This strategy is however giving the highest auxiliary energy need. If good thermal comfort in the building is the main priority control function 4 should be used with low parameters. The row “Over heated building” gives the fraction of the year with indoor temperature above 30° C. The most optimized control strategies and parameters are marked with grey background.

Table 2      Parameter study of different control strategies for the reflectors. The parameter row shows what values were used for lower and upper parameters for the control strategy. Control strategy 1 and 2 have no parameters. The row “Over heated building” gives the fraction of the year with indoor temperature above 30° C.

|                             | Control 1 | Control 2 | Control 3 |         | Control 4 |       |
|-----------------------------|-----------|-----------|-----------|---------|-----------|-------|
| Parameters                  | X         | X         | 100/400   | 100/800 | 22/26     | 26/30 |
| Auxiliary energy need / kWh | 8000      | 7500      | 6900      | 6700    | 6700      | 6500  |
| Produced ther. energy / kWh | 1500      | 2500      | 2300      | 1700    | 2100      | 2000  |
| Produced el. energy / kWh   | 300       | 430       | 400       | 330     | 390       | 370   |
| Over heated building / %    | 27        | 23        | 27        | 33      | 18        | 20    |

In the following simulations the 4:th control function was used. The control parameters were set to 22° C and 26° C.

The annual distribution of the produced thermal and electrical energy can be seen in Fig. 7. The PV cells have a more even annual distribution than solar collectors. This is explained by the thermal losses of the collectors which have to be balanced before heat is delivered. This is why the thermal and the electrical output in December are on the same level while the thermal output is about seven times larger than the electrical output during the summer.

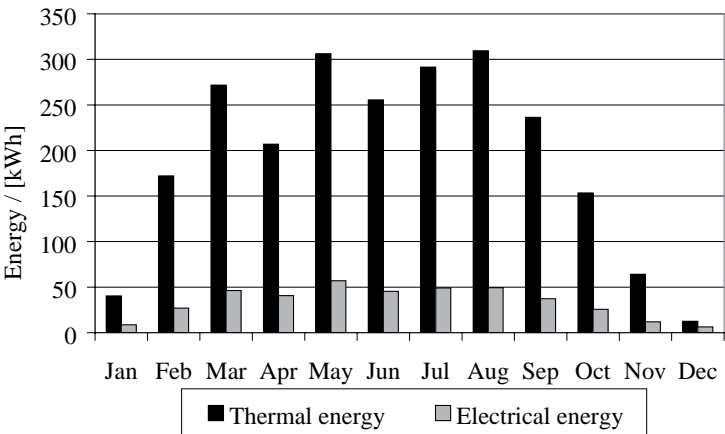


Fig. 7      The annual distribution of delivered solar energy from the window, in black the solar thermal and in grey the solar electricity.

Fig. 8 shows the results for the annual auxiliary energy need from the simulations where the building Solgården was equipped with different types of solar energy systems according to Fig. 4. The first bar is Solgården with a 16 m<sup>2</sup> solar window. The second bar is Solgården with the developed solar window. The third bar is the simulation for system 2 and the last bar is for system 3. In system 3 the solar energy system is placed on the roof tilted 20° to the horizontal.

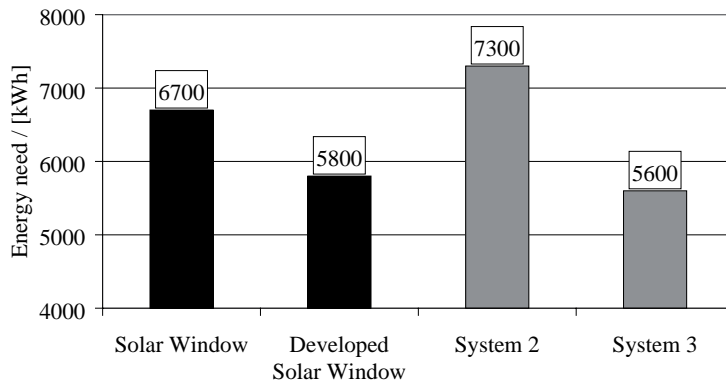


Fig. 8 The auxiliary energy need for Solgården using different types of solar collectors.

Fig. 9 shows the results from a simulation where the solar window or collector area has been increased by 50%. For the solar window case this gives a negative impact since the thermal energy gain from the collector does not compensate for the increased heating required to balance the heat loss due to the larger glazed area. For the roof mounted collector the situation is different, the increase of the collector area increases the thermal production without increasing the thermal losses of the building.

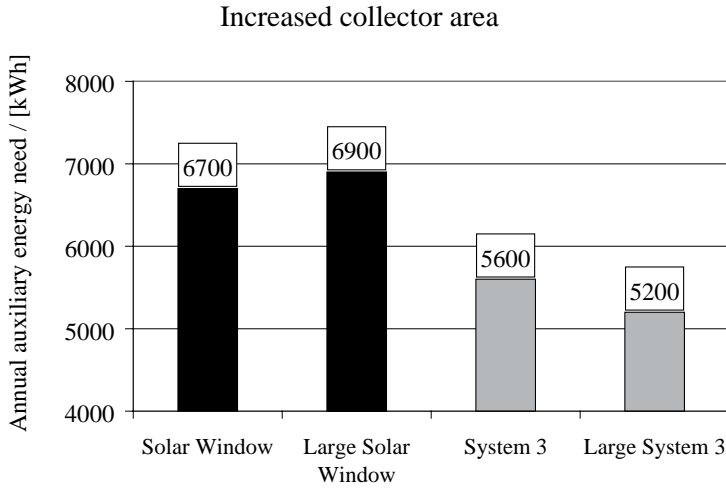


Fig. 9      *The solar window is in black and the reference in grey. The second and fourth bars labelled large are where the solar window or collector area has been increased by 50%.*

#### 4 Discussion and conclusion

The main goal with the solar window is to lower the auxiliary energy need for a building using active solar heating. PV/T hybrid technology, combining thermal and electrical production in one absorber, has the possibility to reduce the total cost of a solar energy system. Another way to reduce the costs of a system is to use relatively cheap reflectors to replace the more expensive PV cells. Building integration of the collectors also has the potential to reduce the costs when building materials can be replaced.

The complicated interaction between the solar window and the building in which it is installed requires an investigation of the thermal performance of the whole system. Depending on how the reflectors are controlled the performance of the solar window will vary substantially. How to control the reflectors depends on the priorities made by the user. If the electrical energy production is highly prioritised, control strategy 2, always closed reflectors, is the best choice. If the annual auxiliary energy need is to be minimized, control strategy 4 is to be preferred as can be seen in table 2.

The rather large difference in thermal comfort shown in table 2 between the third and the fourth strategy is explained by the fact that the third strategy control does not open the reflectors at night even though this would result in larger energy losses and thus lower indoor temperatures in overheating situations. The fourth control function does not only optimize the thermal comfort, it also minimizes the auxiliary energy required for the

building. If the reflectors are not controlled with regard to both radiation and temperature the function of the solar window is not optimized. For instance the overheating in the building is lowered if the reflectors are closed even though the radiation is moderate during a hot period. During winter the reflectors can be tilted to an open mode if the radiation is large. This might not be the case if only a radiation dependent control strategy is used. In this case the reflectors might close since the intensity exceeds the limits. This is unwise since it is much more energetically favourable in this situation to heat the building passively instead of actively via a solar thermal system.

When the solar window is compared to a standard system, with solar collectors and PV modules on the roof, both mounted on similar buildings, the annual auxiliary energy need is considerably higher for the solar window case. The difference between the systems is about 1000 kWh annually. The main reason for this is the high U-value for a building with a solar window. To investigate whether the solar window can be improved, a developed solar window was modelled. The glazing of the standard solar window does not have a low emittance coating in order to maximize the transmitted radiation and thus maximize the electrical and thermal output. The effects of adding a low emittance coating on the glazing and improving the insulation on the absorbers can be seen in Fig 9. The bar labelled “Developed” is for the developed solar window. It is clearly shown that the annual auxiliary energy need is considerably lower compared to the standard solar window. It is thus more important to lower the thermal losses than to maximize the thermal output from the collector part of the window.

Apart from the above stated problems with high U-value of the solar window there is also a problem with competition of the solar radiation between the solar energy system and passive heating and daylighting. If the solar radiation is converted into thermal or electrical energy it can not also be used for passive heating or daylighting of the building, i.e. a photon can only be used once. In Fig 10 this corresponds to the right figure, the solar window system. The “active” area is A whether or not the absorbers, illustrated with black lines, are installed. In system 3 all the radiation that hits the window can be turned into passive heating at the same time as the solar energy system on the roof delivers energy to the hot water tank and to the battery. In Fig. 10 this corresponds to the left figure where the “active” area is A+B. In this case there is no competition.

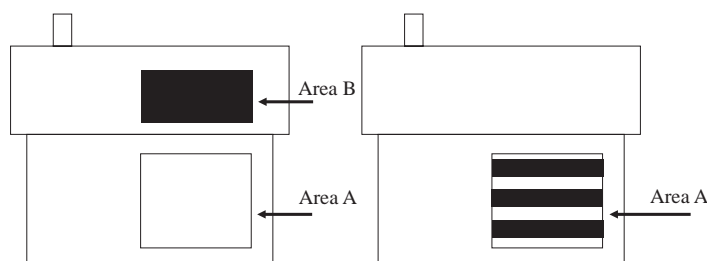


*Fig. 10 Left, Building with a window of size A and a solar collector of size B on the roof. Right, Building with a window of size A in which a solar collector of size B has been placed.*

In Fig. 9 it is shown that a larger solar window will be negative for the energy balance. The larger glazed areas will inevitably lead to larger thermal losses for the building during the winter. At the same time the thermal energy utilization in the solar window collector is becoming saturated. Less thermal energy can be utilized per collector area as the collector areas grow. This is not a problem shared by system 3. In this case the thermal loss from the building is independent of the collector area. The extra energy added to the tank is the only difference and thus the auxiliary energy need is reduced.

If the solar window is to become commercially marketable the U-value of the construction needs to be reduced substantially. At the same time there are many benefits with the solar window. The solar window works both as solar shading and directs the incoming solar radiation to the back of the room when the rays are reflected in the back tilted reflectors. Such benefits are outside the scope of this paper. The reference system also needs to be supplied with a sunshade.

## Acknowledgements

This work was supported by the Swedish Energy Agency through the program Solel 03-07. B. Hellström and H. Håkansson at Lund University and S. Larsson at Vattenfall Development are acknowledged for assistance during measurements and evaluation.

## References

- Anderson, T.N., Duke, M., Morrison, G.L., & Carson, J.K. (2009). Performance of a building integrated photovoltaic/thermal (BIPVT) solar collector. *Solar Energy* 83 (2009), p 445-455.
- Corbin, C.D., & Zhai, Z. J. (2010). Experimental and numerical investigation on thermal and electrical performance of a building integrated photovoltaic-thermal collector system. *Energy and Buildings* 42 (2010), p 76-82.
- Davidsson, H., Perers, B., & Karlsson, B. (2010). Performance of a multifunctional PV/T hybrid solar window. *Solar Energy* 84 (2010), p 365-372.
- Fieber, A., Gajbert, H., Håkansson, H., Nilsson, J., Rosencrantz, T., & Karlsson, B. (2003). *Design, Building integration and performance of a hybrid solar wall element*. Proceedings of ISES Solar World Congress 2003 Gothenburg, Sweden
- Fieber, A., Nilsson, J., & Karlsson, B. (2004). *PV performance of a multifunctional PV/T hybrid solar window*. Proceedings of 19th European photovoltaic solar energy conference and exhibition 2004, Paris, France
- Fieber, A. (2005). *Building Integration of Solar Energy*. Lic. Thesis Report, EBD-T--05/3, p 107-192. Lund: Lund University, Lund Institute of Technology, Department of Construction and Architecture, Division of Energy and Building Design. Available at; [http://www.ebd.lth.se/fileadmin/energi\\_byggnadsdesign/images/Publikationer/AvhandlingWEB\\_alt\\_Andreas.pdf](http://www.ebd.lth.se/fileadmin/energi_byggnadsdesign/images/Publikationer/AvhandlingWEB_alt_Andreas.pdf) visited 2010-01-18.
- Granqvist, C.G., Azens, A., Hjelm, A., Kullman, L., Niklasson, G.A., Rönnow, D., Strømme Mattsson, M., Veszelei, M. & Vaivars, G. (1998). Recent advances in electrochromics for smart windows applications. *Solar energy* 63 (1998), p 199-216.
- Hellgren, D. Hellgrens Ingenjörbyrå, web page visited 2010-01-18 from Hellgrens homepage [www.davidhellgren.se](http://www.davidhellgren.se)
- IEA SHC Task 21. IEA SHC Task 21 Daylight in Buildings, web page visited 2010-01-18 from IEA Task 21 homepage: <http://www.iea-shc.org/task21/index.html>
- Inoue, T., Ichinose, M., & Ichikawa, N. (2008). Thermotropic glass with active dimming control for solar shading and daylighting. *Energy and Buildings* 40 (2008), p 385-393.



- Kalogirou, S.A., & Tripanagnostopoulos, Y. (2006). Hybrid PV/T solar systems for domestic hot water and electricity production. *Energy conversion and management* 47 (2006), p 3368-3382.
- Krauter, S., & Ochs, F. (2003). Integrated solar home system. *Renewable energy* 29 (2003), p 153-164.
- METEONORM 5.0. Global meteorological database for solar energy and applied meteorology, webpage visited 2010-01-18 from Metotest: [www.meteotest.ch](http://www.meteotest.ch)
- Nostell, P., Roos, A., & Karlsson, B. (1999). Optical and mechanical properties of sol-gel antireflective films for solar energy applications. *Thin solid films* 351, p 170-175.
- Tonui, J.K., & Tripanagnostopoulos, Y. (2007). Improved PV/T solar collectors with heat extraction by forced or natural air circulation. *Renewable Energy* 32 (2007), p 623-637.
- TRNSYS Reference Manual. (2000). Klein, S.A., Beckman, W.A., Mitchell, J.W., Duffie, J.A., Daffie, N.A., & Freeman. T.L., Madison: Solar Energy Laboratory, University of Wisconsin.

## Article III





### 364 - Performance of a multifunctional PV/T hybrid solar window

Henrik Davidsson\*, Bengt Perers, Björn Karlsson

Energy and BuildingDesign, Lund University, B.O Box 118, SE 221 00 Lund, Sweden

\*Corresponding Author, henrik.davidsson@ebd.lth.se

#### Abstract

A building-integrated multifunctional PV/T collector have been developed and evaluated. The PV/T solar window is constructed of PV cells laminated on solar absorbers and is placed in a window behind the glazing. To reduce the costs of the solar electricity, reflectors have been introduced in the construction to focus radiation onto the solar cells. The tiltable reflectors render a possibility to control the amount of radiation transmitted into the building. The insulated reflectors also reduce the thermal losses through the window. A model for simulation of the electric and hot water production was developed. The model can perform yearly energy simulations where different effects such as shading of the cells or effects of the glazing can be included or excluded. The simulation can be run with the reflectors in an active, up right, position or with the reflectors in a passive, horizontal, position. The simulation program was calibrated against measurements on a prototype solar window placed in Lund in the south of Sweden and against a solar window built into a single family house, Solgården, in Älvkarleö in the middle of Sweden. The results from the simulation shows that the solar window produces about 56% more electric energy per unit cell area compared to a vertical flat PV module.

Keywords: solar window, PV/T

#### 1. Introduction

A diversity of technical solutions needs to be applied and developed if solar electricity is to become cheap enough to compete with grid electricity. One technique for reducing the price of solar electricity is to use the reflector to focus radiation onto the PV cells, thus allowing expensive PV cells to be replaced by considerably cheaper reflector material. Active water cooling on the back side of the cell gives both relatively cold, high efficient cells, and hot water for domestic use. Further price reduction is possible if the solar modules can be integrated into the building construction. Integration makes it possible to use existing frames and glazing for the solar modules or, alternatively, to replace roofing materials and windows by solar modules. Wall integrated solar collectors using reflectors have been shown to increase the electrical output substantially [1] compared to flat vertical PV modules. All these technologies have been combined in the PV/T hybrid technology presented in this work.

A building integrated multifunctional solar window was proposed and developed by Fieber [2]. The solar window, see figure 1, is constructed of absorbers on which the PV cells have been laminated. The solar window is building-integrated into the inside of a standard window, thus saving frames and glazing and lowering the total price of the construction. In order to minimize the PV cell area, reflectors have been placed behind the absorber. When tilting the foldable reflectors to a vertical position the solar radiation is focused onto the absorbers. When the reflectors are tilted to a horizontal position the solar radiation is let into the building to allow for passive heating. This means that the

reflectors in a closed position increase the radiation on the cells, reduce the thermal losses through the window and also work as a sun shade. The glazing of the window in front of the absorbers is anti reflection treated to maximize the transmittance.

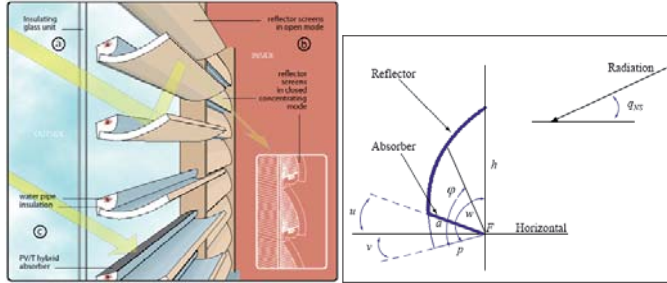


Fig 1. Left; the solar window with water cooled solar cells, insulated and tiltable reflectors and anti reflection treated glazing. Right; illustration of the parabolic reflector and the absorber

## 2.1. Geometry

The geometry of the solar window is shown in figure 1 above. The optical axis,  $v$ , of the parabolic reflector is directed  $15^\circ$  above the horizon with focus on the front edge of the absorber. This means that all radiation from  $15^\circ$  and higher solar altitudes will hit on the absorber between the focal point,  $F$ , and the reflector. The focal length is denoted  $p$ , the height of the glazing  $h$  and  $a$  is the absorber width. The angle  $w$  is the angle between the glazing and the absorber plane and  $q_{NS}$  is the incident angle of the solar radiation projected in the north-south vertical plane. The absorbers are 1.11 m long and 8 cm wide, and the PV cells are 12.5 cm \* 6.25 cm. The solar window in Solgården is constructed of 8 absorbers per window unit, and the prototype solar window is constructed of 5 absorbers, see figure 2. The Solgården solar window has 64 PV cells in series and the prototype solar window has 8 PV cells in series. The total window area is 16 m<sup>2</sup> in Solgården and about 1.2 m<sup>2</sup> for the prototype solar window.

The reflector parabola is described in Eq. (1).  $r$  is a vector from  $F$  to a point on the parabola at angle  $\varphi$ .

$$r(\varphi) = p / \cos^2(\varphi) \quad (1)$$

Both  $h$  and  $a$  can be expressed by  $r$  for the two angles  $w=105^\circ$  and  $u+v=35^\circ$ , respectively for the solar window. The ratio between  $h$  and  $a$ , which is defined as the geometrical concentration factor, can be calculated to be 2.45 for the construction.

The architectural implication such as light distribution has been investigated [2]. Following this, long term measurements were performed regarding energy production, both electrical and hot water. This was carried out on a prototype solar window placed in Lund in the south of Sweden as well as from a solar window built into a residential building in Älvkarleö about 100 km north of Stockholm, Sweden.

In this paper, we describe a model developed to simulate the yearly energy production of the hybrid window system from climatic data. The model uses both experimentally measured parameters and theoretically derived values and functions in the calculations. It takes into account shading caused by the window frames and also includes the transmittance through the glazing and the angular dependence of the PV cells. The model also allows for analyzing different limiting effects such as shading or transmittance through the glazing. This makes it possible to study the potential of development for the solar window.

## Method

Measurements of the performance of the multifunctional PV/T hybrid solar window were carried out during 2006 on a prototype solar window placed in Lund, Sweden (55.44N, 13.12E). A full scale system combining 4 of these solar windows, another 4 is planned, was installed in a single family home called Solgården in Älvkarleö, Sweden (60.57N, 17.45E) and evaluated during 2006-2008. The window was directed 23° towards east. The solar windows can be seen in figure 2. The measurements of the generated current and voltage produced by the prototype solar window were carried out using a Campbell CR1000. The radiation, temperatures and water flow through the absorbers was measured using a Campbell CR10 logger. The temperature measurements were carried out using PT100 sensors. All measurements made in Solgården used a Campbell CR10. Measurements were monitored both with the reflectors in a horizontal and in a vertical position. The prototype solar window was supplied with water of constant inlet temperatures and the measurements were carried out during both day and night. Night time data were used for determining the thermal losses of the window.



Fig 2. Left figure; the prototype solar window with five absorbers. Right figure; the solar window in Solgården with closed reflectors.

A simulation model was developed to evaluate the solar window. The model uses the direct and diffuse radiation together with the inlet water temperature, the ambient temperature and the time, and thus the solar angles, as inputs. The outputs are thermal and electrical delivered power. In order to simplify the calculations the power delivered by the solar window was divided into three components,  $P_{\text{direct}}$ ,  $P_{\text{reflector}}$ , and  $P_{\text{diffuse}}$ . The first is  $P_{\text{direct}}$ , power caused by the direct radiation that hits the absorber directly, the second component is  $P_{\text{reflector}}$ , power caused by the direct radiation that goes via the reflector. The third component,  $P_{\text{diffuse}}$ , is the power contribution caused by the diffuse radiation. Figure

3 graphically explains the three different components of radiation.  $P_{total}$  is the total power delivered by the window.

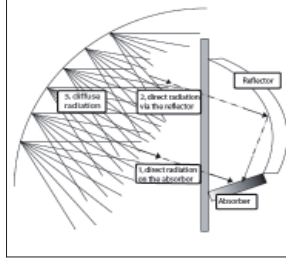


Fig 3. A graphical explanation of the calculation method with the three different radiation components.

The expression for the electrical output is shown below.

$$P_{direct} = I_b * T_{glass}(\Theta_1) * \alpha_{pv}(\Theta_2) * f_{shading}(\Theta_3) * A_{cell} * \eta_{pv} * \cos(\Theta_2) \quad (2)$$

$$P_{reflector} = I_b * T_{glass}(\Theta_1) * \alpha_{pv}(\Theta_4) * f_{reflector}(\Theta_5) * A_{reflector} * \eta_{pv} * R_{reflector} * \cos(\Theta_5) \quad (3)$$

$$P_{diffuse} = I_{diffuse} * C_{1,2} \quad (4)$$

$$P_{total} = P_{direct} + P_{reflector} + P_{diffuse} \quad (5)$$

$I_b$  and  $I_{diffuse}$  are the beam radiation and the diffuse radiation against the window.  $T_{glass}$  describes the angular dependent transmittance through the glazing;  $\alpha_{pv}$  describes the angular dependence of the absorptance of the PV cells, and  $f_{shading}$  describes the shading of the PV cells caused by the window frame.  $f_{reflector}$  is a correction factor for the shadow effects for the radiation which is reflected. This function includes the shading of the reflector. The angles  $\Theta_1$  to  $\Theta_5$  are the different incidence angles for the beam towards the components of the solar window.  $A_{cell}$  and  $A_{reflector}$  are the areas of the PV cell and the reflector, respectively.  $\eta_{pv}$  and  $R_{reflector}$  are the efficiency of the solar cells and the reflectance of the reflector.  $C_{1,2}$  is a response function for the diffuse radiation obtained from measurements during cloudy days, when the beam radiation has negligible influence on the performance. Measurements during cloudy days were performed with the reflector in both horizontal and in vertical positions, allowing both  $C_1$ , horizontal reflector and  $C_2$ , vertical reflector, to be determined. The transmittance,  $T_{glass}$  through the window was calculated using Fresnel's equations and Snell's law. The shading factors  $f_{shading}$  and  $f_{reflector}$  were calculated theoretically from the PV/T window geometry. A measurement was performed to determine  $\alpha_{pv}$ , the angular dependence of the PV cells.

In order to calculate the thermal output a fourth term has to be added to describe the thermal losses in the absorber. The thermal losses,  $P_{thermal\ loss\ prototype}$  for the prototype solar window and the thermal losses  $P_{thermal\ loss\ Solgärden}$  is shown below.

$$P_{thermal\ loss\ Solgärden} = U_{solgärden\ out} * A_{window} * \Delta T_{out} + U_{solgärden\ in} * A_{window} * \Delta T_{in} \quad (6)$$

$$P_{thermal\ loss} = U_{prototype} * A_{window} * \Delta T \quad (7)$$

Since the solar window in Solgården experiences thermal losses to two different temperatures, the ambient temperature and the indoor temperature, two different U-values were used. The  $U_{\text{solgården out}}$  is the thermal loss to the outside and the  $U_{\text{solgården in}}$  is the thermal loss to the inside.  $A_{\text{window}}$  is the total window area.  $\Delta T_{\text{out}}$  is the temperature difference between the ambient temperature and average water temperature and  $\Delta T_{\text{in}}$  is the temperature difference between the indoor temperature and the average water temperature.  $U_{\text{prototype}}$  is the U-value for the prototype solar window and  $\Delta T$  is the temperature difference between the ambient temperature and the average water temperature.

## Result

Two different types of graphs were used to validate the model. The first type is shown in figure 4, where results from measurements and simulations are compared. The short circuit current  $I_{\text{sc}}$  in the right figure is from a cell placed in the solar window. The days were chosen to illustrate different weather conditions, such as different ambient temperatures and cloudy weather with sunny intervals. The days were also chosen to show different seasons and thus different solar angles.

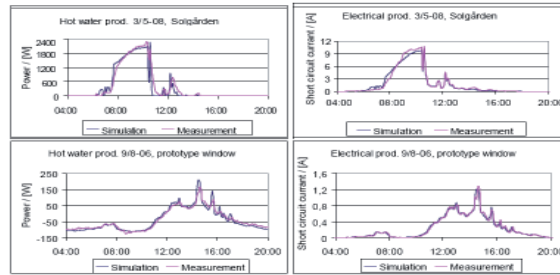


Fig 4. Measured and simulated thermal and electrical output for the window in Solgården (upper) and in the prototype window (lower). Blue is the simulated output and purple is the measured output. On the x-axis is the time of the day.

During the measurements on the prototype solar window two different, not perfectly synchronized, loggers for monitoring the electrical output and the radiation were used. This means that synchronization problems could arise during partly cloudy days. If the electrical output was measured during a cloudless time and the irradiance was measured during a cloudy time the result from the simulation, using the irradiance as input, differs from the measurement. To solve this problem the simulated and the measured output was integrated daily. Then this irregularity will disappear. The result from this analysis is shown below in figure 5 where the integrated daily measured output on the y-axis is plotted against the integrated daily simulated output on the x-axis. A perfect agreement between simulation and measurement would put all the points on the line,  $x=y$ . This analysis was performed both for the thermal output, left figure, and the electrical output, right figures. Validation from the prototype solar window is in blue and the validation from Solgården is in purple. All values have been normalized to the highest output in each series. The correlation is high for all four validations.



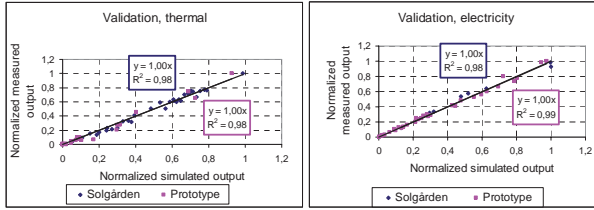


Fig 5. The thermal energy production (left) and the electrical energy production (right). The dots in the graphs are the integrated daily energy production, the simulated value on the x-axis and the measured value on the y-axis. The blue dots are from Solgärden and the pink dots are from the prototype window.

Yearly simulations were made for the solar window and for two flat PV-modules. The PV-modules have the same efficiencies and areas as the string module in the solar window but without shading effects and reflectors. The PV-modules are installed on a wall alternatively tilted  $20^\circ$  on a roof. The wall mounted PV module is not shaded like the solar window but still benefits less from the diffuse radiation due to less favourable angles between the cells and the sky. This is also the case for the direct radiation, as can be seen in figure 6. When the PV module is located on a roof at a low tilt it receives more diffuse radiation than a wall mounted PV module since the module can see a larger part of the diffuse sky. This is clearly visible in figure 6. The increase of the electrical output from the direct radiation on the module is due to less loss in the glazing and the possibility for the roof module to utilize the radiation which comes from directions behind the wall. Note that the increase of the diffuse radiation on the roof mounted module almost compensates the reflector contribution on the cells in the solar window. The diffuse irradiation is treated as isotropic.

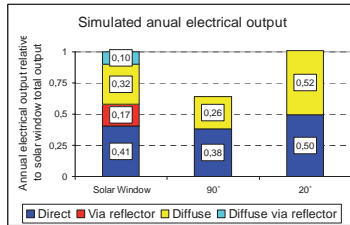


Fig 6. The annual electrical output from the prototype solar window and from two flat PV-modules on a wall at  $90^\circ$  tilt and on a roof at  $20^\circ$  tilt. In the figure the blue part is electricity produced by the direct radiation that hits the absorber directly. The red part is the electricity caused by direct radiation that goes via the reflector. The yellow part is the diffuse radiation that goes directly on the absorber and the light blue is the electricity caused by the diffuse radiation that goes via the reflector. All results have been normalized to the total annual output from the solar window.

The same analysis, in this case using TRNSYS, was performed to investigate the thermal properties. A TRNSYS-deck including the solar window or flat solar collectors, pumps, a storage tank, etc and a heating load was constructed. In the simulation all parameters but the areas of the wall collector and the roof collector was kept constant. Figure 7 shows a graph of the area of the flat collector required to

produce the same annual amount of thermal energy as the solar window in Solgården, turned  $23^\circ$  from south towards east. The roof collector was placed at  $20^\circ$  tilt and the wall collector is placed at  $90^\circ$  tilt to the horizontal. The roof mounted collector can see a larger part of the diffuse sky and has more preferable incidence solar angles and thus gain and produce more energy compared to the wall mounted collector. The absorber area in the solar window is  $5.06 \text{ m}^2$  and the total window area is  $16 \text{ m}^2$ .

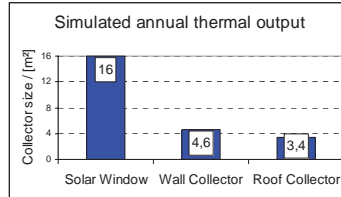


Fig 7. The required areas of the solar window, a wall collector and a roof collector to produce an equal annual amount of thermal energy when installed in Solgården. The wall collector is placed vertically and the roof collector is installed at  $20^\circ$  tilt.

To study the limiting factors in the solar window a simulation was carried out where the factors  $f_{\text{glass}}(\Theta_1)$ ,  $f_{\text{pv}}(\Theta_2)$  and  $f_{\text{shading}}(\Theta_3)$  in Eq. (2,3 and 4) was set to 1, see figure 8. Since the angular dependence of the PV cells is large only for high angles the impact of setting  $f_{\text{pv}}(\Theta_2)$  to 1 will be small, the shading is already deteriorating the performance for high solar angles. If the glazing is omitted the yearly electrical output would increase by about 15% and if the shading effects can be removed completely the increase would be as much as 21%. If the shading effect is very large it is better to have one cell less, since large shading is caused by the window frame on the outer cells.

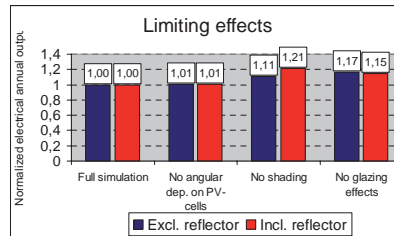


Fig 8. Different limiting factors affecting the solar window. The first bar is the complete simulation. In the second bar the angular dependence of the PV cells have been removed. In the third bar all shading effects have been removed and in the last bar the effects from the glazing have been removed. In blue are simulations performed without the influence of the reflector and in red are simulations including the reflector contribution.

## Discussion

The focus of the work in this article is to reduce the total costs of a building including a solar energy system. One solution is to use building integrated PV/T hybrid collectors using reflectors to focus the

radiation onto the absorbers. Different collectors have been proposed [1]. Using such technique façade elements can be saved to reduce the costs. To further develop the building integration technique a multifunctional PV/T hybrid solar window was proposed by Fieber [2]. Integrating the proposed collector into a window saves both frames and glazing. The total price of the construction is reduced further since the concentrating reflectors are tiltable and thus provide flexible solar shading for the building.

The results from the simulation program developed to evaluate the window closely match the measured data. The simulated annual electrical energy production clearly shows the importance of utilizing the diffuse radiation. About 40% of the electrical energy produced in the window is due to diffuse radiation. The comparison performed in Figure 6 shows that the solar window produces about 56% more electrical energy per unit area of PV cells compared to a flat PV module placed on a wall at a 90° tilt. However the roof mounted PV module performs about 2% better per unit area than the solar window. The roof mounted PV module receives more diffuse radiation than the wall mounted system, and thus produces more electrical energy.

The simulation presented in figure 7 shows that the solar window produces less thermal energy per absorber area compared to a flat vertical solar collector or a roof collector installed at 20° tilt to the horizontal. Due to the complex design of the solar window the U-value of the collector is relatively high. The thermal losses from the solar window collector is approximately 50% larger compared to a normal flat solar collector. However, a large part of the thermal losses will heat the building passively. This positive effect is not included in the values in figure 7. A full investigation including the passive effects, such as passive heating of the building due to thermal losses from the collector and taking into account the decrease of passive heating through the windows due to solar radiation utilized in the collector instead of the passive heating, will be presented in future papers.

The results presented in Figure 8 clearly show the importance of choosing the best available glazing for the window. The importance of avoiding shading caused by the frames of the window is also clear. If the shading is extensive it is better to have one less PV cell per absorber. Heavy shading can occur if the cells on the outer edges are placed too close to the window frame. The angular dependence of PV cells is only apparent for large incident angles, and large incident angles are already heavily shaded by the frames and heavily suppressed by low transmission through the glazing. The annual performance can be increased by up to 30% if the impact of shading and angular effects is minimized.

As can be seen in figure 6 it is possible to run simulations with the reflectors in both active, vertical, or passive, horizontal, positions. This keeps the simulation realistic by allowing control mechanisms, based on human behaviour, to decide whether or not to have closed reflectors. For instance there is a possibility to cool the building at night by simply opening the reflectors and thus increasing the U-value of the window. This is not a possibility for a standard window with low U-value.

### References

- [1] H Gajbert et al, *Solar Energy Materials & Solar Cells* 91 (2007) 1788-1799
- [2] A Fieber, *Building Integration of Solar Energy*, Lic. Thesis (2005) Report EBD-T—05/3









LUND UNIVERSITY

ISSN 1671-8136  
ISBN 978-91-85147-45-8

## System analysis of a PV/T hybrid solar window

Henrik Davidsson

### Errata

---

Page 44, Figure 2.22 Text in figure

|            |   |
|------------|---|
| Reads      | Simulated radiation from direct radaition |
| Shall read | Simulated output from direct radiation    |

---

Page 47, Eq. (2.9)

|            |                                     |
|------------|-------------------------------------|
| Reads      | $h_r = 4\epsilon\sigma \cdot 4T^3m$ |
| Shall read | $h_r = 4\epsilon\sigma \cdot T^3m$  |

---

Page 47, last equation

|            |   |
|------------|---|
| Reads      | $h = \frac{h_{tot}}{c} = \frac{h_c + h_r}{c} = \frac{4\epsilon\sigma \cdot 4T_m^3 + h_r}{c} = \frac{5.5 + 4}{2.45} \approx 3.9 \text{ W/m}^2\text{K}$ |
| Shall read | $h = \frac{h_{tot}}{c} = \frac{h_c + h_r}{c} = \frac{4\epsilon\sigma \cdot T_m^3 + h_c}{c} = \frac{5.5 + 4}{2.45} \approx 3.9 \text{ W/m}^2\text{K}$  |

---

Page 48, Figure 2.25 Text in figure

|            |     |
|------------|-----|
| Reads      | m_h |
| Shall read | m_r |

---

Page 50, Figure number

|            |             |
|------------|-------------|
| Reads      | Figure 2.20 |
| Shall read | Figure 2.26 |

---

Page 73, Table 5.2 Column "Open window / in "

|            |     |
|------------|-----|
| Reads      | 5.8 |
| Shall read | 5.9 |



